



Uniwersytet Przyrodniczy w Poznaniu

Wydział Inżynierii Środowiska i Inżynierii Mechanicznej

Mgr. Paulina Dukat

Ocena wymiany wody i dwutlenku węgla pomiędzy różnowiekowymi lasami sosnowymi a atmosferą w skali drzewa i ekosystemu.

Evaluation of water and carbon dioxide exchange between different-aged pine stands and the atmosphere on a tree and ecosystem scale.

Rozprawa doktorska w dziedzinie nauk inżyniersko-technicznych
w dyscyplinie inżynieria środowiska, górnictwo i energetyka
Doctoral thesis in engineering and technology sciences
in the environmental engineering, mining and energy discipline

Promotor:

Dr hab. inż. Marek Urbaniak, Prof. UPP

Promotor pomocniczy:

Dr Klaudia Ziemblińska

Pracownia Meteorologii,

Katedra Budownictwa i Geoinżynierii,

Wydział Inżynierii Środowiska i Inżynierii

Mechanicznej, Uniwersytet Przyrodniczy w

Poznaniu

Poznań, 2023

Podziękowania

Powstanie przedstawionej pracy doktorskiej niebyło by możliwe bez wpływu wielu osób, którym w tym miejscu szczególnie dziękuję. Dziękuję prof. Januszowi Olejnikowi, za obdarzenie mnie zaufaniem, mimo iż moje umiejętności miałam dopiero udowodnić. Dziękuję też za mentalne wspieranie i dodawanie odwagi. Dziękuję dr hab. Markowi Urbaniakowi za to, że był dla mnie nieocenionym przewodnikiem w drodze do uzyskania stopnia naukowego doktora i zawsze potrafił przeprowadzić mnie przez wszystkie niezbędne etapy powstawania prac naukowych. To, jak również to jakim jest człowiekiem, sprawia, że w moich oczach jest najlepszym promotorem. Dziękuję dr inż. Klaudii Ziemblińskiej, za to, że w każdym momencie mogłam liczyć na wsparcie, zarówno w pracy naukowej jak i życiu prywatnym. Dziękuję Oldze Zawitowskiej-Błacha i Stasiowi Tuchołce, za wsparcie we wszystkich trudnościach, i za to, że dzięki ich obecności praca w biurze była po prostu przyjemna. Dziękuję Piotrowi Kozłowi, za to, że był ze mną, kiedy uczyłam się instalować instrumenty i poznawałam zasady ich działania, za to, że dbał, by dane które wykorzystuję były jak najwyższej jakości oraz za to, że nauczył mnie jeździć na nartach. Dziękuję Damianowi Józefczykowi, dzięki któremu polubiłam pracę w terenie, Pearl Jam, jak i zrozumiałam, jaki ogrom pracy jest potrzebny, aby prowadzić zaawansowane pomiary terenowe. Dziękuję Piotrowi Tomaszewiczowi, za to, że poza zaangażowaniem w pracę, zawsze przynosi dużo uśmiechu, który podnosił mnie na duchu w trudnych momentach. Dziękuję wszystkim współautorom moich prac, za wsparcie merytoryczne i techniczne, i za to, że poświęcili swój czas by efekt końcowy był jak najlepszy.

Dziękuję moim rodzicom, za to, że zawsze mnie wspierają i że zawsze mogę na nich liczyć. Dziękuję mamie za to, że nigdy we mnie nie zwątpiłaś i że wspierasz mnie zawsze w spełnianiu moich marzeń. Dziękuję prof. Timo Vesala, za przyjaźń, za to, że dodaje mi wiary w siebie i zapału do tego, żeby się rozwijać i że zawsze mogę na niego liczyć, nie tylko w kryzysie. Dziękuję Ewie Maciejaszek, za to, że potrafi słuchać, gdy ja chcę mówić. Dziękuję Przemkowi Krajewskiemu, za to, że od lat rozwija mnie filozoficznie i nie pozwala mi spocząć na laurach. Dziękuję wszystkim przyjaciołom, za to, że szli ze mną na różnych etapach życia, w szczególności: Natalii Protasiewicz, Adzie Ogrodnik, Natalii Wierzbickiej, Jadzi Marczewskiej (szczególnie za pomysł, że może powinnam zrobić doktorat), Joannie Biskup, Lauriemu Lindfors, Xin Zhuang, Magdalenie Held, Che Liu – dzięki wam jestem tu, gdzie jestem i wiem, że wybrałam dobrze.

Pracę dedykuję mojemu dziadkowi śp. Stanisławowi Sikorskiemu [1922-2016]

Lista artykułów

Zgodnie z art. 187, ust. 3 Ustawy z dnia 20 lipca 2018 r. Prawo o szkolnictwie wyższym i nauce (Dz. U. 2018 poz. 1668 ze zmianami) oraz w związku z Uchwałą nr 3/21/2021 z dnia 16 grudnia 2021 roku Rady Naukowej Dyscypliny Inżynieria Środowiska, Górnictwo i Energetyka Uniwersytetu Przyrodniczego w Poznaniu, niniejszą rozprawę doktorską stanowi spójny tematycznie zbiór trzech artykułów opublikowanych w czasopismach naukowych, tj.:

- #1. Dukat P., Bednorz E., Ziemblińska K., Urbaniak M., *Trends in drought occurrence and severity at mid-latitude European stations (1951–2015) estimated using standardized precipitation (SPI) and precipitation and evapotranspiration (SPEI) indices*, 2022, Meteorology and Atmospheric Physics, DOI: 10.1007/s00703-022-00858-w. **IF = 2,292** wg Journal Citation Reports (JSR); **70 pkt** wg listy Ministerstwa Edukacji i Nauki (MEN) z grudnia 2021.
- #2. Dukat P., Ziemblińska K., Olejnik J., Małek S., Vesala T., Urbaniak M., *Estimation of Biomass Increase and CUE at a Young Temperate Scots Pine Stand Concerning Drought Occurrence by Combining Eddy Covariance and Biometric Methods*, 2021, Forests, DOI: 10.3390/f12070867. **IF = 3,282** wg JCR; **100 pkt** wg listy MEN.
- #3. Dukat P., Ziemblińska K., Räsänen M., Olejnik J., Vesala T., Urbaniak M. *Scots pine responses to drought investigated with eddy covariance and sap flow methods*, 2023, European Journal of Forest Research, DOI: 10.1007/s10342-023-01549-w. **IF = 3,140** wg JCR; **100 pkt** wg listy MEN.

Spis treści

| | |
|---|------------------|
| <u>LISTA ARTYKUŁÓW</u> | <u>1</u> |
| <u>SPIS TREŚCI.....</u> | <u>2</u> |
| <u>1. STRESZCZENIE.....</u> | <u>3</u> |
| <u>2. WPROWADZENIE</u> | <u>5</u> |
| 2.1. ISTOTNOŚĆ PROBLEMU BADAWCZEGO..... | 5 |
| 2.2. BRAKI WE WSPÓŁCZESNEJ WIEDZY W ZAKRESIE PODJĘTEJ TEMATYKI..... | 6 |
| 2.3. ZAKRES PRACY | 7 |
| 2.4. CELE | 8 |
| 2.5. HIPOTEZY | 9 |
| 2.6. ZNACZENIE PREZENTOWANYCH BADAŃ..... | 9 |
| 2.7. WPROWADZENIE DO ZASTOSOWANEJ METODOLOGII | 10 |
| <u>3. WYNIKI.....</u> | <u>12</u> |
| 3.1. OCENA TRENDÓW INTENSYWNOŚCI I CZĘSTOTLIWOŚCI WYSTĘPOWANIA SUSZY..... | 12 |
| 3.2. PRZYROST BIOMASY I EFEKTYWNOŚĆ WYKORZYSTANIA WĘGLA (CUE) DRZEWOSTANÓW SOSNOWYCH W WARUNKACH SUSZY | 13 |
| 3.3. TRANSPIRACJA I EFEKTYWNOŚĆ WYKORZYSTANIA WODY (WUE) LASÓW SOSNOWYCH W WARUNKACH SUSZY..... | 15 |
| <u>4. PODSUMOWANIE</u> | <u>19</u> |
| <u>5. LITERATURA.....</u> | <u>22</u> |
| <u>6. KOPIE OPUBLIKOWANYCH PRAC WCHODZĄCYCH W SKŁAD ROZPRAWY</u> | <u>25</u> |
| 6.1. PUBLIKACJA #1 | 25 |
| 6.2. PUBLIKACJA #2 | 47 |
| 6.3. PUBLIKACJA #3 | 68 |
| <u>7. OŚWIADCZENIA KANDYDATA ORAZ WSPÓŁAUTORÓW.....</u> | <u>89</u> |

1. Streszczenie

Sosna zwyczajna (*Pinus sylvestris* L.) jest jednym z dominujących gatunków drzew w lasach strefy umiarkowanej i borealnej w Europie. Ze względu na zmiany klimatu lasy sosnowe mogą być narażone na dotkliwe deficyty wody. W Polsce dotyczy to zwłaszcza północno-zachodniej i centralnej części kraju, które obecnie posiadają jedne z najniższych zasobów słodkiej wody na mieszkańca spośród wszystkich krajów Unii Europejskiej.

Celem niniejszej pracy było: ustalenie trendów występowania suszy w latach 1951–2015 dla wybranych krajów Europy środkowej, określenie wpływu suszy na obieg wody i węgla w drzewostanach sosnowych, w szczególności na ich transpirację, wzrost biomasy drzewostanów, fotosyntezę, a także zależności między tymi procesami – zarówno w skali drzewa jak i ekosystemu.

Trendy nasilania suszy meteorologicznych w Europie zostały wykryte w wyniku analizy zmian wskaźnika SPEI (Standardized Precipitation and Evapotranspiration Index), który bierze pod uwagę nie tylko opady, ale także warunki termiczne warunkujące intensywność ewapotranspiracji. W badaniach posłużono się pomiarami metodą kowariancji wirów (EC) do oceny wymiany pary wodnej i dwutlenku węgla w skali ekosystemu oraz metodą przepływu soków, do oceny transpiracji w skali drzewa i drzewostanu. Pomiary były prowadzone na dwóch stanowiskach obejmujących różnowiekowe monokultury sosny zwyczajnej.

W wyniku przeprowadzonych analiz ustalono, że występowanie intensywnych susz w obszarze Europy Środkowej w ostatnich kilku dekadach ma trend wzrostowy. Wykazano również, że mierzona bezpośrednio produktywność pierwotna netto (NPP) w młodym drzewostanie sosnowym była o około $0,6 \text{ t C}\cdot\text{ha}^{-1}$ niższa w roku suchym 2019 niż w umiarkowanie wilgotnym 2020, podobnie jak szacowana efektywność wykorzystania węgla (CUE). Ponadto wysoka efektywność wykorzystania wody (WUE) była związana z niską zawartością wody w glebie, co wskazuje, na silne ograniczanie utraty wody (transpiracji) przy jednoczesnym utrzymaniu intensywnego pochłaniania CO_2 (fotosyntezy).

Istnieje przesłanka, że w okresach występowania suszy i pogłębiających się deficytów wody, monitorowanie lasów pod kątem obiegu wody i węgla, prowadzone w sposób bezpośredni w czasie rzeczywistym, będzie miało coraz większe znaczenie nie tylko dla gospodarki leśnej, ale także lokalnego i globalnego bilansu węgla, wody i energii.

Słowa kluczowe: Sosna zwyczajna, transpiracja, fotosynteza, susza, kowariancja wirów, przepływ soków

Abstract

Scots pine (*Pinus sylvestris* L.) is one of the dominant tree species in temperate and boreal forests in Europe. Due to climate change, pine forests may be exposed to severe water deficits. In Poland, this applies especially to the north-western and central parts of the country, which currently have one of the lowest fresh water resources per capita among all European Union countries.

The aim of this study was to determine trends in drought occurrence for selected Central European countries during the period 1951–2015, determine the impact of drought on water and carbon cycle at pine stands - in particular on their transpiration, stand biomass increase, photosynthesis, as well as the relationships between these processes, both at an individual tree and ecosystem scale.

Trends in the intensification of meteorological droughts in Europe were detected by analyzing the course of SPEI index (Standardized Precipitation and Evapotranspiration Index), which consider not only precipitation, but also thermal conditions determining the intensity of evapotranspiration. The study used eddy covariance (EC) measurements to assess the exchange of water vapor and carbon dioxide (CO₂) on an ecosystem scale, and the sap flow method to assess transpiration on a tree and stand scale. The research was carried out at two Scots pine monoculture sites of different ages.

As a result of performed analyses it was found that the occurrence of severe droughts in the area of Central Europe has an upward trend in the last few decades. The analyzes also showed that the directly measured net primary productivity (NPP) at the young Scots pine monoculture was about 0.6 t C ha⁻¹ lower in the dry year of 2019 than in the moderately wet year 2020, as was the estimated carbon use efficiency (CUE). In addition, high water use efficiency (WUE) was associated with low water content in the soil, which indicates a strong reduction of water loss (transpiration) while maintaining intensive CO₂ uptake (photosynthesis).

There is an indication that during periods of drought and water deficits, forest monitoring in terms of water and carbon cycle, carried out in a direct and real-time manner, will become increasingly important not only for forest management, but also for the local and global carbon, water and energy balance.

Key words: Scots pine, transpiration, photosynthesis, drought, eddy covariance, sap flow

2. Wprowadzenie

2.1. Istotność problemu badawczego

Zakłócenia obiegu węgla i wody są jednym z ważniejszych, negatywnych skutków globalnych zmian klimatu dotyczących różne ekosystemy. Z powodu złożonych powiązań pomiędzy biosferą i nieożywionymi elementami środowiska, a także pewnych opóźnień w łańcuchu przyczynowo - skutkowym, problem ten w dalszym ciągu pozostaje mało rozpoznany. Przyczynia się to do tego fakt, że pojedyncze wystąpienia zjawisk ekstremalnych, takie jak susza, są w przestrzeni publicznej uznawane za objaw zmian klimatycznych (globalnego ocieplenia). Tymczasem, trudno jest wskazać, że wystąpienie konkretnego ekstremalnego zjawiska pogodowego jest bezpośrednim skutkiem zmian klimatycznych. To występowanie trendu - wzrost częstotliwości i intensywności takich zjawisk, powinna być kojarzona z obserwowanym ociepleniem. Susza jest jednym z tych ekstremalnych zjawisk, występującym we wszystkich strefach klimatycznych i tym samym jednym z najpoważniejszych zagrożeń naturalnych (Vogt i Somma 2000). Już na przełomie tysiącleci znaczne obszary Europy doświadczały suszy (Lloyd-Hughes i Saunders 2002). Obserwowane ostatnio dotkliwe i długotrwałe susze ujawniły dużą wrażliwość europejskich ekosystemów, zwłaszcza lasów, na to zagrożenie, które zostało dodatkowo spotęgowane przez zaburzenia antropogeniczne, takie jak zakłócenie cyklu hydrologicznego przez wylesianie lub niewłaściwą gospodarkę leśną (Martínez-Vilalta, Lloret i Breshears, 2012; Dai, 2013; Adams *i in.*, 2015; Cailleret *i in.*, 2017).

Lasy odgrywają ważną rolę w globalnym obiegu wody i węgla, ponieważ zajmują 30% powierzchni lądowej. Z uwagi na to mają ogromny wpływ na klimat zarówno w skali lokalnej, jak i globalnej. Wymiana dwutlenku węgla (CO_2) netto większości lasów jest dodatnia, co oznacza, że CO_2 jest usuwany z atmosfery, co łagodzi ocieplenie klimatu. Ponadto, uwalniając parę wodną w procesie zwanym ewapotranspiracją (ET), mogą przyczyniać się do dalszego „ochładzania” atmosfery. Te niezwykle ważne i pożyteczne funkcje ekosystemów leśnych mogą być jednak zagrożone na skutek zakłóceń obu cykli (węglowego i wodnego) spowodowanych przez częstsze i dotkliwsze susze. Rodzi to potrzebę bardziej szczegółowego (w skali ekosystemu) zbadania poszczególnych składowych strumieni wymiany masy i energii pomiędzy ekosystemami a atmosferą w różnych warunkach reżimu wodnego. Warto również zauważyć, że podział strumieni CO_2 (na produkcję netto i oddychanie) został znacznie lepiej zbadany i jest znacznie częściej stosowany niż podział strumieni pary wodnej (na transpirację i ewaporację). To ostatnie było jednym z głównych celów prezentowanej pracy.

Wyniki analiz, porównujących 81 opublikowanych badań dotyczących podziału ET na jego główne komponenty – transpirację (T) i parowanie (E) – w skali ekosystemu wykazały, że

globalnie transpiracja stanowi średnio 61% ($\pm 15\%$ odchylenia standardowego, SD) ET (Schlesinger i Jasechko, 2014). Oszacowano także, że globalnie T stanowi $\sim 39 \pm 10\%$ sumy opadów atmosferycznych (P). Transpiracja to strumień skierowany z powrotem do atmosfery, a tak duży udział w całkowitej wartości ET świadczy o tym, że jest to dominujące ogniwo w globalnym obiegu wody. Procentowy udział składowych strumieni ET jest oczywiście różny dla różnych ekosystemów. Przykładowo, dla lasów iglastych strefy umiarkowanej obliczono, że stosunek T/ET wynosił średnio 55 ($\pm 15\%$ SD) (Schlesinger i Jasechko, 2014). Ponieważ transpiracja jest między innymi regulowana przez aktywność aparatów szparkowych, co oznacza, że jest to nie tylko proces fizyczny, ale przede wszystkim biologiczny (w przeciwieństwie do ewaporacji, która jest procesem czysto fizycznym; (Gu *i in.*, 2018) – jest także najważniejszą składową leśnego bilansu wodnego a jej badanie jest istotne z punktu widzenia gospodarki leśnej.

2.2. Braki we współczesnej wiedzy w zakresie podjętej tematyki

Kwantyfikacja bilansu węgla ekosystemów lądowych, a zwłaszcza potencjału sekwestracji węgla przez lasy i możliwości wykorzystania tych ekosystemów do łagodzenia zmian klimatycznych, była przedmiotem licznych badań (Lewis *i in.* 2009; Malhi *i in.* 2009; Kunert *i in.* 2019). Produktywność ekosystemu leśnego znajduje odzwierciedlenie w skuteczności usuwania CO₂ z atmosfery i magazynowania węgla w materii organicznej. Zwykle całkowita ilość węgla pochłoniętego przez ekosystem leśny w procesie fotosyntezy (produktywność pierwotna brutto, GPP) oraz węgiel, który pozostał w roślinie, jako saldo produkcji pierwotnej brutto pomniejszonej o oddychanie roślin (tzw. produktywność pierwotna netto, NPP) są przyjętymi miarami tej efektywności (Clark *i in.*, 2001; Kunert *i in.*, 2019). Obserwacja i określenie, jak zmienia się funkcjonowanie lasów wraz ze wzrostem częstotliwości występowania i intensywności susz, jest kluczowe dla prawidłowego oszacowania całkowitego potencjału sekwestracji CO₂ przez ekosystemy lądowe. Ponadto, ponieważ cykle węgla i wody są sprzężone poprzez aktywność aparatów szparkowych – asymilację CO₂ w procesie fotosyntezy i utratę H₂O podczas transpiracji – konieczne jest zbadanie wzajemnych relacji i sprzężeń pomiędzy tymi procesami. W związku z tym efektywność wykorzystania wody (WUE), jako stosunek między absorpcją CO₂ w procesie fotosyntezy a utratą wody w wyniku transpiracji, stała się ważnym wskaźnikiem, zwłaszcza w warunkach suszy (Farquhar, O’Leary *i Berry*, 1982; Gao *i in.*, 2017).

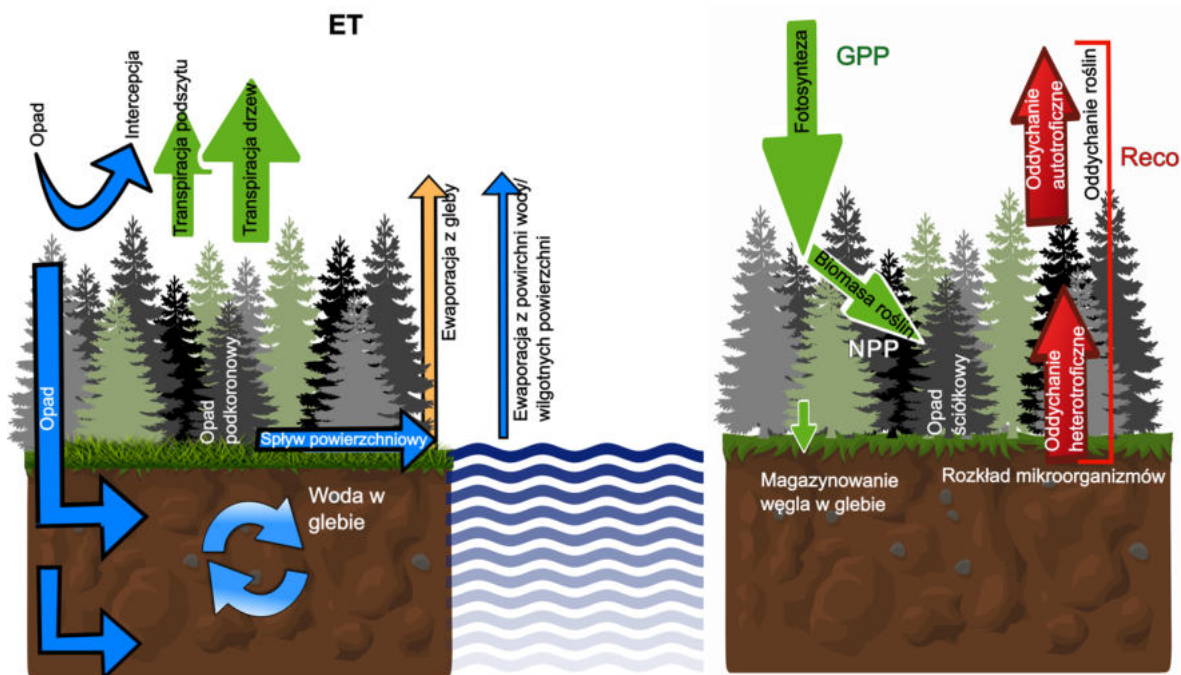
Większa część obszaru Polski jest narażona na występowanie susz meteorologicznych, które wpływają na i tak już niekorzystny bilans wodny oraz skutkują suszami glebowymi, które

dotykają w szczególności lasy (Boczoń i Wróbel, 2015). Wykazano, że susza wpływa na wymianę CO₂ z atmosferą poprzez oddziaływanie zarówno na oddychanie jak i fotosyntezę (M. Reichstein *i in.*, 2013). W literaturze wskazuje się również na fakt, że globalnie ekstremalne zjawiska pogodowe (zwłaszcza susza) miały znacznie większy wpływ na bilans węgla niż wcześniej zakładano (Markus Reichstein *i in.*, 2013), zmniejszając asymilację ekosystemów lądowych o nawet 11 miliardów ton CO₂. Ponadto, to właśnie susza jest głównym czynnikiem powodującym śmiertelność sosny zwyczajnej, zwłaszcza w Europie Środkowej w klimacie umiarkowanym (Buras *i in.*, 2018).

Badania przedstawione w niniejszej pracy są kompleksowym spojrzeniem na opisane wyżej zagadnienia. Przedstawiono tu zastosowanie kilku niezależnych metod, które pozwalają w sposób bezpośredni lub pośredni oszacować wartości nie tylko strumieni wymiany netto węgla i pary wodnej pomiędzy lasem sosnowym a atmosferą, ale także ich składowe. Za wartość dodaną pracy można również uznać to, że podobnych badań dla drzewostanów sosnowych nie prowadzono dotychczas w Polsce, a na świecie jedynie w ograniczonym zakresie, zarówno jeśli chodzi o czas, jak i o rodzaj ekosystemu objęte badaniami.

2.3. Zakres pracy

W pracy dokonano oceny wykorzystania wskaźników suszy do wyznaczenia wieloletnich trendów występowania suszy w strefie umiarkowanej w Europie (publikacja #1). Stało się to przyczynkiem do badań reakcji najliczniejszych w naszym kraju drzewostanów sosnowych na ograniczenia w dostępie do wody, rozumiane jako zakłócenia składowych obiegu wody i węgla poprzez ogniwo atmosferyczne. Wśród ujętych w badaniach składowych wspomnianych obiegów, znalazły się: transpiracja (T), ewapotranspiracja (ET), stosunek opadów (P) do transpiracji (T), produktywność pierwotna brutto (GPP), produktywność pierwotna netto (NPP), oddychanie ekosystemów (Reco) (publikacja #2, #3), a także interakcje między tymi strumieniami wyrażone jako: efektywność wykorzystania wody (WUE), efektywność wykorzystania węgla (CUE) (publikacja #3). Ponadto, porównano dwa oszacowania transpiracji: wykorzystujące pomiary przepływu soków (T_{SF}) i uzyskaną przez wyodrębnienie ze strumienia ewapotranspiracji (ET), zmierzonego systemem kowariancji wirów (EC) (T_{EC}). Wymienione składowe obiegu wody i węgla w lesie dla wygody czytelnika przedstawiono schematycznie na Ryc. 1. Skrócony opis miejsca badań i metodyki zamieszczono w podrozdziale 4.7.



Rycina 1. Schematy obiegu wody (po lewej) i węgla (po prawej), zmodyfikowane na podstawie (Straka i Layton, 2010; Riebeek i Simmon, 2011). Elementy stanowiące przedmiot badań w tej rozprawie doktorskiej to przede wszystkim - Ewapotranspiracja całego ekosystemu ET (ilość pary wodnej uwalnianej do atmosfery); Transpiracja – para wodna uwalniana do atmosfery poprzez aparaty szparkowe w liściach, GPP – produktywność pierwotna brutto (ilość CO_2 pochłoniętego podczas fotosyntezy), NPP – produktywność pierwotna netto (ilość CO_2 wbudowanego w biomasę roślinną), Reco – całkowite oddychanie ekosystemu (ilość CO_2 wyemitowanego łącznie w wyniku oddychania auto- i heterotroficznego).

2.4. Cele

Nadrzędnym celem pracy było przedstawienie znaczenia monitorowania zależności strumieni wymiany węgla i wody od występowania suszy w ekosystemie leśnym różnymi metodami. Wiele wysiłku poświęcono uzyskaniu solidnych szacunków transpiracji (T), jako skuteczniejszego wskaźnika stanu funkcjonowania lasów podczas suszy, w porównaniu do powszechnie stosowanego całkowitego strumienia wody wymienianego z atmosferą (ET). Wydaje się, że drzewostany, które z powodzeniem monitorowane są jedynie stosunkowo kosztownymi systemami kowariancji wirów, powinny być wsparte również pomiarami na poziomie pojedynczych drzew, które dają wgląd w szczegóły mechanizmu transportu wody w drzewach, pozwalając na obserwację ich reakcji na zmieniające się warunki pogodowe.

Biorąc pod uwagę powyższe, **szczegółowe** cele pracy doktorskiej ujęto w następujących sformułowaniach:

- (1) Określenie trendów w częstotliwości i intensywności suszy w Europie Środkowej i Wschodniej, gdzie sosna zwyczajna stanowi jeden z głównych gatunków lasotwórczych.
- (2) Określenie wpływu suszy na transpirację, fotosyntezę, wzrost biomasy oraz ich wzajemne relacje wyrażone efektywnością wykorzystania węgla i wody w wybranych ekosystemach sosnowych.
- (3) Określenie przydatności pomiarów przepływu soków na poziomie poszczególnych drzew w diagnostyce funkcjonowania lasu w skali ekosystemu, zwłaszcza w warunkach suszy.

2.5. Hipotezy

W wyniku przeprowadzonych badań literaturowych i w związku z rozpoznaniem lukami w wiedzy, przed rozpoczęciem badań sformułowano następujące hipotezy:

1. wzrostowy trend występowania i intensywności suszy w ciągu ostatnich 50 lat będzie wyraźnie widoczny także w Europie Środkowo-Wschodniej, dla której nie jest to charakterystyczna cecha klimatu (**publikacja #1**)
2. ekstremalna susza, jaka wystąpiła w poszczególnych miesiącach 2019 roku na badanych obszarach leśnych, miała istotny wpływ na transpirację tych drzewostanów, fotosyntezę, efektywność wykorzystania wody i węgla oraz przyrost nowej biomasy (**publikacja #2 i #3**).
3. transpiracja (T) oszacowana na podstawie pomiarów przepływu soków (T_{SF}) jest bardziej odpowiednia do wykrywania skutków wywołanych suszą niż T uzyskane z pomiarów metodą kowariancji wirów EC (T_{EC}) (**publikacja #3**).

2.6. Znaczenie prezentowanych badań

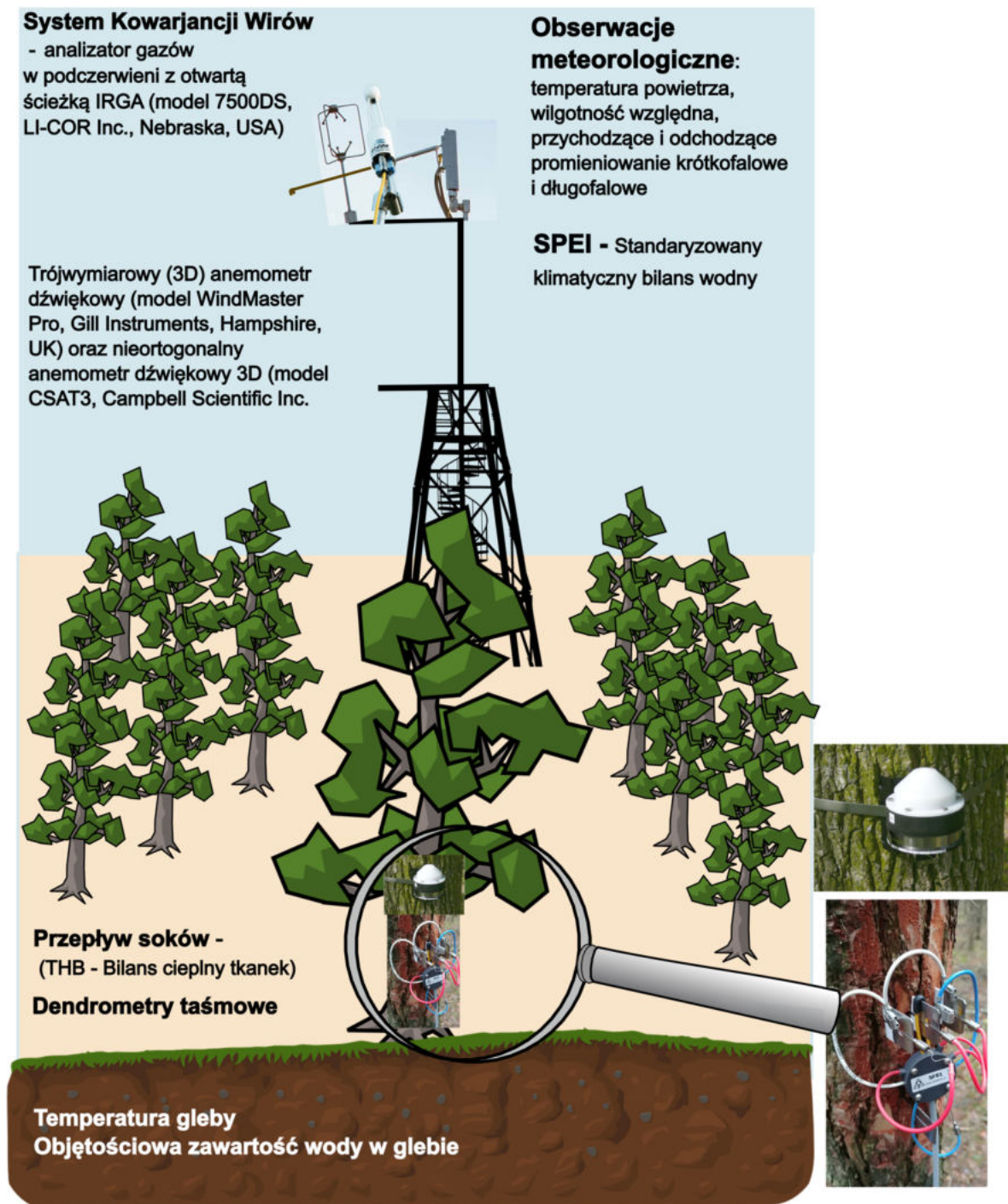
Globalne ocieplenie prowadzi do zaburzeń obiegu węgla i wody. Zaburzenia te mogą być widoczne w różnych skalach czasowych i wpływać na stan ekosystemów, ich trwałość oraz zdolność do akumulacji i magazynowania węgla. Nie jest do końca jasne czy globalne ocieplenie spowoduje tendencję do zwiększania częstotliwości i dotkliwości susz w strefie umiarkowanej. Publikacja #1 była próbą weryfikacji tego stwierdzenia. Uzyskane wyniki zdają się potwierdzać tendencję wzrostową częstości występowania tych niekorzystnych zjawisk, co wiąże się z hipotezą nr 1. W związku z tym w publikacji #2 i #3 podjęto badania mające na celu odpowiedź na pytanie, w jaki sposób nasilenie zjawiska suszy wpływa na obieg węgla i wody w różnowiekowych drzewostanach sosnowych w północno-zachodniej Polsce.

Praca ta przyczynia się zatem do lepszego zrozumienia procesów wpływających na obiegi węgla i wody w kontinuum gleba-roślina-atmosfera na przykładzie powszechnie występującego w Europie gatunku lasotwórczego w warunkach suszy. W świetle postępującego ocieplenia klimatu oraz potrzeby dywersyfikacji metod równoważenia emisji, podjęta tematyka zyskuje coraz większe znaczenie, chociażby w kontekście potrzeby prognozowania stanu środowiska na podstawie dostępnych baz danych czy identyfikowania zagrożeń mogących wpływać na stan i funkcjonowanie ekosystemów naturalnych. Wszystkie powyższe problemy badawcze mają charakter interdyscyplinarny, wpisują się zarówno w obszar zainteresowań dyscypliny inżynieria środowiska, górnictwo i energetyka jak i leśnictwo.

2.7. Wprowadzenie do zastosowanej metodologii

Dane empiryczne, które posłużyły do dalszej analizy, pozyskano z dwóch powierzchni badawczych zlokalizowanych w monokulturowych drzewostanach sosnowych (*Pinus sylvestris* L.): „Tuczno” - TU (Nadleśnictwo Tuczno) - drzewostan w wieku 68 lat oraz młodszym „Mezyk” - ME (polska pisownia „Mężyk”, jednak dla zachowania zgodności z artykułami zastosowano pisownię bez polskich znaków diaktrycznych, Nadleśnictwo Potrzebowice) w wieku 26 lat w czasie prowadzenia badań.

Sposób obliczania standaryzowanego klimatycznego bilansu wodnego SPEI oraz wskazanie bazy danych, z której można go pozyskać na potrzeby oszacowań w skali lokalnej, przedstawiono w publikacji #1. Bezpośrednie pomiary strumieni wymiany CO₂ i H₂O przeprowadzono za pomocą systemów kowariancji wirów (EC). W obszarze źródłowym (ang. footprint)* systemów EC (*reprezentatywny obszar „widziany/analizowany” przez system EC) umieszczono system do pomiaru przepływu soków oraz dendrometry opaskowe do pomiaru zmian pierśnicy (na 25 drzewach na każdej powierzchni badawczej). Przepływ soków (*ang. sap flow*) został zmierzony techniką pomiaru propagacji impulsu termicznego w tkance przewodzącej pnia. W celu wyznaczenia biomasy drzew, wykorzystano pomiary biometryczne przeprowadzone na stanowisku Mezyk. Utworzono równania allometryczne korelujące a) całkowitą suchą biomasę drzew [kg] z pierśnicą (M1), jak również korelujące suchą biomasę wydzielonych poszczególnych części drzewa i pierśnicy (M2). Ponadto, wykonano podstawowe pomiary meteorologiczne, glebowe. Metodyka pomiaru i obliczeń została szczegółowo opisana w artykułach #2 i #3. Zastosowane w pracy doktorskiej metody pomiarowe – od drzewostanu do skali pojedynczego drzewa – przedstawiono schematycznie na Ryc. 2.

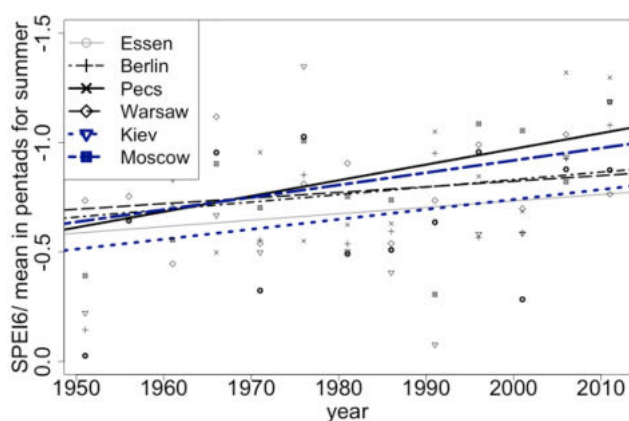


Rycina 2. Schemat systemu pomiarowego na powierzchniach badawczych w Tucznie i Mezyku.

3. Wyniki

3.1. Ocena trendów intensywności i częstotliwości występowania suszy

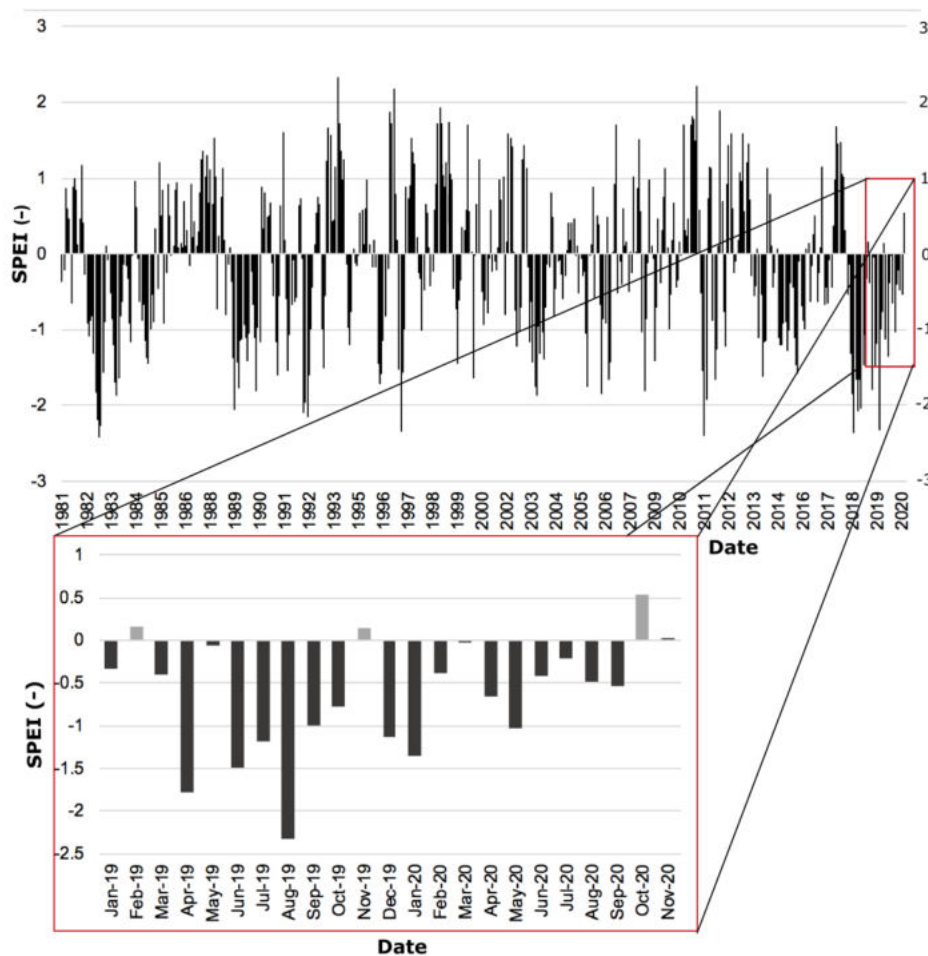
Standaryzowany klimatyczny bilans wodny (SPEI) oraz znormalizowany wskaźnik opadów (SPI) są powszechnie stosowane do diagnozowania i monitorowania intensywności i częstotliwości występowania suszy (Beguería, Vicente-Serrano i Angulo-Martínez, 2010; Vicente-Serrano, Beguería i López-Moreno, 2010; Vicente-Serrano *i in.*, 2012; Bezdán *i in.*, 2019). W niniejszej pracy indeksy SPEI i SPI zostały obliczone dla 6 lokalizacji w Europie (Essen, Berlin, Warszawa, Pecz, Kijów, Moskwa), dla lat 1950-2015 (publikacja #1). Analiza wyników pozwoliła wykazać, że warunki termiczne i opadowe oraz ewapotranspiracja potencjalna miały tendencję rosnącą dla wszystkich lokalizacji (co jest zgodne z wynikami (Spinoni *i in.*, 2019)). Wykazano istotne i pozytywne trendy średniej rocznej temperatury powietrza, przy czym najsilniejszy trend wzrostowy odnotowano dla Moskwy. Najważniejszy wynik dotyczący intensywności i częstości suszy w Europie w strefie umiarkowanej przedstawiono na Ryc. 3. Trend SPEI sugeruje, że we wszystkich badanych lokalizacjach susze – nie tylko meteorologiczne, ale przede wszystkim glebowe – najprawdopodobniej będą miały w najbliższej przyszłości jeszcze bardziej dotkliwy charakter.



Rycina 3. Średni wskaźnik SPEI dla pentad w skali 6-miesięcznej, dla wszystkich zdarzeń o wartości wskaźnika poniżej 0, w miesiącach letnich – czerwcu, lipcu i sierpniu. Źródło: Ryc. 7c w publikacji #1 (Dukat *i in.*, 2022).

Wskaźnik SPEI wykorzystano również do określenia intensywności suszy w poszczególnych miesiącach w latach 2019 - 2020 na powierzchniach badawczych Mezyk i Tuczno (publikacja #2). Na Ryc. 4 przedstawiono wynik dla powierzchni badawczej Mezyk.

Z ryciny tej wynika, że w badanym okresie susza o różnym nasileniu występowała przez większą część, istotnego z punktu widzenia funkcjonowania ekosystemu, sezonu wegetacyjnego. Najintensywniejsze susze wystąpiły w kwietniu i czerwcu oraz sierpniu 2019 r. Rok 2020 był bardziej wilgotny, jednak również w tym roku w kwietniu i maju stwierdzono suszę. Występowanie tak intensywnej suszy na początku sezonu wegetacyjnego jest szczególnie niekorzystne dla wzrostu drzew.



Rycina 4. Wartości SPEI (Standaryzowany klimatyczny bilans wodny) oszacowane w skali 3-miesięcznej w okresie 1981-2020 (górny panel) i 2019-2020 (dolny panel) dla poszczególnych miesięcy. Okres referencyjny – 1950-2020, na podstawie bazy danych SPEI Global Drought Monitor (Vicente-Serrano, Beguería i López-Moreno, 2010). Źródło: Ryc. 5 w publikacji #1 (Dukat *i in.*, 2021).

3.2. Przyrost biomasy i efektywność wykorzystania węgla (CUE) drzewostanów sosnowych w warunkach suszy

W wyniku wyżej opisanych analiz wskazano, że lata 2019 i 2020 (dla których dostępna była pełna baza danych) różniły się liczbą i stopniem nasilenia okresów suszy. Porównano wyniki

średniego przyrostu pierśnicy drzew, przyrostu biomasy drzewostanów oraz wskaźnika efektywności wykorzystania węgla CUE, otrzymane na powierzchni badawczej Mezyk w tym okresie. Różnice w całkowitym przyroście pierśnicy przeciętnego drzewa zaobserwowano zwłaszcza w sierpniu 2019 roku, który wg wskaźnika SPEI był miesiącem ekstremalnie suchym ($SPEI < -2$) (Ryc. 4, Ryc. 5a). W takich warunkach stres wodny doprowadził zarówno do odwracalnego kurczenia się pnia (co związane jest z większym gradientem między zapotrzebowaniem wody a wodą dostępną; (Zweifel, Item i Häsler, 2000; Güney *i in.*, 2020), jak i znacznego zahamowania przyrostu biomasy w tym najistotniejszym dla produkcji pierwotnej netto okresie. W 2019 r. pierśnica przeciętnego drzewa zwiększyła się o 0,14 mm, a w 2020 r. o 0,16 mm. Przeliczając tę różnicę (0,02mm) w rocznym przyroście pierśnicy drzew na jednostkę powierzchni, przy liczbie ponad 4200 drzew na hektar, można oszacować, że przełożyła się ona na zmniejszenie akumulacji węgla w biomase aż o 0,6 tony na hektar w suchym 2019 roku w porównaniu do przeciętnie wilgotnego 2020 (Ryc. 5a).

Na podstawie pomiarów i analiz zaprezentowanych powyżej, przy wykorzystaniu równań allometrycznych stwierdzono, że bezwzględny przyrost suchej biomasy pojedynczego drzewa na powierzchni badawczej Mezyk, wyniósł około 0,9 kg w 2019 r. i 1,2 kg w 2020 r. (w zależności od zastosowanego równania allometrycznego, opracowanego i przedstawionego w publikacji #2, w Tabeli 1). Przyrost suchej biomasy drzew w przeliczeniu na jednostkę powierzchni badanego drzewostanu wyniósł ok. 4,3 /4,4 t C ha⁻¹ w 2019 r. i 5,5/5,7 t C ha⁻¹ w 2020 r. (obliczone odpowiednio metodą równań allometrycznych M1 / M2). Uwzględniając zawartość węgla w suchej biomase drzewnej, roczna wartość węgla zasymilowanego i wbudowanego w tkanki nowo wytworzonego drewna (NPP) w skali całego ekosystemu osiągnęła 2,1/2,2 t C ha⁻¹ w 2019 r. i 2,7/2,8 t C ha⁻¹ w 2020 r. Pomimo, iż NPP było wyższe w 2020 r., całkowita roczna wartość CO₂ pochłoniętego w procesie fotosyntezy (strumień GPP), zarówno w sezonie wegetacyjnym, jak i w okresie przyrostu biomasy drzewa (B – Ryc. 5) był nieco wyższy w 2019 r. Mimo to, wskaźnik CUE, będący względną miarą tego, ile CO₂ pochłoniętego w procesie fotosyntezy zostało trwale związane i wbudowane w biomasę drzew, było wyższe w 2020 r. W badanym okresie wartości CUE uzyskane dla okresu przyrostu drewna (0,18/0,19 [-] w 2019 r.; 0,23/0,24 [-] w 2020) były stosunkowo niskie, zbliżone do tych obserwowanych w lasach strefy borealnych (De Lucia *i in.*, 2007). Na wykresie zamieszczonym na rycinie 5 można również zauważyć, że start okresu, w którym w latach 2019-2020 ekosystem był pochłaniaczem węgla, pokrywał się z rozpoczęciem maksymalnego skurczu zimowego pnia, który jest sygnałem pobudzenia aktywności drzew w nowym sezonie

wegetacyjnym. Koniec okresu, w którym las był pochłaniaczem CO₂ pokrywał się z przejściem drzew do posezonnej fazy odpoczynku.

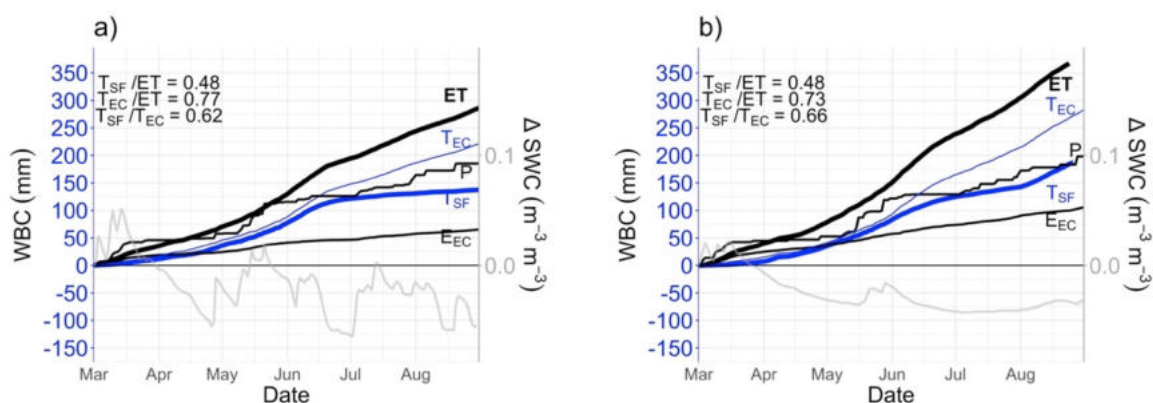


Rycina 5. Główne momenty i okresy w procesie przyrostu drzew na podstawie bezpośrednich pomiarów: a) dendrometrycznych (skala pojedynczego drzewa) oraz b) metodą kowariancji wirów (skala całego ekosystemu). SG – przyrost pnia w ciągu roku, związany z sezonowym wzrostem, MWC – maksymalne zimowe skurczenie pnia, B – okres przyrostu biomasy drzewa, PO – punkt zerowy dla bieżącego roku, odpowiadający punktowi kulminacji przyrostu w roku poprzednim, Reh – okres rehydracji tkanek drzewa po maksymalnym zimowym skurczeniu pnia, terminologia przyjęta za (Zweifel *i in.*, 2010)), NEP – produktywność ekosystemu netto, CO₂ sink – okres, w którym ekosystem był netto pochłaniaczem CO₂ (okres sekwestracji węgla). Źródło: Ryc. 5, **Publikacja #2** (Dukat *i in.*, 2021).

3.3. Transpiracja i efektywność wykorzystania wody (WUE) lasów sosnowych w warunkach suszy.

Oba oszacowane strumienie transpiracji (z pomiarów przepływu soków indywidualnych drzew, przeskalowanych na cały drzewostan, T_{SF} i oszacowany na podstawie pomiarów metodą EC uśredniony dla całego ekosystemu, T_{EC}) porównano w różnych warunkach

higrotermicznych, w tym podczas ekstremalnej suszy. W okresie marzec-wrzesień 2019 r., który w nawiązaniu do publikacji 3# będzie odąd nazywany sezonem wegetacyjnym, łączna suma T_{SF} była niższa na powierzchni badawczej Mezyk (137 mm) niż Tuczno (189 mm), (Ryc. 6). Podobnie, wartość T_{EC} wyniosła 222 mm i 283 mm odpowiednio dla Mezyka i Tuczna. Zmierzone sumy ET również różniły się w zależności od miejsca badań (287 mm w Mezyku i 389 mm w Tucznie). Mimo to udział T_{EC} w całkowitym strumieniu ET był porównywalny dla obu lokalizacji i osiągnął 0.77 dla Mezyka i 0.73 dla Tuczna w sezonie wegetacyjnym. Stosunek transpiracji oszacowanej drugą metodą – przepływu soków – T_{SF}/ET stanowił jednak tylko 0.49 strumienia ET zarówno w młodym, jak i dojrzałym drzewostanie sosnowym (Ryc. 6). Chociaż sumy opadów w sezonie wegetacyjnym były prawie równe dla

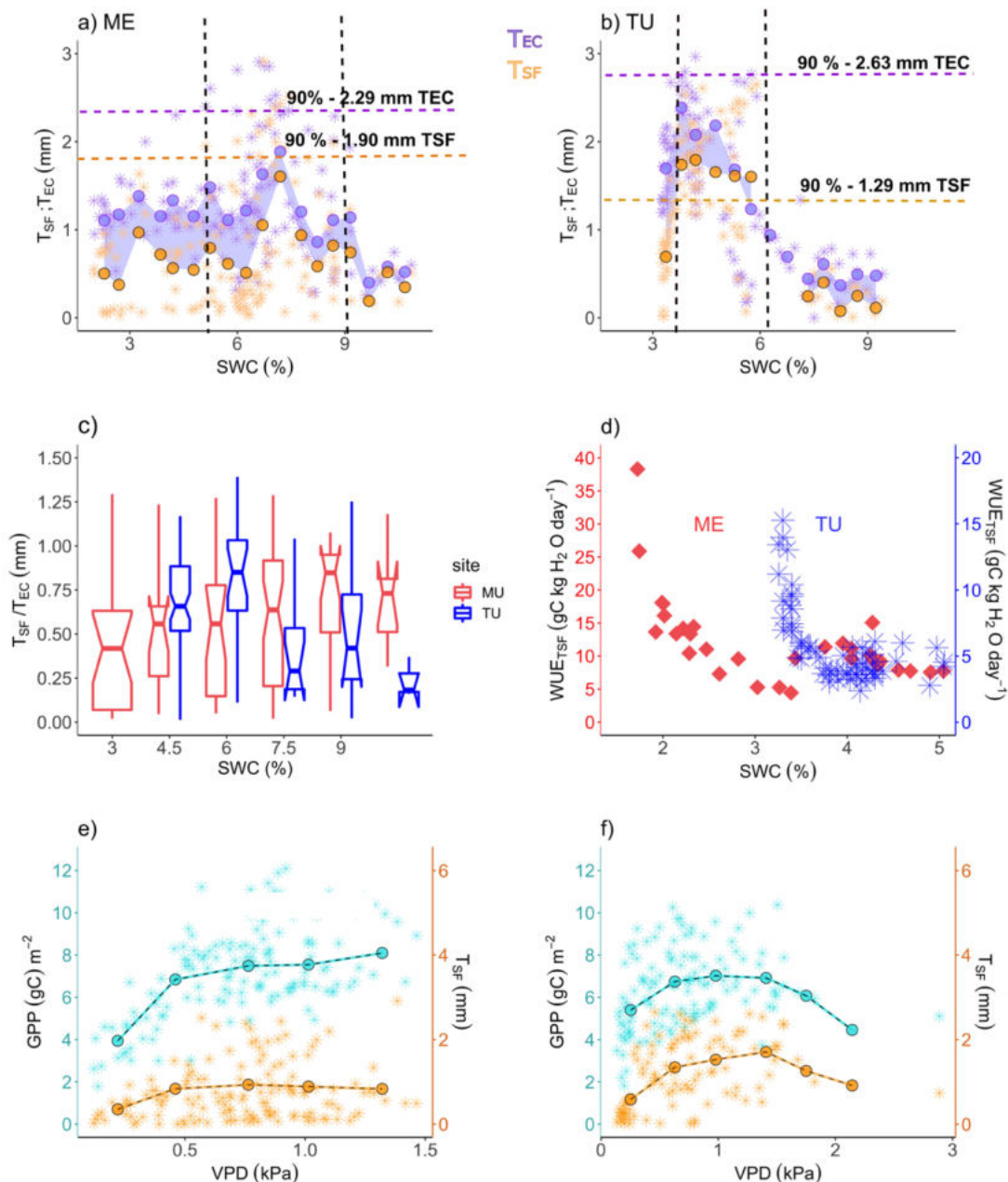


Rycina 6. Kumulowane krzywe składowych bilansu wodnego (WBC) w sezonie wegetacyjnym 2019 w Mezyku (ME - a) i Tucznie (TU - b) w tym: ewapotranspiracja (ET), transpiracja oszacowana metodą przepływu soków (T_{SF}), transpiracja obliczona na podstawie strumienia ET zmierzonego metodą kowariancji wirów (T_{EC}), ewaporacja ($E_{EC} = ET - T_{EC}$) i opad atmosferyczny (P). Wskaźniki T_{SF}/ET , T_{EC}/ET i T_{SF}/T_{EC} przedstawiają stosunki ich sumarycznych wartości w okresie wegetacyjnym (marzec-wrzesień). Dodatkowo, zmiany średnich dobowych wartości wilgotności gleby (SWC) przedstawiono na osi Y umieszczonej po prawej stronie. Źródło: Ryc. 4, **Publikacja #3** (Dukat *i in.*, 2023).

obu powierzchni badawczych, stosunek transpiracji do opadu - T_{SF}/P osiągnął 0.74 dla Mezyka i aż 0.95 dla Tuczna. Suma T_{EC} w obu przypadkach przekroczyła sumę opadów w sezonie wegetacyjnym w 2019 r. Odwrotnie było w przypadku opadów rocznych ogółem, co może wskazywać na konieczność wykorzystywania wody zmagazynowanej w pniu i glebie w cieplej porze roku (Ryc. 6).

Do wskazania wystąpienia suszy w skali dobowej wykorzystano pomiary wilgotności gleby/zawartości wody w glebie (SWC). Gdy w okresie letnim SWC na głębokości 10 cm w glebie (w poziomie mineralnym) spadała poniżej 3,5%, co miało miejsce zwłaszcza

w czerwcu i sierpniu w Mezyku oraz w lipcu, w Tucznie, różnice pomiędzy otrzymanymi wartościami transpiracji oszacowanymi dwoma metodami (T_{SF} i T_{EC}) znacznie się zwiększyły – zaobserwowano spadek wartości T_{SF} w odniesieniu do odpowiadających im wartości T_{EC} . Należy w tym miejscu przypomnieć, że oszacowana wartość T_{EC} obejmuje cały ekosystem, w tym również podszyt i runo leśne (o ile występują), podczas gdy T_{SF} reprezentuje transpirację tylko głównego gatunku drzew (sosny zwyczajnej). Mimo to, zarówno T_{SF} , jak i T_{EC} miały podobną dynamikę w odpowiedzi na zmieniające się warunki SWC. W celu określenia zakresu wilgotności gleby, dla których transpiracja była największa, ustalono próg, powyżej którego wartości T_{SF} i T_{EC} uznano za wysokie – 9 decyl z rozkładu wartości średnich dobowych T obliczonych dla okresu wegetacyjnego w roku 2019 (Ryc. 7a, b). Większość wartości wyższych niż 9 decyl dla obu strumieni T wystąpiła w podobnych warunkach SWC, co pozwoliło na wyznaczenie optymalnego dla tego procesu przedziału wartości wilgotności gleby na obu powierzchniach badawczych (Ryc. 7 a, b), które wynosiły: 5 – 9% dla powierzchni badawczej Mezyk i 4 – 6% dla Tucznie. Ponadto, dla tych samych wartości SWC stosunek pomiędzy T_{SF} i T_{EC} przyjmował zbliżone wartości na obu powierzchniach (Ryc. 8c). Efektywność wykorzystania wody (obliczona jako stosunek GPP do T_{SF} , reprezentującego transpirację głównego gatunku drzew) gwałtownie wzrastała poniżej wartości SWC= 4%. Wynikało to z faktu utrzymywania się intensywności procesu fotosyntezy (ilości pochłanianego CO_2 , GPP) na stosunkowo wysokim poziomie (Ryc. 7d) przy jednoczesnym ograniczeniu procesu transpiracji. Ten wzrost efektywności wykorzystania wody przy niskim SWC odzwierciedla strategię drzew polegającą na minimalizowaniu strat wody przy jednoczesnym utrzymaniu poziomu absorpcji CO_2 . Ponieważ intensywność parowania jest zwykle niska przy wysokim SWC (w opisywanych badaniach poziom powyżej 9%), ze względu na wysoką wilgotność względną i tym samym niską wartość deficytu ciśnienia pary wodnej (VPD), zaobserwowano spadek wartości tak T_{SF} jak i GPP (Ryc. 7e, f). Natomiast, przy wysokich średnich dobowych wartościach VPD (> 1 – 1,5 kPa) zaobserwowano spadek wartości T_{SF} i w mniejszym stopniu GPP w drzewostanie dojrzałym (TU), który nie był jednak widoczny w przypadku drzewostanu znacznie młodszego na powierzchni Mezyk. Pokazuje to, że chociaż oba procesy są sprzężone przez aktywność aparatów szparkowych, drzewa dostosowują się do warunków stresu wodnego i priorytetowo traktują oszczędzanie wody i utrzymanie asymilacji węgla.



Rycina 7. Związek pomiędzy wilgotnością gleby (SWC) a transpiracją wyznaczoną dwiema metodami: T_{SF} (pomarańczowy) i T_{EC} (fioletowy) na powierzchni badawczej a) Mezyk (ME) i b) Tuczo (TU); c) wykres pudełkowy przedstawiający stosunek T_{SF}/T_{EC} na różnych poziomach SWC (szerokość wyznaczonych klas = 1,8% SWC), w ME (czerwony) i TU (niebieski); d) związek pomiędzy wskaźnikiem wykorzystania wody (WUE_{TSF}) i SWC w ME (czerwony) i TU (niebieski) dla $SWC < 5,5\%$; e, f) zależność pomiędzy dziennymi sumami GPP, T_{SF} i VPD na powierzchniach badawczych ME i TU; jaśniejsze punkty reprezentują wszystkie wartości dziennych sum T i GPP; wyróżnione ciemniejszym kolorem punkty i linie reprezentują dane uśrednione w przyjętych klasach VPD; przerywane linie poziome (a, b) wskazują dziewiąty decyl (90%) średniej dziennej wartości transpiracji ekosystemu oszacowanej na podstawie pomiarów przepływu soków (T_{SF} - kolor pomarańczowy) i metodą kowariancji wirów (T_{EC} - kolor fioletowy). Źródło: Ryc. 8, **Publikacja #3** (Dukat *i in.*, 2023).

4. Podsumowanie

W związku z nasilającym się ociepleniem klimatu i wzmożoną antropopresją, konieczne jest monitorowanie nie tylko ekosystemów szczególnie wrażliwych, ale także tych, które do tej pory uważano za odporne. Rosnąca globalnie temperatura najprawdopodobniej spowoduje dalsze zwiększenie intensywności i częstotliwości występowania suszy i wynikające z tego zaburzenia w ekosystemach naturalnych. W **publikacji #1** wskazano, że w strefie klimatu umiarkowanego Europy należy spodziewać się wzrostu średniej temperatury powietrza i częstotliwości występowania zjawiska suszy (**cel szczegółowy 1**). Mając na względzie powyższy trend, zbadano, jak zjawisko suszy wpływa na zdolność drzewostanów sosnowych w polskich warunkach klimatycznych m.in. do sekwestracji węgla. Wykazano, że w suchym roku 2019 (następującym po jeszcze bardziej suchym 2018 roku), w związku z intensywną suszą, która wystąpiła zwłaszcza wiosną (kwiecień) i latem (czerwiec i sierpień), ilość węgla wbudowanego w biomasę drzew (NPP) w młodym drzewostanie sosnowym (Mezyk) była o około $0,6 \text{ t C} \cdot \text{ha}^{-1}$ niższa niż w umiarkowanie wilgotnym 2020 r. (**publikacja #2**). Można zatem stwierdzić, że wystąpienie suszy wpłynęło negatywnie na jedną z najważniejszych składowych bilansu węgla lasów z punktu widzenia gospodarki leśnej – ilość produkowanego drewna. Susza występująca w cieplej porze roku wiąże się z podwyższoną temperaturą i przedłużającym się okresem bezopadowym, a tym samym większą ilością docierającego promieniowania słonecznego. Teoretycznie, może się to zatem przełożyć na nieco wyższą wartość całkowitego GPP (ilość dwutlenku węgla zasymilowanego w wyniku fotosyntezy z uwagi na większą ilość promieniowania słonecznego) jak i wyższą wartość oddychania ekosystemu. Taki efekt zaobserwowano na badanych powierzchniach leśnych wykazując, że wartość GPP w suchym 2019 roku była nieco wyższa niż w 2020 roku. Jednakże, efektywność wykorzystania węgla (CUE) była w 2019 roku niższa niż w 2020 roku. Wartości CUE w obu latach były jednocześnie zaskakująco niskie – tak niskie, jak te obserwowane w lasach borealnych (De Lucia *i in.*, 2007). Można zatem stwierdzić, że badanie reakcji lasu sosnowego na niedobory wody w aspekcie obiegu wody i węgla na obszarze narażonym na susze, jest szczególnie ważne nie tylko dla rozwoju nauk z zakresu inżynierii środowiska, nauk o Ziemi, ale także dla ekonomii sektora leśnego (**cel szczegółowy 2**). Wynika to z faktu, że w Polsce struktura gatunkowa lasów jest zdominowana przez sosnę zwyczajną, która jest tym samym najważniejszym surowcem do produkcji drewna.

Znacznie większego wpływu suszy oczekiwano w odniesieniu do badanych elementów bilansu wodnego. Szczegółowym celem publikacji #3 było porównanie dwóch metod

oszacowania transpiracji na poziomie całego ekosystemu: opartej na bezpośrednich pomiarach relatywnie tanim systemem do badania przepływu soków pojedynczych drzew (T_{SF}) oraz uśrednionej wartości na poziomie ekosystemu, oszacowanym na podstawie bezpośrednich pomiarów zdecydowanie droższą i znacznie bardziej wymagającą metodycznie techniką kowariancji wirów (T_{EC}). Wartość transpiracji uzyskana w wyniku podziału strumienia ET (T_{EC}) przekroczyła sumaryczną wartość opadów w sezonie wegetacyjnym, co oznacza, że badane drzewostany musiały wykorzystywać wodę zmagazynowaną w glebie i pniu do przetrwania długotrwałych okresów suszy. Stwierdzono również, że najprawdopodobniej drzewa musiały mieć dostęp do wody zmagazynowanej w głębszych niż badane warstwach gleby (poniżej 2 m). Chociaż transpiracja jako proces była najprawdopodobniej podobnie wrażliwa na suszę w obu badanych drzewostanach sosnowych: relatywnie młodym - Mezyku i dojrzałym - Tucznie w suchym 2019 r., zaobserwowano wyraźnie większy spadek T_{SF} niż T_{EC} , gdy zawartość wody w glebie (SWC) była bardzo niska. Wynika to z faktu, że T_{EC} obejmuje cały ekosystem - w tym transpirację runa leśnego i podszytu, co nie zostało ujęte w T_{SF} . Efekt zamaskowania tych elementów mógł zatem odegrać istotną rolę. Jak można się było spodziewać, różnice pomiędzy tymi dwoma oszacowaniami była znacznie bardziej widoczna na powierzchni badawczej Tucznie, gdzie poza gatunkiem głównym występuje także podrost bukowy oraz znacznie bardziej rozwinięta i bioróżnorodna warstwa runa leśnego niż w Mezyku. Można zatem stwierdzić, że w przypadku lasów gospodarczych, które często są monokulturami bez drugiego piętra, transpiracja uzyskana na podstawie pomiarów przepływu soków jest wystarczająca do prawidłowego monitorowania i diagnozowania kondycji drzew i całego ekosystemu w warunkach suszy. Także, metoda ta jest znacznie szybsza w diagnozowaniu stresu wodnego niż obserwacje już zaistniałych skutków, jak na przykład zmiany fizjologiczne czy zamieranie drzew. Chociaż zarówno T_{SF} , jak i T_{EC} miały ogólnie podobną zmienność sezonową, dobową i miesięczną, a także podobne reakcje na zmiany czynników meteorologicznych, to dla niższych wartości SWC rozbieżności między T_{SF} i T_{EC} wzrosły zarówno dla młodego, jak i dojrzałego drzewostanu. Ponieważ zawartość wody w glebie mierzono w wierzchniej warstwie (w poziomie mineralnym), obserwacje wykazały niskie wartości wilgotności gleby w okresach bezopadowych. Niemniej jednak, pomiar ten został wykorzystany jako indykator suszy w skali dobowej, na podstawie którego stwierdzono, że dla niższego SWC (np. 3,5%) intensywność fotosyntezy była utrzymywana na względnie wysokim poziomie (GPP), tymczasem transpiracja (uzyskana na podstawie pomiarów przepływu soków - T_{SF}) była znacznie ograniczana w obu badanych ekosystemach leśnych. Jeden z końcowych wniosków w **publikacji #3** stwierdza, że funkcjonowanie sosny zwyczajnej

w czasie suszy odzwierciedla strategię drzew polegającą na minimalizowaniu strat wody na korzyść sekwestracji węgla, co zostało odzwierciedlone w znacznie zwiększonej efektywności wykorzystania wody (WUE) w tych warunkach. Dowodzi to wytrzymałości sosny zwyczajnej na okresowo występujący stres wodny. Kwestią otwartą pozostaje jednak wartość progowa tej odporności i skala czasowa trwania suszy, po przekroczeniu których dochodzi do zamierania drzew. Oznacza to, że w okresach deficytu wody i występowania suszy bieżące monitorowanie lasów pod kątem wykorzystania i dostępności wody prowadzone w sposób bezpośredni w czasie rzeczywistym, będzie miało coraz większe znaczenie nie tylko dla gospodarki leśnej, ale także lokalnego i globalnego bilansu węgla, wody i energii (**cel nadrzędny**).

5. Literatura

- Adams, H. D. *i in.* (2015) „Experimental drought and heat can delay phenological development and reduce foliar and shoot growth in semiarid trees”, *Global Change Biology*, 21(11), ss. 4210–4220. doi: 10.1111/gcb.13030.
- Beguéría, S., Vicente-Serrano, S. M. i Angulo-Martínez, M. (2010) „A multiscalar global drought dataset: The SPEI base: A new gridded product for the analysis of drought variability and impacts”, *Bulletin of the American Meteorological Society*, 91(10), ss. 1351–1356. doi: 10.1175/2010BAMS2988.1.
- Bezdan, J. *i in.* (2019) „SPEI-based approach to agricultural drought monitoring in Vojvodina region”, *Water (Switzerland)*, 11(7). doi: 10.3390/w11071481.
- Boczoń, A. i Wróbel, M. (2015) „The influence of drought on the water uptake by Scots pines (*Pinus sylvestris* L.) at different positions in the tree stand ”, *Forest Research Papers*, 76(4), ss. 370–376. doi: 10.1515/frp-2015-0036.
- Buras, A. *i in.* (2018) „Are Scots pine forest edges particularly prone to drought-induced mortality?”, *Environmental Research Letters*, 13(2). doi: 10.1088/1748-9326/aaa0b4.
- Cailleret, M. *i in.* (2017) „A synthesis of radial growth patterns preceding tree mortality”, *Global Change Biology*, 23(4), ss. 1675–1690. doi: 10.1111/gcb.13535.
- Clark, D. A. *i in.* (2001) „Measuring net primary production in forests: Concepts and field methods”, *Ecological Applications*, 11(2), ss. 356–370. doi: 10.1890/1051-0761(2001)011[0356:MNPPIF]2.0.CO;2.
- Dai, A. (2013) „Increasing drought under global warming in observations and models”, *Nature Climate Change*. Nature Publishing Group, 3(1), ss. 52–58. doi: 10.1038/nclimate1633.
- Dukat, P. *i in.* (2021) „Estimation of biomass increase and cue at a young temperate scots pine stand concerning drought occurrence by combining eddy covariance and biometric methods”, *Forests*. MDPI, 12(7). doi: 10.3390/f12070867.
- Dukat, P. *i in.* (2022) „Trends in drought occurrence and severity at mid-latitude European stations (1951–2015) estimated using standardized precipitation (SPI) and precipitation and evapotranspiration (SPEI) indices”, *Meteorology and Atmospheric Physics*. Springer, 134(1). doi: 10.1007/s00703-022-00858-w.
- Dukat, P. *i in.* (2023) „Scots pine responses to drought investigated with eddy covariance and sap flow methods”, *European Journal of Forest Research*. Springer Berlin Heidelberg. doi: 10.1007/s10342-023-01549-w.

- Farquhar, G. D., O'Leary, M. H. i Berry, J. A. (1982) „On the relationship between carbon isotope discrimination and the intercellular carbon dioxide concentration in leaves.”, *Australian Journal of Plant Physiology*, 9(2), ss. 121–137. doi: 10.1071/PP9820121.
- Gao, Y. *i in.* (2017) „Response of water use efficiency to summer drought in a boreal Scots pine forest in Finland”, *Biogeosciences*. Copernicus GmbH, 14(18), ss. 4409–4422. doi: 10.5194/bg-14-4409-2017.
- Gu, Chunjie *i in.* (2018) „Partitioning evapotranspiration using an optimized satellite-based ET model across biomes”, *Agricultural and Forest Meteorology*, 259(May), ss. 355–363. doi: 10.1016/j.agrformet.2018.05.023.
- Güney, A. *i in.* (2020) „Drought responses and their effects on radial stem growth of two co-occurring conifer species in the Mediterranean mountain range”, *Annals of Forest Science*, 77(4). doi: 10.1007/s13595-020-01007-2.
- Kunert, N. *i in.* (2019) „Understanding the controls over forest carbon use efficiency on small spatial scales: Effects of forest disturbance and tree diversity”, *Agricultural and Forest Meteorology*. Elsevier B.V., 269–270, ss. 136–144. doi: 10.1016/j.agrformet.2019.02.007.
- Lewis, S. L. *i in.* (2009) „Increasing carbon storage in intact African tropical forests”, *Nature*, 457(7232), ss. 1003–1006. doi: 10.1038/nature07771.
- Lloyd-Hughes, B. i Saunders, M. A. (2002) „A drought climatology for Europe”, *International Journal of Climatology*, 22(13), ss. 1571–1592. doi: 10.1002/joc.846.
- De Lucia, E. H. *i in.* (2007) „Forest carbon use efficiency: Is respiration a constant fraction of gross primary production?”, *Global Change Biology*, 13(6), ss. 1157–1167. doi: 10.1111/j.1365-2486.2007.01365.x.
- MALHI, Y. *i in.* (2009) „Comprehensive assessment of carbon productivity, allocation and storage in three Amazonian forests”, *Global Change Biology*, 15(5), ss. 1255–1274. doi: 10.1111/j.1365-2486.2008.01780.x.
- Martínez-Vilalta, J., Lloret, F. i Breshears, D. D. (2012) „Drought-induced forest decline: Causes, scope and implications”, *Biology Letters*, 8(5), ss. 689–691. doi: 10.1098/rsbl.2011.1059.
- Reichstein, M. *i in.* (2013) *CARBO-Extreme project brochure: The Terrestrial Carbon Cycle under Climate Variability and Extremes – a Pan-European Synthesis*. Jena. Dostępne na: http://www.carbo-extreme.eu/uploads/Main/News/C-Extreme_bro_med.pdf. 2014-03-20.
- Reichstein, Markus *i in.* (2013) „Climate extremes and the carbon cycle”, *Nature*, 500(7462), ss. 287–295. doi: 10.1038/nature12350.
- Riebeek, H. i Simmon, R. (2011) *NASA Earth Observatory*. Dostępne na:

<https://earthobservatory.nasa.gov/features/CarbonCycle>.

Schlesinger, W. H. i Jasechko, S. (2014) „Transpiration in the global water cycle”, *Agricultural and Forest Meteorology*. Elsevier B.V., 189–190, ss. 115–117. doi: 10.1016/j.agrformet.2014.01.011.

Spinoni, J. i in. (2019) „A new global database of meteorological drought events from 1951 to 2016”, *Journal of Hydrology: Regional Studies*, 22(October 2018). doi: 10.1016/j.ejrh.2019.100593.

Straka, T. J. i Layton, P. A. (2010) „Natural resources management: Life cycle assessment and forest certification and sustainability issues”, *Sustainability*, 2(2), ss. 604–623. doi: 10.3390/su2020604.

Vicente-Serrano, S. M. i in. (2012) „Performance of drought indices for ecological, agricultural, and hydrological applications”, *Earth Interactions*. American Meteorological Society, 16(10), ss. 1–27. doi: 10.1175/2012EI000434.1.

Vicente-Serrano, S. M., Beguería, S. i López-Moreno, J. I. (2010) „A multiscalar drought index sensitive to global warming: The standardized precipitation evapotranspiration index”, *Journal of Climate*, 23(7), ss. 1696–1718. doi: 10.1175/2009JCLI2909.1.

Vogt, J.V., Somma, F. (eds). (2000) „Drought and Drought Mitigation in Europe.”, *Kluwer Academic Publishers: Dordrecht, The Netherlands*, 336.

Zweifel, R. i in. (2010) „Link between continuous stem radius changes and net ecosystem productivity of a subalpine Norway spruce forest in the Swiss Alps”, *New Phytologist*, 187(3), ss. 819–830. doi: 10.1111/j.1469-8137.2010.03301.x.

Zweifel, R., Item, H. i Häslér, R. (2000) „Stem radius changes and their relation to stored water in stems of young Norway spruce trees”, *Trees - Structure and Function*, 15(1), ss. 50–57. doi: 10.1007/s004680000072.

6. Kopie opublikowanych prac wchodzących w skład rozprawy

6.1. Publikacja #1

Trends in drought occurrence and severity at mid-latitude European stations (1951–2015) estimated using standardized precipitation (SPI) and precipitation and evapotranspiration (SPEI) indices



Trends in drought occurrence and severity at mid-latitude European stations (1951–2015) estimated using standardized precipitation (SPI) and precipitation and evapotranspiration (SPEI) indices

Paulina Dukat¹ · Ewa Bednorz² · Klaudia Ziemblińska¹ · Marek Urbaniak¹

Received: 9 March 2020 / Accepted: 2 January 2022
© The Author(s) 2022

Abstract

One of the negative consequences of climate change is the also increase in the severity, frequency and length of droughts appearing in Europe. The effects of meteorological drought are often substantial, not only for the natural environment but also for humans. Hence, the main purpose of this research was to determine the trends in the severity and occurrence of droughts in Europe during the period 1951–2015 using the standardized precipitation index and the standardized precipitation and evapotranspiration index (SPEI). For six European sites located in mid latitudes, the number of dry months was determined and the trend of their occurrence was examined. Moreover, for the summer months in which the indicators fell below 0, the trend related to the severity of the drought was determined for each site. Despite the absence of a statistically significant trend of an increase in the occurrence of dry months in general, an increase in the severity of droughts occurring in summer was observed for the SPEI over a 6-month scale for all the investigated stations. The highest number of dry months since the 1970s appeared during the last 5 years of analysis.

1 Introduction

The 2009 report of the European Environment Agency (Collins et al. 2009) on the water resources in Europe stated that the relationship between the demand and availability of water has reached a critical point in many parts of the continent as a result of both excessive consumption of water and prolonged droughts. This has led to harmful effects on the functioning of freshwater ecosystems, such as decreases in the water levels of lakes and river flow as well as a reduction in the total surface area of wetlands, which is particularly important for the existence of local fauna. These effects are also accompanied by deterioration in water quality due to the

reduction of water resources. Climate changes will most certainly lead to further serious problems with water availability in the future and there will be more frequent and intense episodes of drought throughout Europe (Collins et al. 2009).

Drought is a natural event that occurs in all climates and is one of the most severe natural hazards that causes significant economic, social and environmental losses (Vogt and Somma 2000). At the end of the twentieth century and the beginning of the twenty-first century, significant parts of Europe were affected by drought (Lloyd-Hughes and Saunders 2002); in particular, the latter severe and prolonged droughts revealed the sensitivity of European ecosystems to this natural disturbance which was further intensified by human activities, such as disruption of the hydrological cycle by deforestation or improper drainage. More frequent occurrences of drought made the inhabitants of the European continent and the governments realize the risk of the many socioeconomic problems associated with water shortages, which resulted in activating a search for appropriate methods to mitigate the effects of drought. In the past 60 years, an increase in the frequency, duration, and intensity of droughts has already been observed in western, central, and south-eastern Europe (Spinoni et al. 2016). Along with the changing climate, this trend is likely to strengthen further in the twenty-first century. In Europe in the period from 1976 to

Responsible Editor: Stephanie Fiedler.

✉ Paulina Dukat
paulina.dukat05@gmail.com

¹ Meteorology Lab, Department of Construction and Geoengineering, Faculty of Environmental Engineering and Mechanical Engineering, Poznań University of Life Sciences, Piątkowska 94, 60-649 Poznań, Poland

² Climatology Department, Adam Mickiewicz University in Poznań, Bogumiła Krygowskiego St. 10, 61-680 Poznań, Poland

2006, economic losses related to drought were estimated at approximately 100 million euros (Vogt et al. 2011).

Different definitions of meteorological drought have been presented and used by authors depending on the scope and purpose of their research. For the present study, the definition of drought proposed in the IPCC report (Seneviratne et al. 2012a, b) was adopted. According to this definition, drought is a period of abnormally dry weather long enough to cause a serious hydrological imbalance. Thus, a period of anomalously low rainfall is defined as a meteorological drought. Water shortage, during the growing season, leads to the occurrence of an agricultural drought (due to the lack of moisture in the soil), while the reduction of water resources is defined as a hydrological drought (Seneviratne et al. 2012a, b). In addition to low rainfall, the occurrence of drought is associated with an increase in the actual rate of evapotranspiration. Lack of rainfall is the first factor favoring the occurrence of a meteorological drought, with this phenomenon enhanced by the potential increase in evapotranspiration reinforced by radiation, higher wind speed, and water vapor deficit due to temperature rises (Seneviratne et al. 2012a, b). It is now assumed that global warming and its regional aspects are one of the factors increasing the frequency of anomalous weather phenomena (IPCC 2001). Therefore, understanding the regional causes and the features of meteorological drought is important when investigating and understanding its specific impact (Trnka et al. 2016).

The variability of drought conditions can be assessed along with climatic changes using the standardized precipitation index (SPI), which uses precipitation totals only and thus can be used anywhere by simply transforming its skewed distribution to a normal distribution (Tsakiris and Vangelis 2005). The main advantage of the SPI is its simplicity, wherein the main disadvantage is the use of only one meteorological element to describe water deficit. This index has been used by many authors for the analysis of drought occurrences in Europe (Blain 2011; Krajcinović 2010; Livada and Assimakopoulos 2007; Lloyd-Hughes and Saunders 2002), and in the United States (Hayes et al. 1999) where this index calculation method was developed (McKee and Nolan 1993, 1995). Since the input variable for the SPI is precipitation, rainfall increases or decreases will likely result in a wetting or drying tendency for the SPI, respectively. Nevertheless, in some countries rainfall variability plays a more important role than the average change: Poland is an example of a country where the SPI over a 12-month scale shows a slight wetting tendency despite a general decrease in precipitation (Spinoni et al. 2019). On the contrary, for small countries such as Oman or Tajikistan, where dry and semi-dry areas predominate, the results of SPI-12 calculations suggest a tendency toward drying, despite a slight increase in precipitation, so the SPI calculations may be biased.

The standardized precipitation evapotranspiration index (SPEI) is based on precipitation and potential evapotranspiration data (Vicente-Serrano et al. 2010), which, in principle,

is a modification of the standardized precipitation index to include the impact of temperature. The SPEI, similarly to the SPI, is one of the most widely used drought indicators in Europe (Spinoni et al. 2015). Due to the fact that the SPEI includes the potential evaporation factor (PET), it is recommended especially as an indicator for monitoring agricultural drought. In principle, PET can be calculated using more or less complex models/equations, e.g. Thornthwaite (TH), FAO-56 Penman–Monteith (PM), Hargreaves–Samani (HG) (Bezdan et al. 2019) but simultaneously this is its biggest disadvantage. The Thornthwaite (TH) method is the simplest way to calculate potential evapotranspiration due to the factors used, which are easily accessible—average air temperature for the investigated period and the latitude of the location. Significant differences were found when the SPEI was calculated using different PET equations wherein the differences were bigger in semi-arid and mesic areas (Beguería et al. 2014).

1.1 Hypotheses and aims

Appropriate recognition of the climate features related to occurrences of drought in the past is crucial. In addition, proper monitoring and development of drought mitigation strategies using appropriate tools, including indicators, are required. Drought can be identified based on various variables depending on data availability. Thus, one of the most desirable tools for determining drought in the future and its subsequent mitigation is a method based on easily accessible data, which includes air temperature and precipitation as key elements. It is expected that there would be an increasing trend in the occurrence of drought, determined with the help of both the selected indicators. Climate change is visible, inter alia, by increasing global air temperature and changing precipitation distribution. We hypothesize that this can lead to an increase in the occurrence of drought, also in those parts of Europe for which this has not been a characteristic climate feature. Our main aim is thus to define trends in the frequency and severity of drought events for mid-latitude European countries using data from six meteorological stations located in this region covering both marine and continental temperate climate conditions.

2 Materials and methods

2.1 Data

For the meteorological station in Warsaw, data were obtained from the Institute of Meteorology and Water Management—National Research Institute, while for all other stations this was obtained from the Home European Climate Assessment & Dataset portal (ECAD 2018). Average daily values of

temperature and precipitation totals were used to calculate mean monthly air temperatures and monthly precipitation totals, respectively, which were then used to calculate the selected indices.

2.2 Site descriptions

The meteorological stations selected for the analysis are located in the mid latitudes of the European continent (Fig. 1). On the basis of the Köppen Geiger classification (Kottek et al. 2006), stations in Essen (Germany, 150 m above sea level [a.s.l.]), Berlin (Germany, 48 m a.s.l.), Pécs (Hungary, 203 m a.s.l.), and Warsaw (Poland, 110 m a.s.l.) were categorized as areas with a moderate warm and humid climate with an average temperature lower than 18 °C and higher than −3 °C in the coldest month (Cfb). The stations in Kiev (Ukraine, 166 m a.s.l.) and Moscow (Russia, 156 m a.s.l.) were categorized under the Dfb class, which is characterized as a snow-forest climate (boreal) with the coldest month having an average air temperature below −3 °C and the warmest month having a temperature higher than 10 °C

(Kozuchowski et al. 2012; Woś 2010). Long-term average air temperatures and the average precipitation totals for each site are shown in Table 1. Among the investigated stations, the highest long-term average annual temperature calculated for the period 1951–2015 occurred in Pécs, which was equal to 10.8 °C, while the lowest temperature occurred in the station in Moscow, which was 5.3 °C (Fig. 2, Table 1). The highest average annual precipitation total was measured in Essen (923 mm), while the lowest, estimated to be only 521 mm, was recorded in the station in Poland. At all the stations, the highest precipitation occurred in the summer months: in June in Essen, Berlin and Moscow and in July in Pécs, Warsaw and Kiev (Fig. 2). From the perspective of climate type analysis, determined by means of the two meteorological elements (temperature and precipitation) on a monthly basis, it was evident that not only is the total precipitation value significant but also its distribution throughout the year. The standard deviation of the total monthly precipitation from the annual mean for the entire period (1951–2015) was the highest in Essen and Pécs. Lower values were found for the stations in Warsaw (31) and Berlin (30) (Table 1).

Fig. 1 Locations of the meteorological stations in Europe included in the research

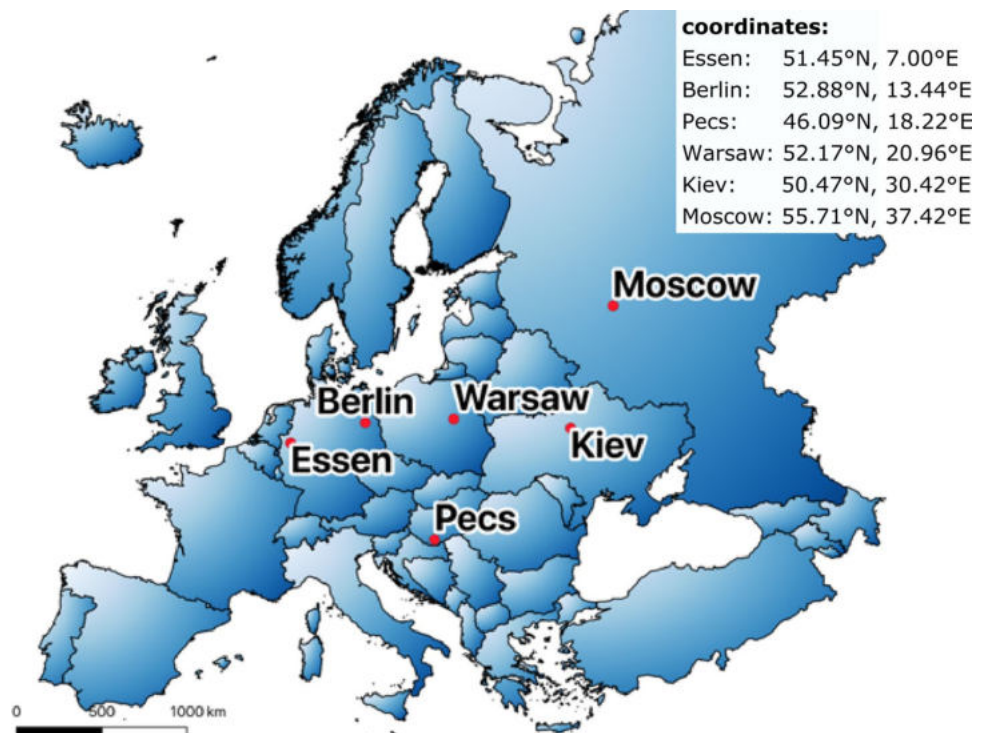


Table 1 Mean annual precipitation total (P) (mm) and mean annual air temperature (C) for each station included in the research, SD—standard deviation from the period 1951–2015

| | ESSEN | BERLIN | PÉCS | WARSAW | KIEV | MOSCOW |
|--------------------------------------|-------|--------|-------|--------|------|--------|
| Mean annual precipitation total (mm) | 923 | 580 | 644 | 521 | 628 | 680 |
| Annual P SD | 144 | 98 | 129 | 94 | 116 | 116 |
| Monthly P SD | 38 | 30 | 38 | 31 | 37 | 33 |
| Mean annual air temperature (°C) | 9.87 | 9.69 | 10.79 | 8.15 | 8.11 | 5.32 |

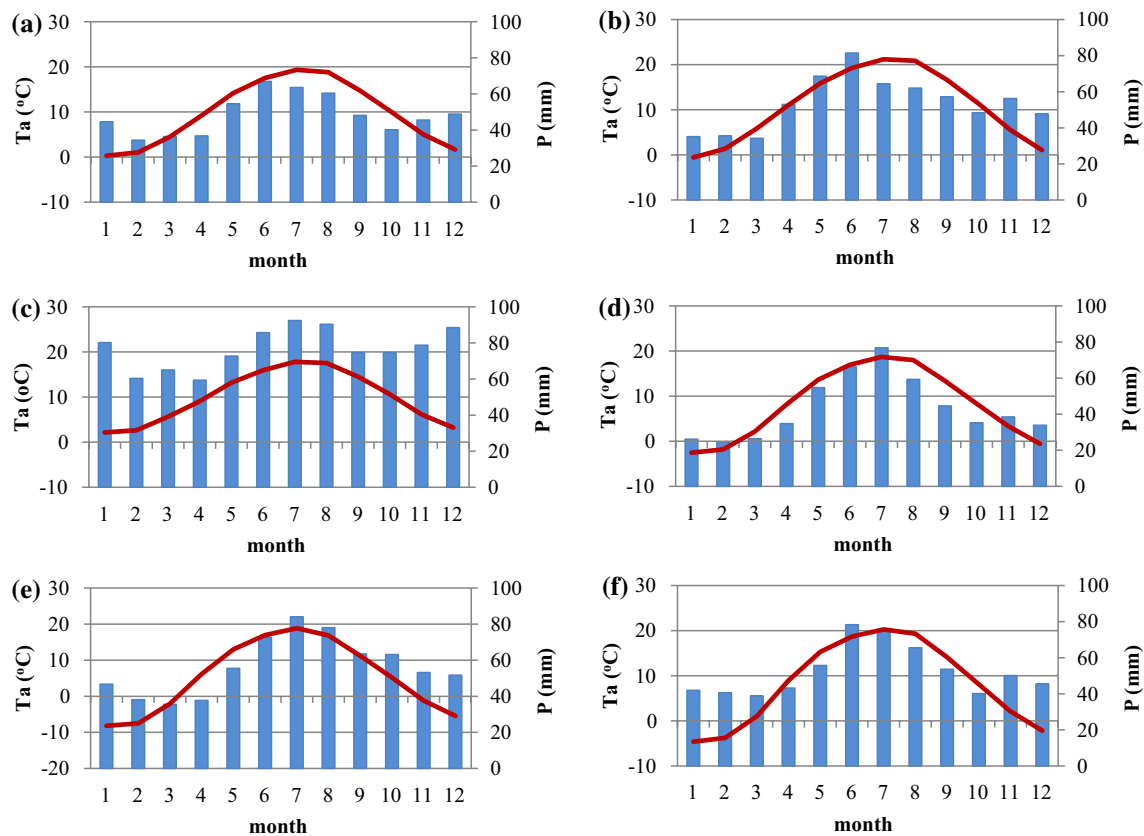


Fig. 2 Climatograms for **a** Essen, **b** Berlin, **c** Pécs, **d** Warsaw, **e** Kiev, and **f** Moscow, based on the data from the period 1951–2015. T_a average monthly air temperature ($^{\circ}\text{C}$) (red line), P monthly precipitation totals (mm)

2.3 Methods

To determine the number of dry months in the analyzed period at each station, two indicators were used: SPI and SPEI. The SPI is calculated by fitting a probability density function to a given frequency distribution of historical precipitation (Faye et al. 2019) and then the probabilities are transformed into a normalized distribution with a mean equal to zero and a variance of one, which was developed by McKee and Nolan (1993, 1995). Originally, the SPI was calculated for 1-, 2-, 3-, 6-, 12-, 24-, 36-, and 48-month scales to recognize the different impacts, but in general this index can be calculated for any weekly or monthly timescale (Hayes et al. 2012). Because the SPI is normalized based on the statistical representation of historical records in each location separately, drought conditions can be recognized equally well for both humid and drier climate conditions. In addition, it can be used for assessing the severity of the drought and to issue warnings regarding the possibility of it occurring. The method to derive the SPEI index is based on the original SPI calculation procedure but

includes an additional variable, i.e. potential evapotranspiration. It is recommended considering the thermal factor (here indirectly by the inclusion of PET in SPEI index), especially for applications such as the analysis of future climate scenarios which is useful for studying the effects of global warming and drought (Beguería et al. 2010; Vicente-Serrano et al. 2010).

Here, in order to calculate the SPEI index, the potential evapotranspiration was estimated according to the Thornthwaite equation (Thornthwaite 1948) (Eq. 1), which is part of the package “SPEI” in R software (version 3.5.0; The R Foundation for Statistical Computing, 2018/04/23). The variables used in the PET calculations presented below are the monthly precipitation totals, monthly mean air temperature and the latitude of the station’s location. The exact methodology for calculating the SPEI has been presented by Vicente-Serrano et al. (2010).

$$\text{PET} = 16K \left(\frac{10T}{I} \right)^m, \quad (1)$$

where: T is the mean monthly temperature ($^{\circ}\text{C}$); I is the heat index, which is calculated as the sum of the 12 monthly index values i according to the following formula:

$$i = \left(\frac{T}{5}\right)^{1.514}, \quad (2)$$

K is a correction coefficient computed as a function of the latitude and month (Vicente-Serrano et al. 2010) and m is a coefficient depending on I :

$$m = 6.75 \times 10^{-7} I^3 - 7.71 \times 10^{-5} I^2 + 1.79 \times 10^{-2} + 0.492. \quad (3)$$

Vicente-Serrano et al. (2010) concluded that log-logistic distribution is the best option among other distributions for obtaining an SPEI series in standardized z units (mean = 0, SD = 1). Therefore, for the purposes of this study, standardization of the meteorological variables was also carried out by using a log-logistic distribution. The probability distribution function of monthly precipitation (SPI) or the difference between precipitation and potential evapotranspiration for each month (SPEI) is given by the equation described, for example, by (Beguería et al. 2014):

$$F(D) = \left[1 + \left(\frac{\alpha}{D - \gamma}\right)^{\beta}\right]^{-1}, \quad (4)$$

where: α scale parameter, β shape parameter, γ location parameter, – all estimated from sample D , which for the SPEI is the difference between precipitation (P) and potential evapotranspiration (PET).

After calculating the α , β and γ parameters (the detailed methodology for calculating these is given by Singh et al. 1993), the unbiased probability weighted moments (PWMs) were calculated, based on a method described by Hosking (1986):

$$w_s = \frac{1}{N} \sum_{i=1}^N \frac{\binom{N-i}{s} D_i}{\binom{N-i}{s}}, \quad (5)$$

where w_s is the PWM of order s , N is the number of data and D_i is the difference between precipitation (P) and potential evapotranspiration (PET) for the month i . D_i is therefore the climatic water balance (CWB).

Beguería et al. (2014) have suggested that the unbiased PWM method should be preferred for the computation of an SPEI series. When the two indicators are both normalized variables (the average SPI and SPEI values are 0 and the standard deviation is 1) they can be compared with other SPI and SPEI values, computed for different times and locations. A zero value of SPI or SPEI corresponds to 50% of the cumulative precipitation probability (SPI) or Climatic

Water Balance probability (SPEI), according to the logistic distribution (Vicente-Serrano et al. 2010). Each index value corresponds to the characteristic of the analyzed period (month); positive values of the SPI and SPEI indicate wetter months while negative ones—dry periods. McKee and Nolan (1993) proposed the following SPI categorization for conditions in Colorado (Table 2), which was applied in the presented study.

To calculate the SPI and SPEI, R software was used, in particular the “SPEI” package (Beguería and Vicente-Serrano 2017a, b). Corresponding indicator values were calculated for 1-, 3- and 6-month scales since it was suggested that estimations of the occurrence of dry periods based on such time perspectives are appropriate for recognizing the impact of meteorological drought on agriculture (Rhee and Carbone 2010). Statistical calculations were determined using “base” and “ggplot” packages for preparing the figures. Drought occurrence, severity and trends have been analyzed using data outcome from SPEI package in R environment (R Core Team 2020).

3 Results and discussion

3.1 Temporal courses of climatic factors

Due to climate changes and multidirectional anthropopressure, it is important to analyze trends occurring in the climatic system on both a global and local scale. Nevertheless, it should be emphasized that in case of multi-year research on climate-related trends, even less statistically significance trends may already be relevant for the climatic system. Due to the length of the period covered by the presented analysis, long-term trends in key meteorological elements, namely average annual air temperatures, annual precipitation totals and potential evapotranspiration, have been calculated according to the methodology presented above (Thornthwaite 1948), as well as deriving the climatic water balance (the difference between the annual precipitation total and the potential evapotranspiration), and are presented below (Fig. 3, Table 3).

Table 2 Classification of the months based on SPI index values (source: Hayes et al. 1999 after McKee and Nolan 1993), also applicable for the SPEI index (Faustin Katchele et al. 2017; Wang et al. 2020)

| | |
|----------------|------------------|
| Extremely dry | < – 2.0 |
| Severely dry | – 1.99 to – 1.50 |
| Moderately dry | – 1.49 to – 1.00 |
| Near normal | – 0.99 to 0.99 |
| Moderately wet | 1.00 to 1.49 |
| Very wet | 1.50 to 1.99 |
| Extremely wet | > 2.00 |

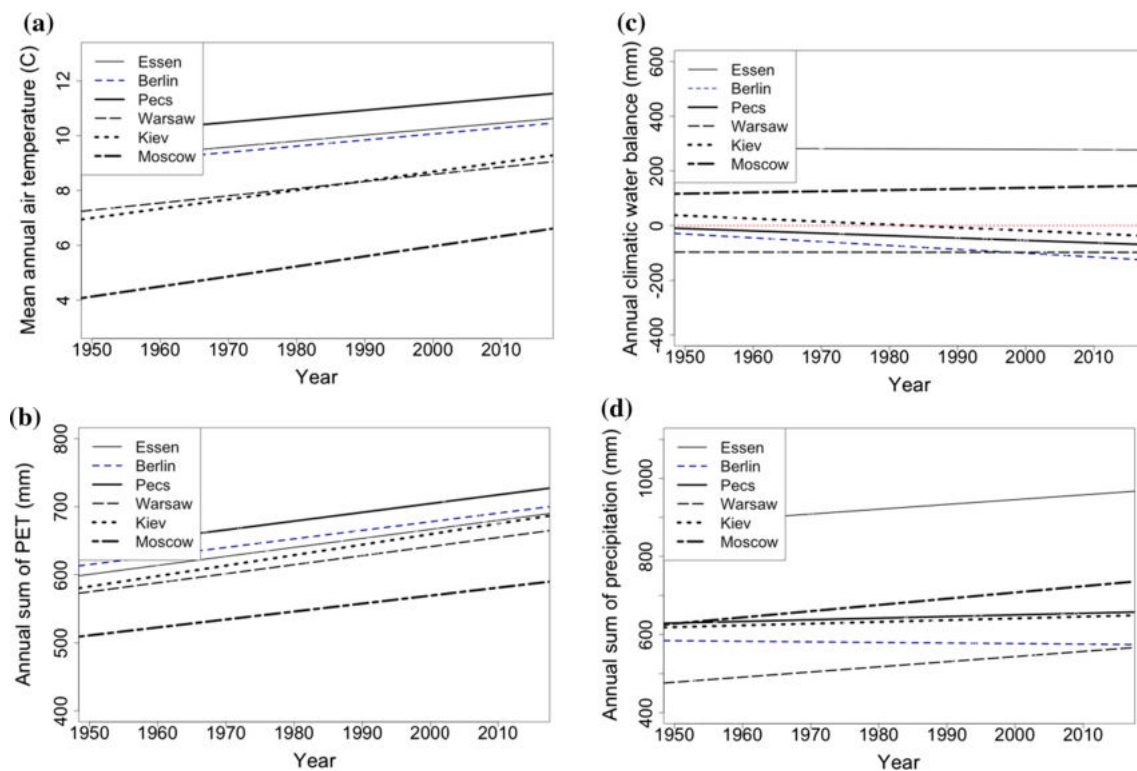


Fig. 3 Long-term trends of average annual air temperatures (a), annual potential evapotranspiration totals (b), annual climatic water balance totals (c), and annual precipitation totals (d), for all the investi-

gated European meteorological stations. The red dotted line in plot c represents the balance = 0 between precipitation and PET

Table 3 Simple linear regression parameters fitted to the long-term data for the annual potential evapotranspiration (PET) total, the mean annual air temperature (T) and the annual precipitation total (PREC) presented in Fig. 3

| | PET R^2 | PET a | $T R^2$ | $T a$ | PREC R^2 | PREC a |
|--------|-----------|---------|---------|-------|------------|----------|
| ESSEN | 0.312 | 1.325 | 0.260 | 0.022 | 0.010 | 1.228 |
| BERLIN | 0.278 | 1.257 | 0.233 | 0.022 | -0.015 | -0.145 |
| PÉCS | 0.259 | 1.288 | 0.242 | 0.022 | -0.012 | 0.420 |
| WARSAW | 0.308 | 1.330 | 0.272 | 0.026 | 0.056 | 1.316 |
| KIEV | 0.333 | 1.540 | 0.360 | 0.034 | -0.011 | 0.445 |
| MOSCOW | 0.254 | 1.168 | 0.395 | 0.037 | 0.053 | 1.596 |

R^2 coefficient of determination, calculated using Pearson's correlation, a linear regression slope; significance level $\alpha=0.005$

The performed analyses revealed that there is a positive trend for the average annual air temperature (Fig. 3a) and potential evapotranspiration (Fig. 3c) at all the stations included in this research. It turned out that during the last 60 years, the average annual air temperature has risen fastest in Moscow and Kiev. Simultaneously, the Russian station

was also one of the two locations where the most significant positive trend of annual precipitation totals has been recorded. A negative trend of precipitation, even though quite insignificant in terms of its impact, was determined only for the Berlin meteorological station, and thus the annual amount of precipitation in that location can be expected to decrease in the future.

There were no statically significant trends in the long-term climate water balance for any of the chosen European stations, therefore the corresponding parameters for the linear regression in this case are not shown in Table 2. Nevertheless, these trends are still shown in Fig. 3d, because this gives an idea of where to place particular stations in accordance with the threat of shrinking water resources ($CWB < 0$ —too little precipitation to balance potential evapotranspiration).

4 Long-term changes in the number of droughts

The long-term (1951–2015) values of the SPI and SPEI indexes over 1-, 3-, and 6-month scales for all the stations are presented in the Figs. 8, 9, 10, 11, 12, 13 in Appendix 1. For Essen and Berlin, the analysis performed at 6-months revealed that according to both SPI and SPEI, in recent years (especially until the middle of the 2010–2015 pentad), the dominance of values below zero, suggesting a deviation toward dry conditions, is clearly visible. Certain cyclical deviations on this timescale were also recognized, with other periods of dry months in Germany, identified by both indicators. That conditions have been recognized at the beginning of the analyzed period: the 1950s, longer culmination in 1960 and before 1965, in Essen especially between 1970 and 1975 and before 1990, in Berlin after 1990 and especially in 2015. For these sites, much wetter months were indicated in the 1980s and additionally for Essen at the beginning of the twenty-first century. In Pécs, analysis of the SPI values estimated over the same timescales allowed four especially dry periods to be distinguished: between 1955 and 1960, at the beginning of 1970, 1990 and also in 2011–2012. Meanwhile, according to the SPEI, assessment of the occurrence of dry conditions was generally similar to the SPI, but the increasing duration of dry months in 2011–2013 was much more pronounced. For Warsaw, both indicators show, over a 6-month timescale, drought periods at the beginning of the 1950s, before 1965, after 1975, at the beginning of the 1990s and at the end of the last pentad. On the other hand, during 1970–1975, in the early 1980s and the beginning of the last decade, the conditions were more humid in the Polish station. In Kiev, particularly long dry periods occurred during the 1955–1965 period and after 1975, according to both indicators. According to the SPI, the year 2015 and, according to the SPEI, the last five years were characterized by drier conditions in comparison with

all other years. In Moscow, unusually long dry periods determined by both indicators over a 6-month timescale occurred in 1960–1965 and then for 1995–1997. During the last 20 years, the values of the SPEI index suggest the occurrence of much drier conditions in 2010–2012 and in 2015, similarly to that estimated using the SPI, although with higher severity. Despite the quite large dispersion of the stations in the mid latitudes of Europe, similar fluctuations/periodicity were noticeable among all the investigated locations. In general, both indicators suggested that dry periods occurred mostly at the beginning and at the end of period covered by the analysis.

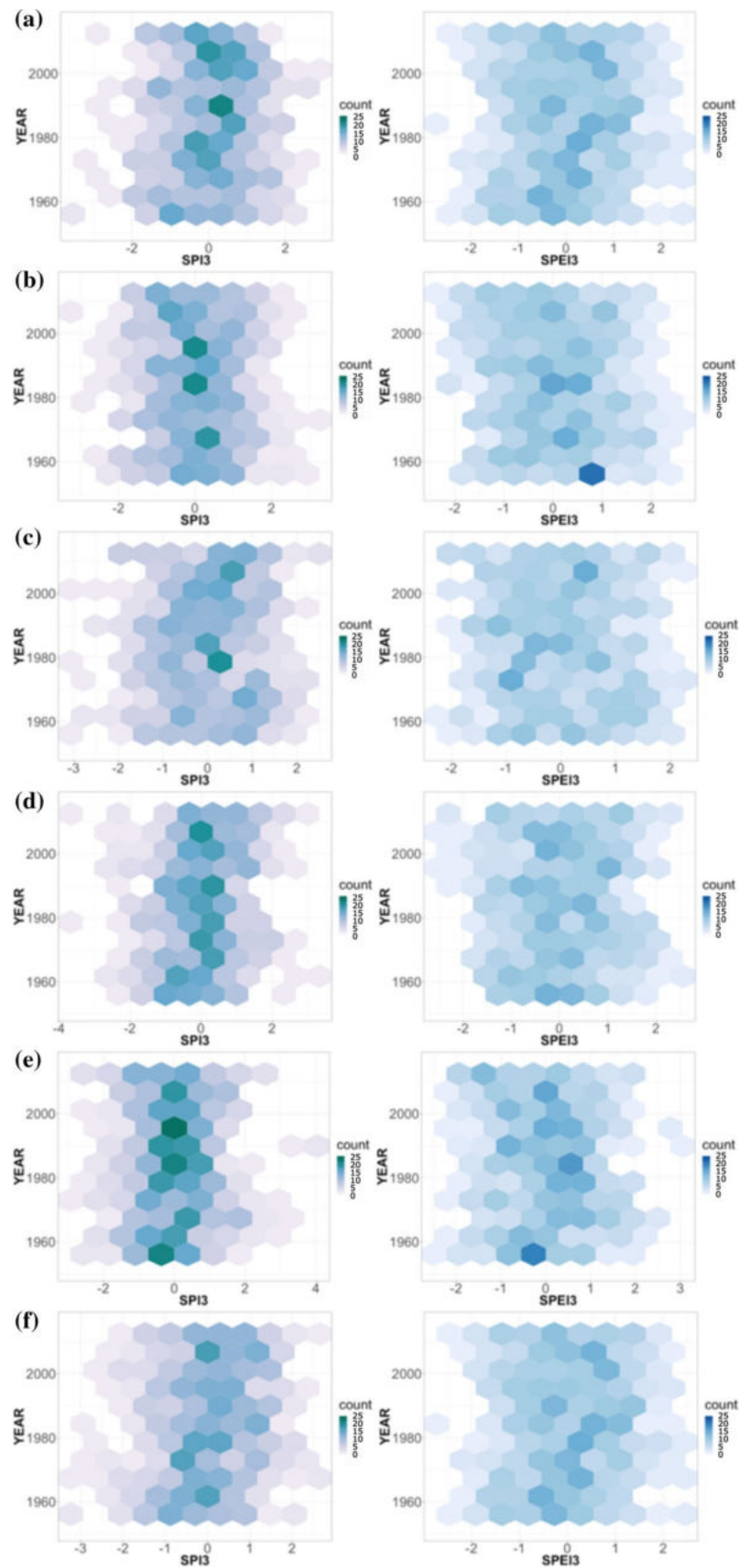
Using the 3-month SPI and SPEI index values, surface plots were created by dividing the plane into regular hexagons. Then, the number of observations in each hexagon was counted and finally mapped to fill the hexagons (Fig. 4). Such a graphical presentation of the results allows, for example, during the long-term period when the indicators were spread over a wider spectrum of values, to show whether and when the number of occurrences shifted toward negative values.

Compared to the other stations, Kiev had the largest concentration of values around 0, according to the SPI index. In Berlin and Warsaw, during the most recent years, the distribution of the SPEI index has moved to more negative values, which means drier conditions. In Moscow, the number of occurrences of extremely dry months (SPEI index values close to -2) is also currently increasing compared to previous years, and approaching the value from before the 1960s. The irregular shapes obtained for the SPI index show, as previously stated, similarly irregular distributions for the precipitation factor. In Essen and Berlin, however, an increase in the severity of drought conditions in recent years can already be seen. Only in case of Moscow does the SPI index show an increase in the number of months characterized by wetter conditions, which most likely resulted from a similar long-term precipitation trend (Fig. 3b). For Pécs and Warsaw, broadening of the spectrum of SPEI index values has been found. This is associated with a flattening of the SPEI density distribution, which is the anticipated consequence of climate change—an increase in the number of extreme events.

4.1 Trends in the occurrence of drought

In the following section, trends in the occurrence of drought in the six different locations with a temperate climate on the continent of Europe covered by the analysis were determined. All the months in which the SPI and SPEI indexes

Fig. 4 Distribution of the SPI (on the left) and SPEI (on the right) values for a 3-month scale presented on hexagonal surface plots for the six European meteorological stations: **a** Essen, **b** Berlin, **c** Pécs, **d** Warsaw, **e** Kiev, and **f** Moscow



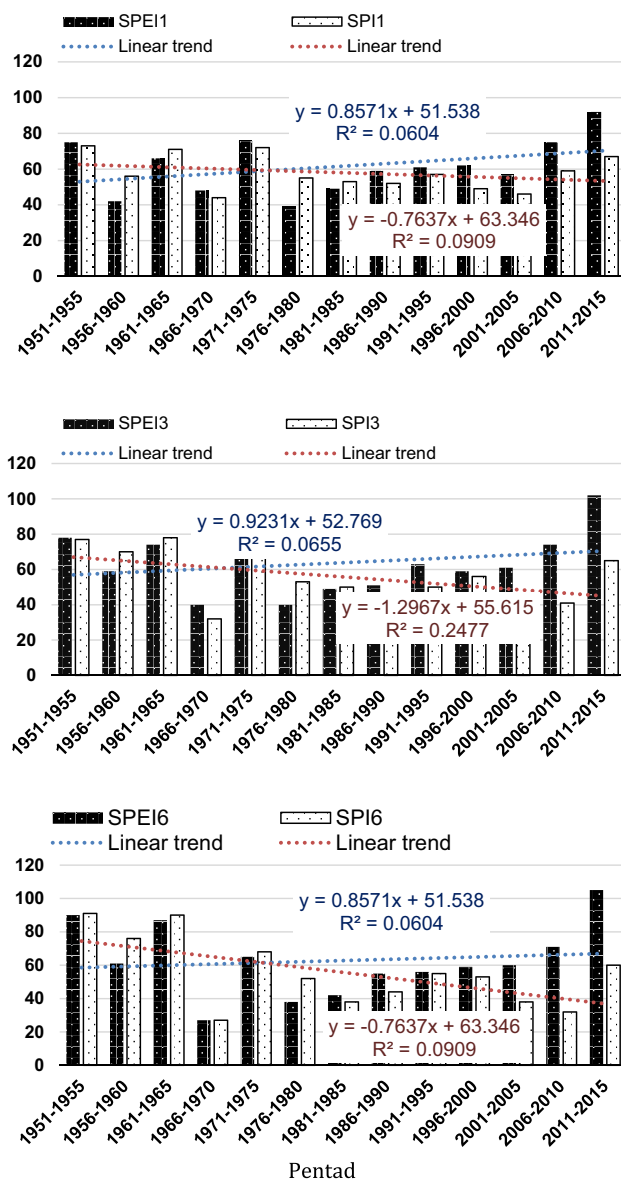


Fig. 5 Number of months in which the SPEI and SPI, calculated at 1-, 3- and 6-month timescales, fell below -1.00 . The figures given by the bars are the total numbers of dry periods in the pentads for all stations

fell below -1 were added up for each site, which according to the classification (McKee and Nolan 1993) means drought-representative conditions (see Table 2). In order to show trends, the analyzed period was divided into pentads (Fig. 5). According to both indicators for all timescales (1-, 3- and 6-month perspectives), there are, in general, three

periods in which the number of droughts in relation to the other 5-year periods was higher. For the SPEI index, these periods were: 1951–1956, 1961–1966 and 2010–2015 for all timescales, and additionally for the 1-month timescale during 1971–1976. Moreover, it should be emphasized that such presentation of the obtained results (aggregation of all the dry months from all the stations during 5-year periods) helps to show that there is a slight negative linear trend in the SPI index for all the timescales, which suggests a decrease in the number of droughts in the analyzed region. Analyzing the data on a monthly basis due to the large number of droughts in 1951–1966 (SPI), we found a lack of statistically significant trends in the occurrence of dry months within the studied period, which very likely has a large impact on the linear trend estimation. On the contrary, the SPEI index indicates an upward trend in drought occurrence regardless of the timescale. The most pronounced upward trend was found for the SPEI for a 3-month timescale. The possible explanation might already be in the increasing trend of the potential evapotranspiration totals in this part of Europe (Fig. 3). Figure 5 shows that in the last pentad (2011–2015) there were more dry months than in any other periods since 1976 as indicated by both the SPI and SPEI. For the SPEI for all three timescales, the number of droughts recorded in the last five years of the analyzed period significantly exceeded the earlier occurrences of this phenomenon.

4.2 Trends in drought severity

Index values below -1 , according to the adopted classification for the SPI and SPEI indices, detect the beginning of moderately dry conditions, which was the threshold used to estimate drought occurrence trends in the previous chapter. Whereas drought severity trends were derived by subtracting all negative SPEI and SPI index values from 0 for each station, which designates all drier than normal conditions in the chosen period. Afterwards, linear trends were calculated for both drought indicators at 1-, 3- and 6-month timescales, which, as they approach lower, negative values, indicate an increase in the severity of the drought (Fig. 6). Detailed information on these linear regression parameters is not presented here since they had very low values and were not statistically significant. An increasing trend in the severity of droughts for the SPEI and SPI indicators in the summer was recognized for the 1-month timescale in Essen, Berlin and Pécs, while in Essen and Berlin the upward trend of the SPEI was much more pronounced in comparison with

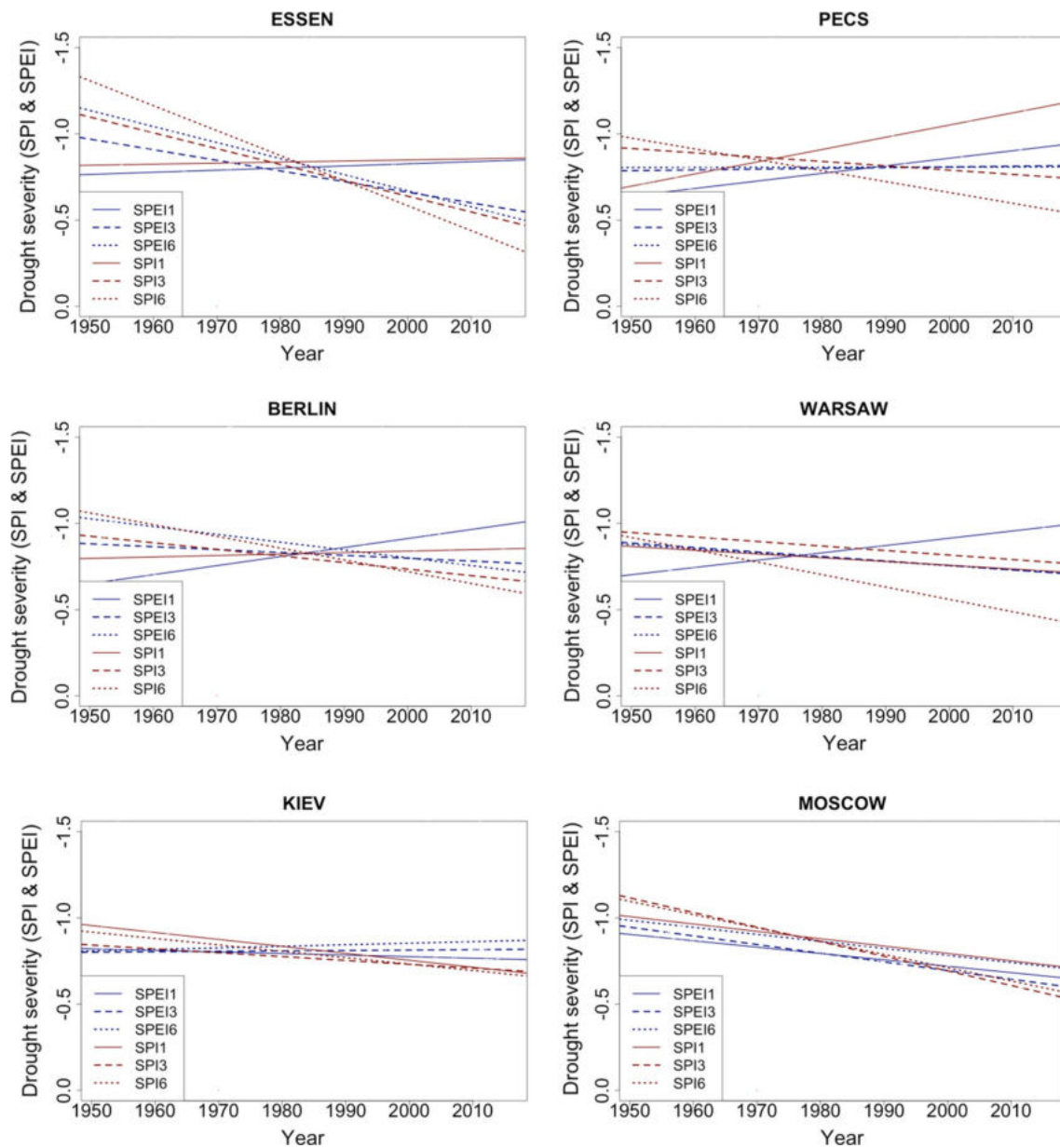


Fig. 6 Trends in drought severity for all stations included in the analysis. The lower the indicator value, the higher the severity of the drought

Pécs. In Kiev, a weak increasing trend of drought severity appeared for the SPEI for the 3- and 6-month timescales. In Warsaw, however, the increase in drought severity was pronounced only for the SPEI index for the 1-month timescale. The most consistent results were obtained for Moscow—all trend lines had similar courses with positive slopes for both the SPI and SPEI for all timescales, which suggests that there is a persistent tendency toward wetter conditions.

Considering that in Central and Eastern Europe droughts are the most dangerous for crops and other vegetation as well human wellbeing in the summer, similar linear trends of drought severity for June to August were investigated (Fig. 7, Table 4). This analysis included only the SPEI index calculated for the 3-month timescale since temperature plays a crucial role in the summer, and the “severity analysis” for the indicator based on precipitation only (SPI)

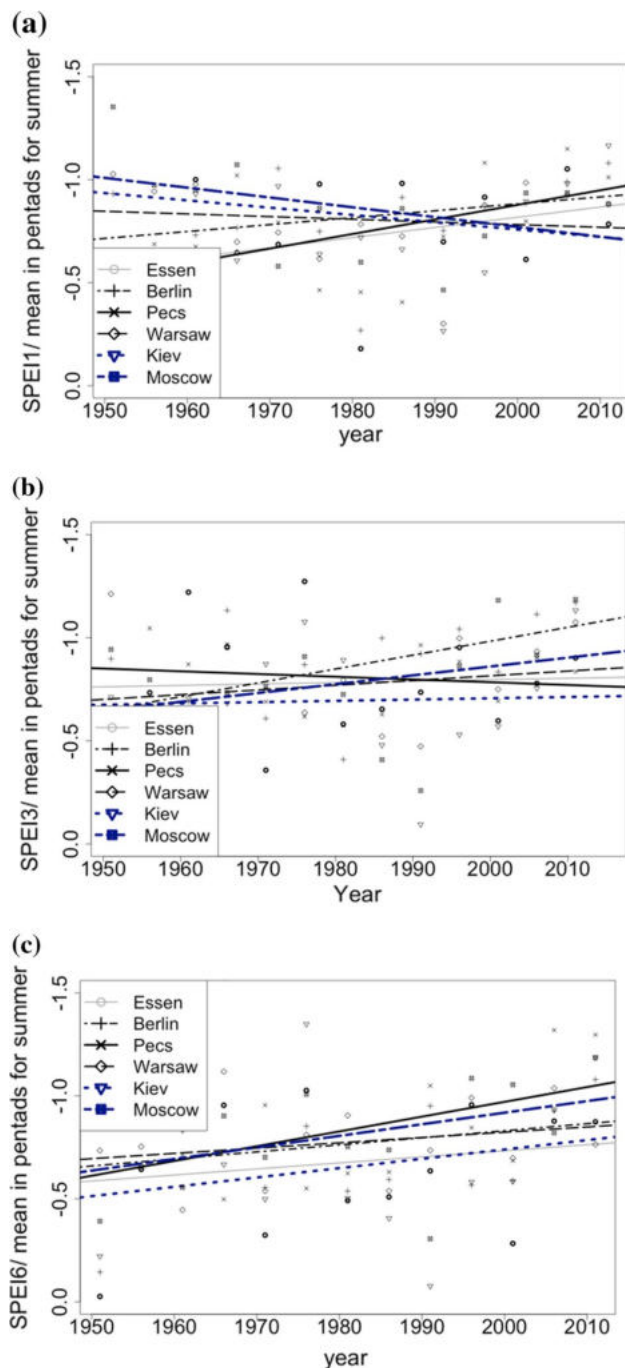


Fig. 7 The average SPEI index for pentads for the **a** 1-month, **b** 3-month, and **c** 6-month timescales, for all events with an indicator value below 0, in the summer months–June, July and August

would not give a full picture of the real conditions. This is also associated with the fact that in the investigated region, summer precipitation very often falls as torrential rains,

Table 4 Simple linear regression parameters fitted to the negative summertime SPEI values averaged for 5-year periods (pentads) for the 1-, 3- and 6-month timescales for all the stations included in the analysis (the trends of summer drought severity are presented in Fig. 13)

| | Parameter | SPEI1 | SPEI3 | SPEI6 |
|--------|-----------|--------|--------|--------|
| ESSEN | R^2 | 0.053 | -0.088 | -0.060 |
| | a | -0.005 | -0.001 | -0.003 |
| BERLIN | R^2 | 0.014 | 0.200 | -0.051 |
| | a | -0.003 | -0.007 | -0.003 |
| PÉCS | R^2 | 0.207 | -0.075 | 0.132 |
| | a | -0.007 | 0.001 | -0.007 |
| WARSAW | R^2 | -0.073 | -0.057 | -0.023 |
| | a | 0.001 | -0.002 | -0.003 |
| KIEV | R^2 | -0.049 | -0.089 | -0.024 |
| | a | 0.004 | -0.001 | -0.005 |
| MOSCOW | R^2 | 0.085 | 0.008 | 0.085 |
| | a | 0.005 | -0.004 | -0.006 |

R^2 coefficient of determination, calculated using Pearson's correlation, a linear regression slope

which, even though they are very intense and result in high monthly totals, are short and most of the water is lost due to runoff. The negative values of the SPEI index were filtered for the selected time interval (summer months), and then the average values of the index in pentads were calculated. The trends obtained from fitting the linear regression to the mean values of the summer SPEI in pentads are shown in Fig. 7. For SPEI1 (1-month timescale), an increasing trend of drought severity in the summer was determined for Essen, Berlin and Pécs, wherein such a trend was the most pronounced for this timescale in Pécs. The SPEI for the 3-month timescale for Pécs was also positive, but it also became positive for Warsaw, Kiev and Moscow. The average SPEI for the 6-month timescale for all stations indicates an increase in the severity of drought over time, with the greatest increase in its intensity during the summer in Pécs (highest linear regression slope value).

4.3 Discussion

Referring to the analyzes carried out by Spinoni et al. (2019) on a regional scale, based on the SPI index for a 12-month timescale, it was forecasted that both the precipitation amount as well as the value of the indicator itself will most probably increase in Germany, Russia and Ukraine in the future. According to the same study, an increase in the precipitation amount is also expected in Poland and Hungary.

However, in Poland, the 12-month timescale SPI index analysis showed a positive trend of this indicator value, which suggests a tendency to wetter conditions, whereas in Hungary, a trend toward drought was expected. Nevertheless, the SPEI index for the 12-month timescale predicts a decline in the value of that index in Poland, Germany and Hungary, where the potential evapotranspiration is also expected to increase.

In the presented study, a similar investigation was carried out but it was a point analysis (considering a few locations in a temperate zone in Europe, not a spatial distribution), and was based on drought indices calculated for shorter timescales (1-, 3- and 6-months). Moreover, thermal and precipitation data allowed the calculation of potential evapotranspiration which showed an increasing trend for all the locations, which is consistent with the results of Spinoni et al. (2019). The most noticeable upward trend of potential evapotranspiration was found for Kiev. This translates into a slight increase in the drought strengthening—according to the SPEI, an increase in the severity of droughts was shown (Fig. 7). Significant and positive trends in the increase in the average annual air temperature were also determined for all sites, with the strongest increasing trend for Moscow. Regarding available datasets, the obtained results indicated an increasing trend in precipitation in Warsaw, while a decreasing trend occurred in Berlin at the same time, which is only partly in agreement with the study of Spinoni et al. (2019). In Kiev and Pécs, long-term precipitation trends were statistically insignificant, thus indicating neither a reduction nor an increase in the amount.

The SPEI and SPI indices can be computed for different timescales (Vicente-Serrano et al. 2010; Beguería and Vicente-Serrano 2017a, b). The multi-scalar character of these two indices is their important advantage compared to other existing indices (Vicente-Serrano et al. 2012). Such an approach allows estimation of the influence of past thermal and humidity conditions in drought analysis. Thus, computation enabled the index to adapt to the memory of the system under study in terms of the intended purpose of the research (meteorological, agriculture-soil, hydrological drought detection). The quantity of this memory is controlled by the parameter scale (Vicente-Serrano et al. 2010; Beguería and Vicente-Serrano 2017a, b). It was shown that short timescales (1 or 3 months) can be used to describe meteorological drought while a 3-month or 6-month scale is usually used to evaluate an agricultural drought, and a

longer scale, such as 12 or 24 months, is more suitable for investigating hydrological drought and water resources (Mishra and Singh 2010; Pei et al. 2020). For example, the SPEI index for a 6-month scale, calculated for a timeseries in Indonesia presented the best accuracy for modeling soil moisture (95%) compared to the rest of the timescales used (3-, 6-, 12-months) (Ariyanto et al. 2020). Nevertheless, the type of the soil was Alfisol, which has a clay texture and very stable aggregate. In Wang et al.'s (2015) study investigating data from 40 soil moisture stations in China, it was defined that the optimum timescale for monthly SPI and SPEI which shows the most significant correlation with soil moisture at a specific soil layer was the 1-month timescale. On the other hand, their results also suggest an increasing, direct proportional relationship between the length of the index timescale and the depth of the soil for which the moisture content is measured. By using indices in three different timescales in this study we presented trends for the occurrence of drought and its severity regarding meteorological and soil (agricultural) drought, where it was assumed that the 1- and 3-month timescales are the most suitable for predicting meteorological drought, whereas the 6-month timescale is best for detecting soil drought.

The increase in the average annual temperature as well as the potential evapotranspiration at all stations translates into the results obtained for the SPEI index, however, the irregular distribution of precipitation throughout the year with a generally increasing tendency of its total annual value, makes determining drought risk more complex.

Taking into consideration all the months when the SPI and SPEI indices dropped below -1 (representing dry periods/drought conditions), an analysis of the trends in the occurrence of drought was performed in this study. An increasing trend in the occurrence of drought has been determined for the SPEI index for all considered timescales. It is worth emphasizing that according to this indicator, for the last five years included in this study, i.e. 2011–2015, an incomparably higher number of droughts has occurred, compared to previous pentads since 1951. However, in the latest study by Stagge et al. (2017), it was found that drought trends in continental Europe show that the total area experiencing an SPI6 drought has decreased significantly during the last 56 years which contradicts previous studies. Also, in the same study, spatial patterns of drought occurrence investigated by the SPI6 index turned out to be similar to the results obtained by the SPEI for a 6-month scale, showing an increasing drought occurrence across southern Europe and the Mediterranean area, while decreasing for broad parts of northern

Europe (Stagge et al. 2017). Another recent study also showed that the SPEI is probably a more suitable index than the SPI to investigate the spatio-temporal variability of drought in Europe under climate change, especially for Mediterranean region and Central Europe (Ionita and Nagavciuc 2021). Moreover, this same study suggests that the increasing mean air temperature and the potential evapotranspiration can enhance drought intensity over the southern and central parts of Europe. In light of the projected increase in potential evapotranspiration in a warming climate, this result has implications regarding the future occurrence of drought (Ionita and Nagavciuc 2021). In Spinoni et al.'s (2018) study regarding the RCP4.5 emission scenario (which for the end of the twenty-first century assumes a CO₂ equivalent of about 650 ppm), it was predicted that over the period 2011–2100 in Central Europe, a moderate increase in drought frequency will occur on an annual scale. Then, under scenario RCP8.5 (the equivalent of about 1370 ppm), a strong increase in drought frequency in most of the region was predicted, with an increase in drought occurrence mainly over the summer. These two scenarios correspond to global temperature increases of approximately 1.8 and 4.0 °C, respectively, compared to past conditions.

The severity of drought varied depending on the temporal scale used to calculate both indicators. Nevertheless, an increasing trend in drought severity for the 6-month timescale was identified for the SPEI indicator for all stations during the summer. In regions that already experience difficulties with water resources, being below or close to zero climatic water balance, as indicated in this study in the cases of Berlin, Warsaw and Pécs, can cause problems associated with crop irrigation as well as worsening biometeorological human health conditions. The awareness of the impact of drought on human health is reflected in the development of this branch of medicine which is currently becoming an independent field of science. In our study, the average SPEI index for pentads showed that considering the SPEI indicator for three different timescales (1-, 3- and 6- months), the 6-month timescale appeared to present the most pronounced trend of increasing drought severity across all the investigated stations. Therefore, it can be assumed that agrometeorological drought (soil drought) will most probably show an increasing trend in the mid latitudes of Europe.

It has been stated in IRC technical reports on meteorological drought in Europe by Spinoni et al. (2016) that due to climate change and the ever-increasing pressure on water resources, the effects of droughts are likely to be more severe

in the future. Consequently, they will require constant monitoring, evaluation and adaptation (Spinoni et al. 2016).

Even though a cyclical nature of drought occurrence in 5-year periods was found (SPI index), the role of an increase in the average annual air temperature by more than 1 degree at each site over 65 years should not be neglected. This is reflected well in the higher number of droughts indicated by the SPEI in 2010–2015 which leads to the assumption that, even with the cyclical occurrence of certain climate features (precipitation pattern), the overall effect on drought occurrence and severity is enhanced by other factors, such as the already mentioned increase in the average annual temperature and thus intensified potential evaporation.

Even though the fluctuations in the number of dry periods were noticeable as indicated by the SPI index, which is solely based on precipitation data, the number of droughts in the most recent period (2011–2015) was the highest since 1976 and higher than ever before in the period under analysis for the SPEI. The negative effects of global climate change are still enhanced by anthropogenic activities (constantly increasing emissions), which are most profoundly noticeable as an increase in air temperature. Sometimes two (or more) climate extremes can mutually strengthen each other (Seneviratne et al. 2012a, b). Then, a positive feedback occurs between the two extremes. For example, there can be the mutual enhancement of droughts and heatwaves in transitional regions between dry and wet climates. This feedback has been recognized as having an impact on predicted changes in temperature variability and heatwave occurrence in, among others, Central and Eastern Europe (Seneviratne et al. 2012a, b). Thus, one can expect a greater number of more intense droughts in the future, for which the indicators combining precipitation and thermal conditions will be more sensitive. Further “flattening” of the probability distribution of drought indices, as in the example presented on the hexagonal surface plots for Warsaw and Pécs regarding the SPEI indicator, is also expected, which means the more frequent occurrence of very dry and very wet periods causing more extreme events.

Appendix

See Figs. 8, 9, 10, 11, 12, 13.

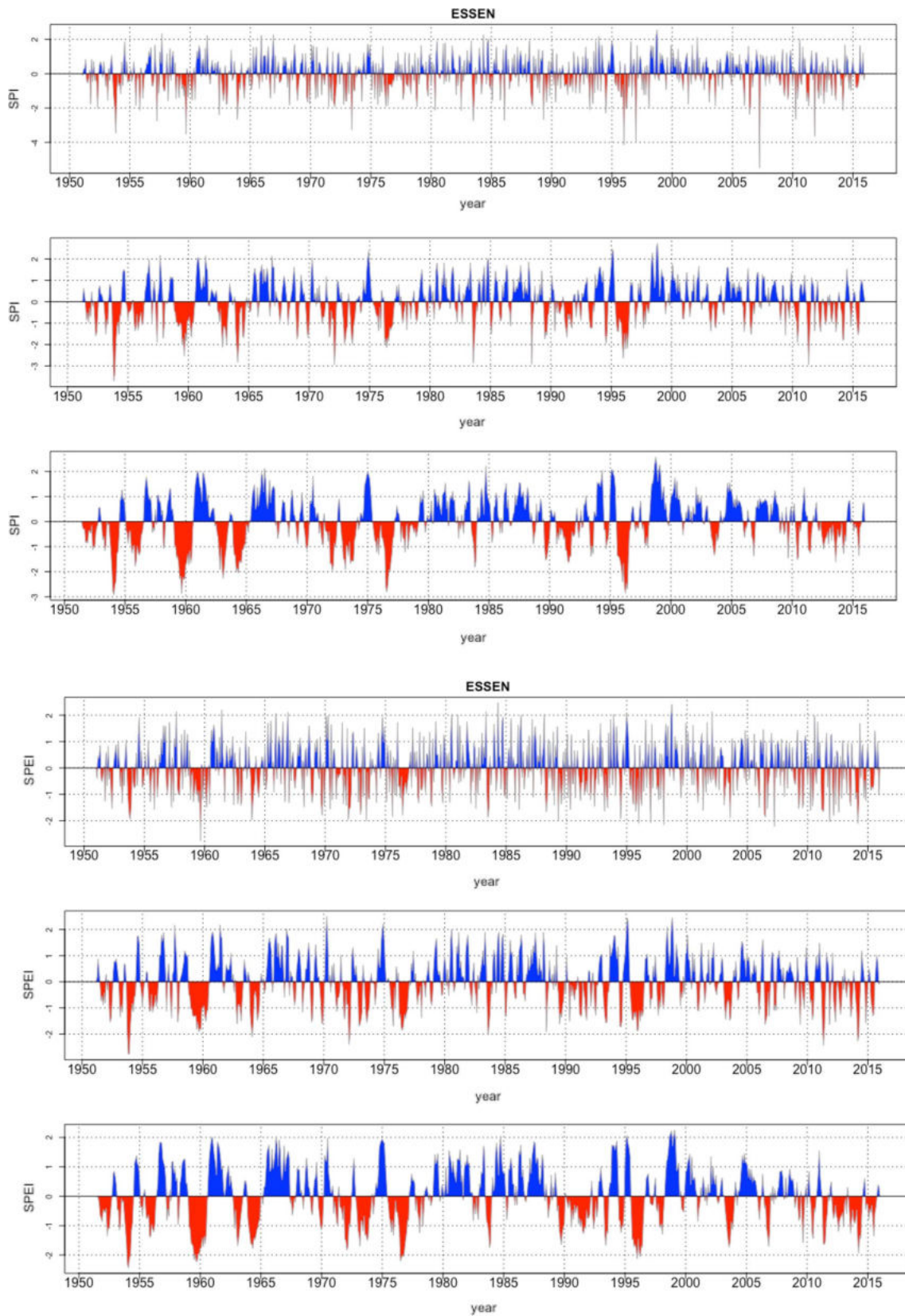


Fig. 8 Long-term (1951–2015) index values **a** SPI on a 1-, 3-, and 6-month scale, and **b** SPEI on a 1-, 3-, and 6-month scale for Essen

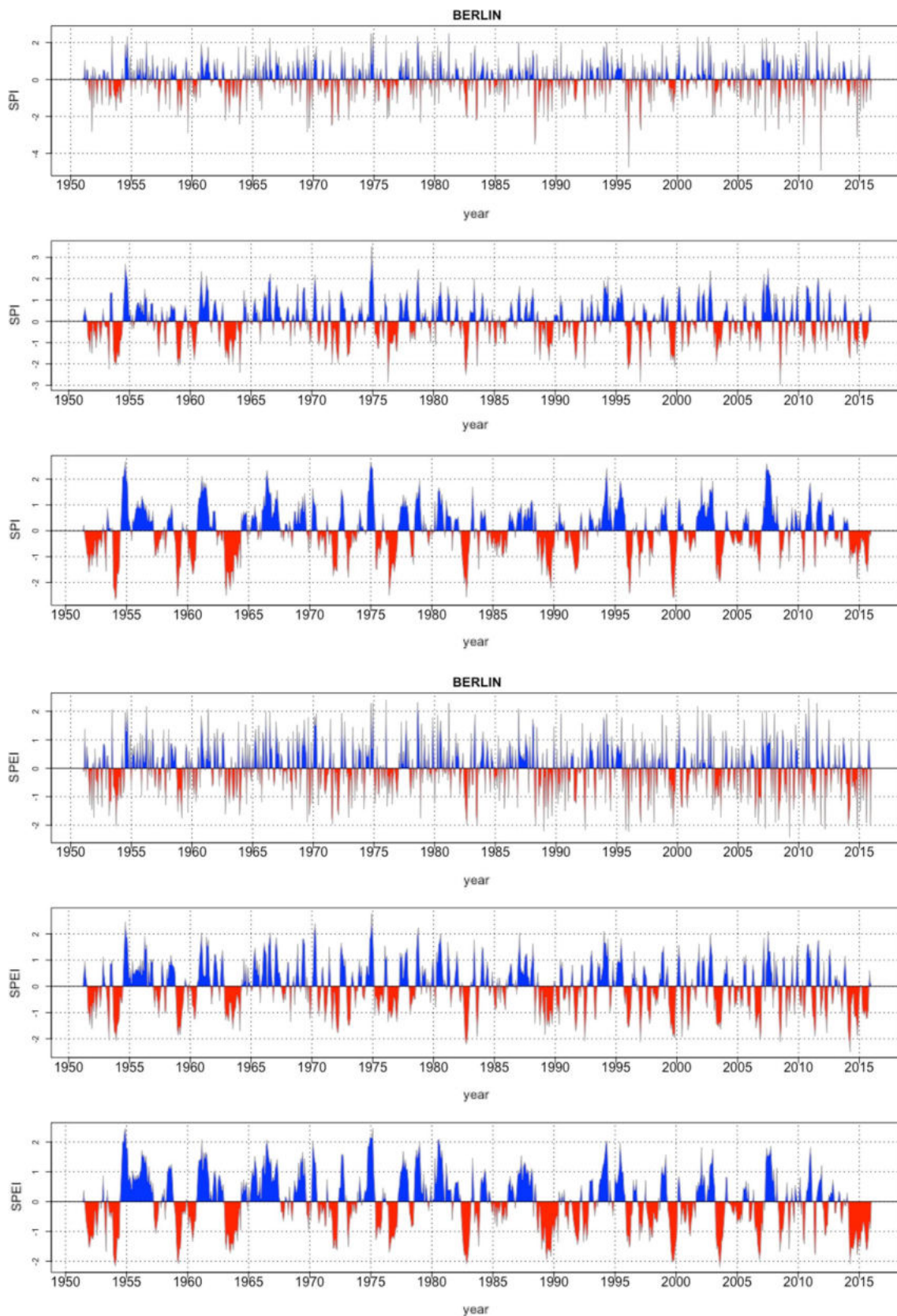


Fig. 9 Long-term (1951–2015) index values **a** SPI on a 1-, 3-, and 6-month scale, and **b** SPEI on a 1-, 3-, and 6-month scale for Berlin

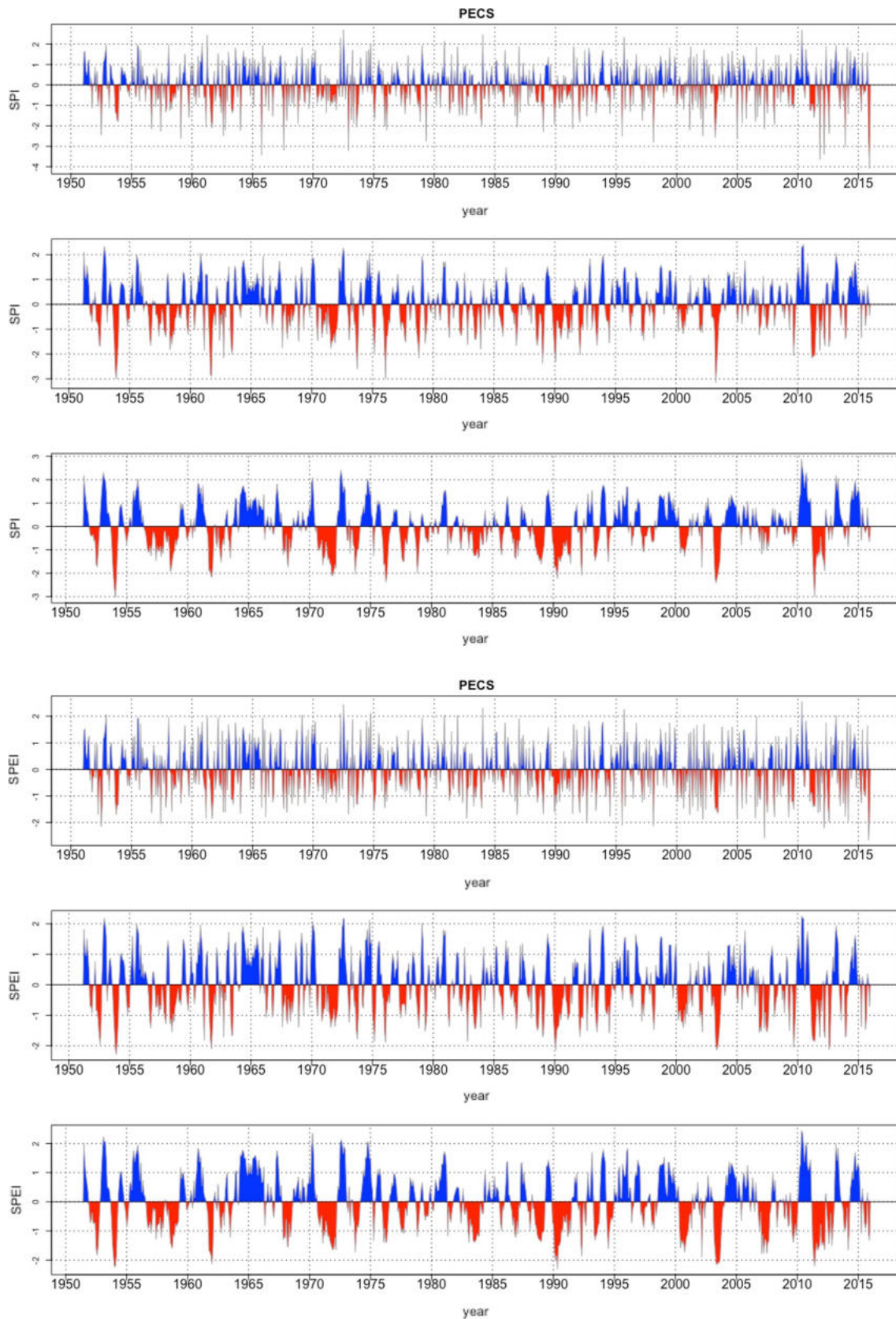


Fig. 10 Long-term (1951–2015) index values **a** SPI on a 1-, 3-, and 6-month scale, and **b** SPEI on a 1-, 3-, and 6-month scale for Pecs

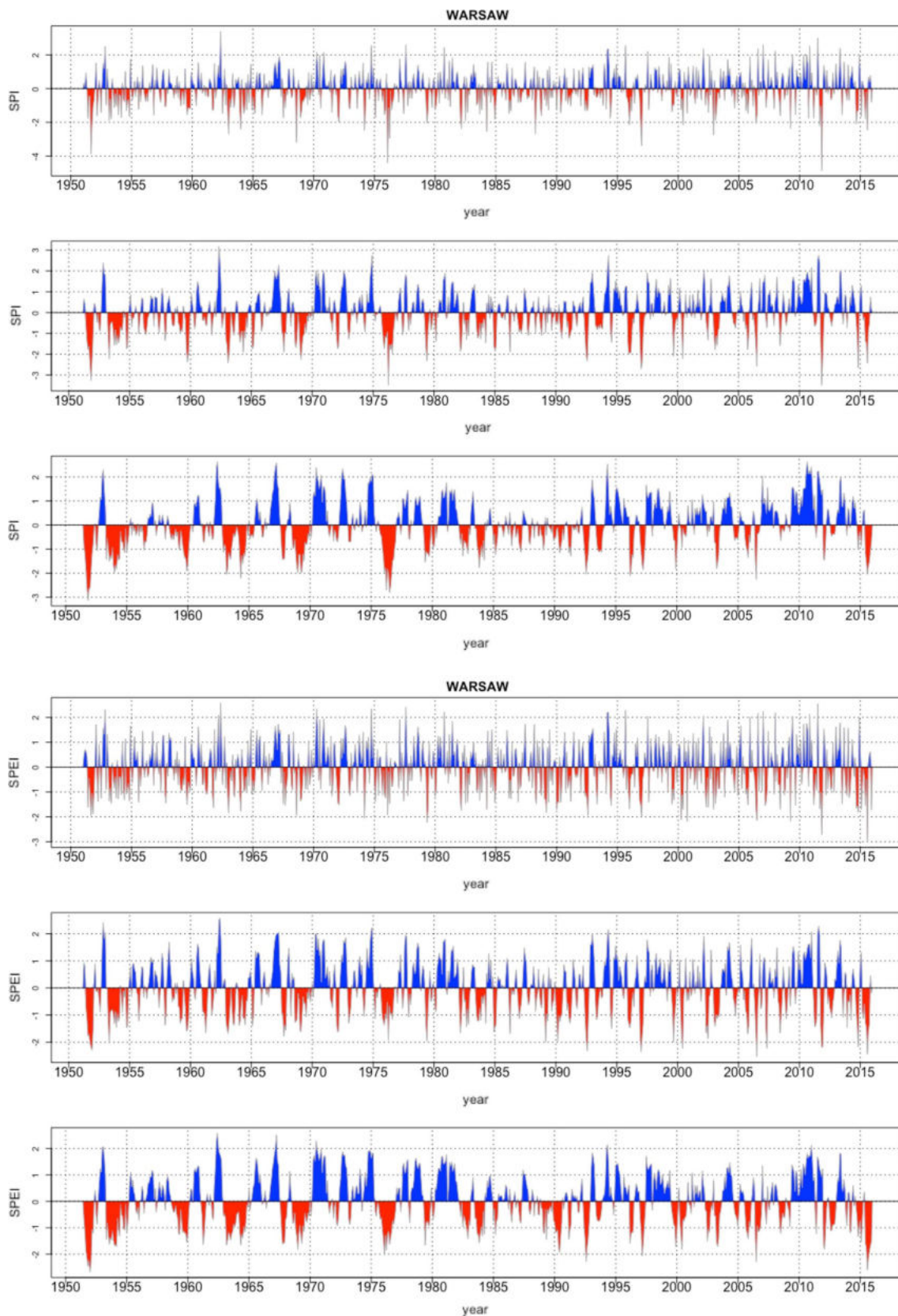


Fig. 11 Long-term (1951–2015) index values **a** SPI on a 1-, 3-, and 6-month scale, and **b** SPEI on a 1-, 3-, and 6-month scale for Warsaw

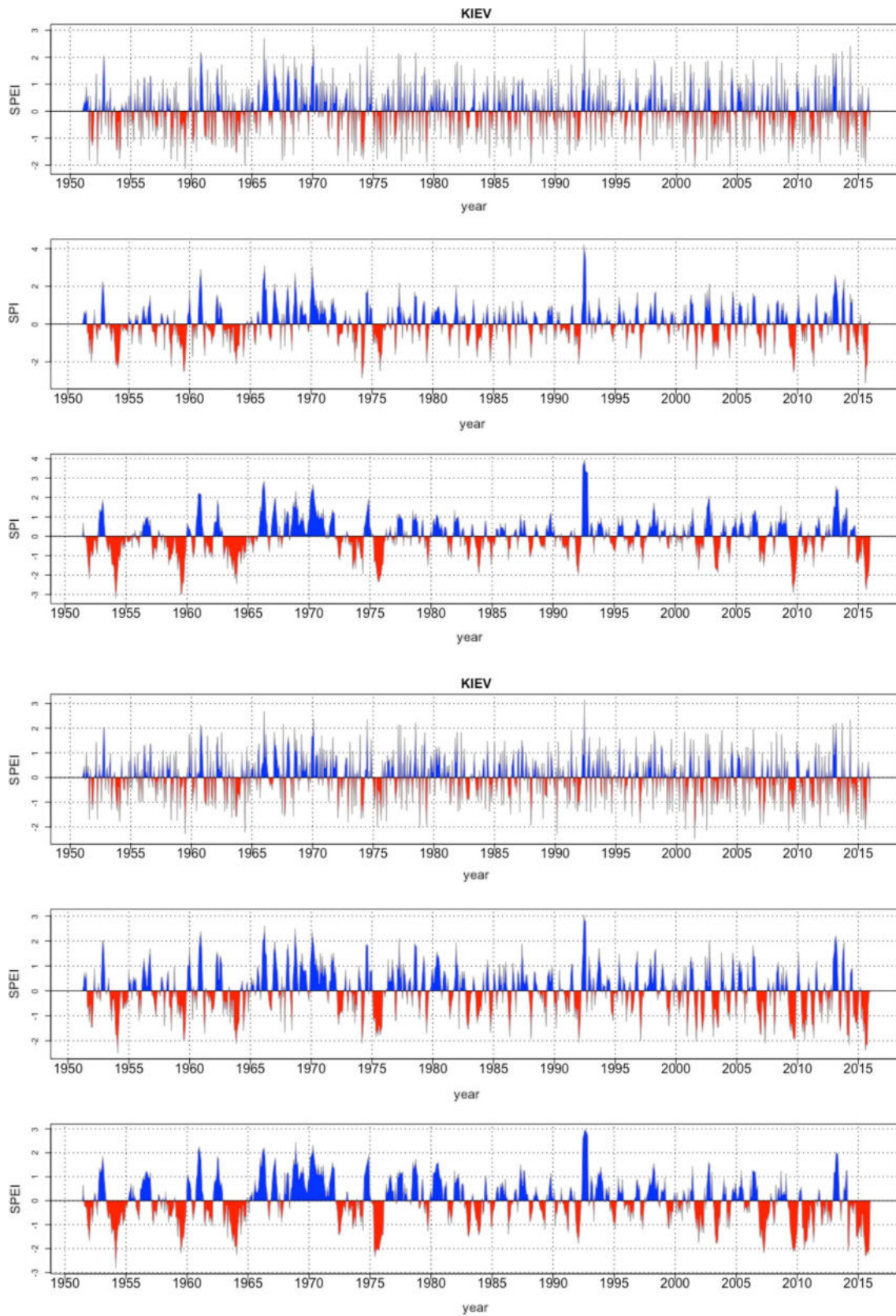


Fig. 12 Long-term (1951–2015) index values **a** SPI on a 1-, 3-, and 6-month scale, and **b** SPEI on a 1-, 3-, and 6-month scale for Kiev

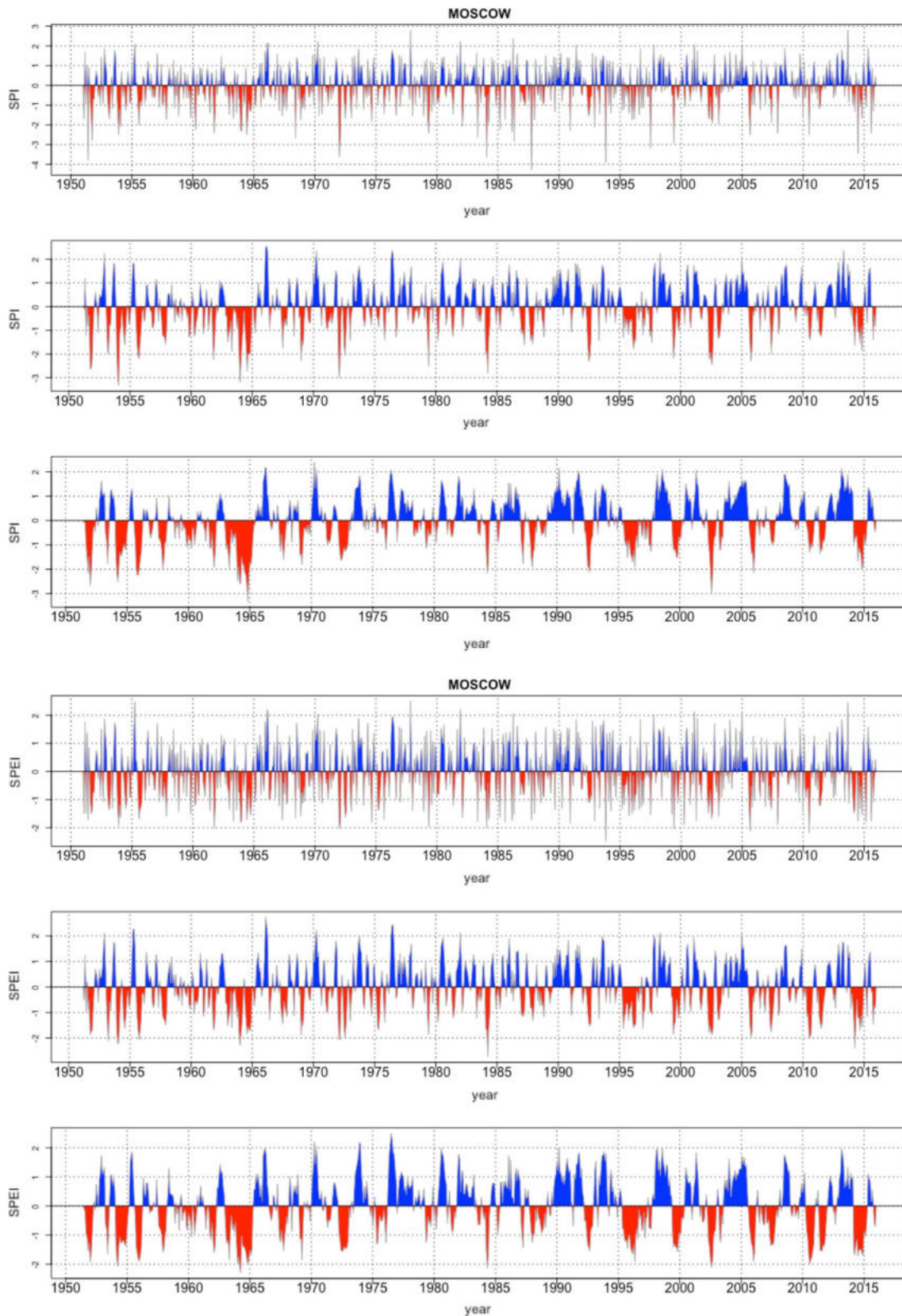


Fig. 13 Long-term (1951–2015) index values **a** SPI on a 1-, 3-, and 6-month scale, and **b** SPEI on a 1-, 3-, and 6-month scale for Moscow

Funding Not applicable.

Data availability statement The climatological data that support the findings of this study during manuscript preparation were available from the portal of European Climate Assessment & Dataset project and Polish Institute of Meteorology and Water Management portal (IMGIW), under links: <https://www.ecad.eu> and <https://danepubliczne.imgw.pl>.

Availability of data and material The data used in this paper are in the public domain: <https://www.ecad.eu/dailydata/index.php> and https://dane.imgw.pl/data/dane_pomiarowo_obserwacyjne/dane_meteorologiczne/dobowe/klimat/.

Code availability Not applicable.

Declarations

Conflict of interest The authors declare no conflict of interest.

Open Access This article is licensed under a Creative Commons Attribution 4.0 International License, which permits use, sharing, adaptation, distribution and reproduction in any medium or format, as long as you give appropriate credit to the original author(s) and the source, provide a link to the Creative Commons licence, and indicate if changes were made. The images or other third party material in this article are included in the article's Creative Commons licence, unless indicated otherwise in a credit line to the material. If material is not included in the article's Creative Commons licence and your intended use is not permitted by statutory regulation or exceeds the permitted use, you will need to obtain permission directly from the copyright holder. To view a copy of this licence, visit <http://creativecommons.org/licenses/by/4.0/>.

References

- Ariyanto DP, Aziz A, Komariah et al (2020) Comparing the accuracy of estimating soil moisture using the standardized precipitation Index (SPI) and the standardized precipitation evapotranspiration index (SPEI). *Sains Tanah* 17:23–29. <https://doi.org/10.20961/stjssa.v17i1.41396>
- Beguéría S, Vicente-Serrano SM, Angulo-Martínez M (2010) A multiscalar global drought dataset: the SPEI base: a new gridded product for the analysis of drought variability and impacts. *Bull Am Meteorol Soc* 91:1351–1356. <https://doi.org/10.1175/2010BAMS2988.1>
- Beguéría S, Vicente-Serrano SM, Reig F, Latorre B (2014) Standardized precipitation evapotranspiration index (SPEI) revisited: parameter fitting, evapotranspiration models, tools, datasets and drought monitoring. *Int J Climatol* 34:3001–3023. <https://doi.org/10.1002/joc.3887>
- Beguéría S, Vicente-Serrano SM (2017) SPEI: calculation of the standardised precipitation-evapotranspiration index. R package
- Beguéría S, Vicente-Serrano SM (2017) Package ‘SPEI’. Calculation of the Standardised Precipitation-Evapotranspiration Index
- Bezdan J, Bezdan A, Blagojević B et al (2019) SPEI-based approach to agricultural drought monitoring in Vojvodina region. *Water (switzerland)*. <https://doi.org/10.3390/w11071481>
- Blain GC (2011) Standardized precipitation index based on pearson type III distribution. *Rev Bras Meteorol* 26:167–180. <https://doi.org/10.1590/s0102-77862011000200001>
- Collins R, Kristenses K, Thyssen N (2009) Water resources across Europe – confronting water scarcity and drought. EEA Report 2/2009. Denmark. <https://doi.org/10.2800/16803>
- ECAD (2018) Home European Climate Assessment & Dataset portal
- Faustin Katchele O, Ma ZG, Yang Q, Batebana K (2017) Comparison of trends and frequencies of drought in central North China and sub-Saharan Africa from 1901 to 2010. *Atmos Ocean Sci Lett* 10:418–426. <https://doi.org/10.1080/16742834.2017.1392825>
- Faye C, Grippa M, Wood S (2019) Use of the Standardized Precipitation and Evapotranspiration Index (SPEI) from 1950 to 2018 to determine drought trends in the Senegalese territory, *Climate Change*
- Hayes MJ, Svoboda MD, Wilhite DA, Vanyarkho OV (1999) Monitoring the 1996 drought using the Standardized Precipitation Index. *Bull Am Meteor Soc* 31:429
- Hayes MJ, Svoboda MD, Wardlow BD et al (2012) Drought monitoring: Historical and current perspectives. *Remote Sens Drought Innov Monit Approach*. <https://doi.org/10.1201/b11863>
- Hosking JRM (1986) The theory of probability weighted moments. *Res Rep RC 12210 IBM Res Div Yorkt Height NY* 10598
- Ionita M, Nagavciuc V (2021) Changes in drought features at European level over the last 120 years. *Nat Hazards Earth Syst Sci*. <https://doi.org/10.5194/nhess-2021-46>
- IPCC 2001: climate change (2001) Contribution of working group I to the third assessment report of the intergovernmental panel on climate change [Houghton, J.T. Ding, Y. Griggs, D.J. Noguer, M. Linden, P.J. van der Dai, X. Maskell, K. Johnson, C.A.]. Cambridge Univ Press, p 94
- Kottek M, Grieser J, Beck C et al (2006) World map of the Köppen-Geiger climate classification updated. *Meteorol Zeitschrift* 15:259–263. <https://doi.org/10.1127/0941-2948/2006/0130>
- Kożuchowski K, Wibig J, Degirmendzić J (2012) *Meteorologia i Klimatologia*, Wydawnictwo Naukowe PWN. Warsaw
- Krajinović Z (2010) Implementation of standardised precipitation index—SPI, Republic Hydrometeorological Service of Serbia
- Livada I, Assimakopoulos VD (2007) Spatial and temporal analysis of drought in Greece using the Standardized Precipitation Index (SPI). *Theor Appl Climatol* 89:143–153. <https://doi.org/10.1007/s00704-005-0227-z>
- Lloyd-Hughes B, Saunders MA (2002) A drought climatology for Europe. *Int J Climatol* 22:1571–1592. <https://doi.org/10.1002/joc.846>
- McKee TBJ, Nolan JK (1993) The relationship of drought frequency and duration to time scales. In: *Prepr eighth conf appl climatol Anaheim, CA, Amer Meteor, Soc* pp 179–184
- McKee TBJ, Nolan JK (1995) Drought monitoring with multiple time scales. In: *Prepr ninth conf appl climatol Dallas, TX, Amer Meteor Soc*, pp 233–236
- Mishra AK, Singh VP (2010) A review of drought concepts. *J Hydrol* 391:202–216. <https://doi.org/10.1016/j.jhydrol.2010.07.012>
- Pei Z, Fang S, Wang L, Yang W (2020) Comparative analysis of drought indicated by the SPI and SPEI at various timescales in Inner Mongolia, China. *Water (switzerland)*. <https://doi.org/10.3390/w12071925>
- R Core Team (2020) R: a language and environment for statistical computing
- Rhee J, Im J, Carbone GJ (2010) Monitoring agricultural drought for arid and humid regions using multi-sensor remote sensing data. *Remote Sens Environ* 114:2875–2887
- Seneviratne SI, Nicholls N, Easterling D, Goodess CM, Kanae S, Kossin J, Luo Y, Marengo J, McInnes MRK, Reichstein M, Sorteberg A, Vera C, Zhang X (2012a) Changes in climate extremes and their impacts on the natural physical environment in book: managing the risks of extreme events and disasters to advance climate change adaptation (SREX). In: Field CB, Barros V, Stocker TF, Qin D, Dokken DJ, Ebi KL, Mastrandrea MD, Mach KJ, Plattner

- SKA, Tignor M, PMM (eds) A special report of working groups I and II of the Intergovernmental Panel on Climate Change (IPCC). Cambridge University Press, Cambridge, pp 109–230
- Seneviratne SI, Nicholls N, Easterling D et al (2012b) Changes in climate extremes and their impacts on the natural physical environment. Manag Risks Extrem Events Disasters Adv Clim Chang Adapt Spec Rep Intergov Panel Clim Chang 9781107025:109–230. <https://doi.org/10.1017/CBO9781139177245.006>
- Singh VP et al (1993) Parameter estimation for 3-parameter log-logistic distribution (LLD3) by Pome. Stoch Hydrol Hydraul 7:163–177
- Spinoni J, Naumann G, Vogt JV, Barbosa P (2015) The biggest drought events in Europe from 1950 to 2012. J Hydrol Reg Stud 3:509–524. <https://doi.org/10.1016/j.ejrh.2015.01.001>
- Spinoni J, Naumann G, Vogt J, Barbosa P (2016) Meteorological droughts in Europe: events and impacts—past trends and future projections. Publ off Eur Union. Luxemb. EUR 27748 EN. <https://doi.org/10.2788/450449>
- Spinoni J, Vogt JV, Naumann G et al (2018) Will drought events become more frequent and severe in Europe? Int J Climatol 38:1718–1736. <https://doi.org/10.1002/joc.5291>
- Spinoni J, Barbosa P, De Jager A et al (2019) A new global database of meteorological drought events from 1951 to 2016. J Hydrol Reg Stud 22:100593. <https://doi.org/10.1016/j.ejrh.2019.100593>
- Stagge JH, Kingston DG, Tallaksen LM, Hannah DM (2017) Observed drought indices show increasing divergence across Europe. Sci Rep 7:1–10. <https://doi.org/10.1038/s41598-017-14283-2>
- Thornthwaite CW (1948) An approach toward a rational classification of climate. Geogr Rev 38:55–94
- Trnka M, Semerádová D, Novotný I et al (2016) Assessing the combined hazards of drought, soil erosion and local flooding on agricultural land: a Czech case study. Clim Res 70:231–249. <https://doi.org/10.3354/cr01421>
- Tsakiris G, Vangelis H (2005) Establishing a Drought Index incorporating evapotranspiration. Eur Water 9(10):3–11
- Vicente-Serrano SM, Beguería S, López-Moreno JI (2010) A multi-scalar drought index sensitive to global warming: the standardized precipitation evapotranspiration index. J Clim 23:1696–1718. <https://doi.org/10.1175/2009JCLI2909.1>
- Vicente-Serrano SM, Beguería S, Lorenzo-Lacruz J et al (2012) Performance of drought indices for ecological, agricultural, and hydrological applications. Earth Interact. <https://doi.org/10.1175/2012E1000434.1>
- Vogt JV, Somma F (eds) (2000) Drought and drought mitigation in Europe. Kluwer Acad Publ Dordrecht, Netherlands, p 336
- Vogt JV, Barbosa P, Hofer B, Magni D, De Jager A, Singleton A, Horion S, Sepulcre G, Micale F, Sokolova E, Calcagni L, Marioni M, Antofie TE (2011) Developing a European drought observatory for monitoring, assessing and forecasting droughts across the European continent. AGU Fall Meet Abstr 1, NH24A-07
- Wang H, Rogers JC, Munroe DK (2015) Commonly used drought indices as indicators of soil moisture in China. J Hydrometeorol 16:1397–1408. <https://doi.org/10.1175/JHM-D-14-0076.1>
- Wang Q, Zeng J, Qi J et al (2020) A multi-scale daily SPEI dataset for drought monitoring at observation stations over the mainland China from 1961 to 2018. Earth Syst Sci Data Discuss. <https://doi.org/10.5194/essd-2020-172>
- Woś A (2010) Klimat polski w drugiej połowie XX wieku. Wydawnictwo Naukowe UAM, Poznań




Publisher's Note Springer Nature remains neutral with regard to jurisdictional claims in published maps and institutional affiliations.

6.2. Publikacja #2

Estimation of Biomass Increase and CUE at a Young Temperate Scots Pine Stand Concerning Drought Occurrence by Combining Eddy Covariance and Biometric Methods

Article

Estimation of Biomass Increase and CUE at a Young Temperate Scots Pine Stand Concerning Drought Occurrence by Combining Eddy Covariance and Biometric Methods

Paulina Dukat ^{1,2,*} , Klaudia Ziemblińska ¹ , Janusz Olejnik ¹ , Stanisław Małek ³, Timo Vesala ^{2,4,5} and Marek Urbaniak ¹

- ¹ Meteorology Lab., Department of Construction and Geoengineering, Faculty of Environmental Engineering and Mechanical Engineering, Poznan University of Life Sciences, Piątkowska 94, 60-649 Poznań, Poland; klaudiaziam@up.poznan.pl (K.Z.); janusz.olejnik@up.poznan.pl (J.O.); marek.urbaniak@up.poznan.pl (M.U.)
- ² Faculty of Science, Institute for Atmospheric and Earth System Research/Physics, University of Helsinki, FI-00014 Helsinki, Finland; timo.vesala@helsinki.fi
- ³ Department of Ecology and Silviculture, Faculty of Forestry, University of Agriculture in Krakow, Al. 29-go Listopada 46, 31-425 Kraków, Poland; rlmalek@cyf-kr.edu.pl
- ⁴ Faculty of Agriculture and Forestry, Institute for Atmospheric and Earth System Research/Forest Sciences, University of Helsinki, FI-00790 Helsinki, Finland
- ⁵ Department of Environmental Dynamics and Global Climate Change, Yugra State University, 628012 Khanty-Mansiysk, Russia
- * Correspondence: paulina.dukat05@gmail.com



Citation: Dukat, P.; Ziemblińska, K.; Olejnik, J.; Małek, S.; Vesala, T.; Urbaniak, M. Estimation of Biomass Increase and CUE at a Young Temperate Scots Pine Stand Concerning Drought Occurrence by Combining Eddy Covariance and Biometric Methods. *Forests* **2021**, *12*, 867. <https://doi.org/10.3390/f12070867>

Academic Editor: Francesco Pirrotti

Received: 27 May 2021

Accepted: 29 June 2021

Published: 30 June 2021

Publisher's Note: MDPI stays neutral with regard to jurisdictional claims in published maps and institutional affiliations.



Copyright: © 2021 by the authors. Licensee MDPI, Basel, Switzerland. This article is an open access article distributed under the terms and conditions of the Creative Commons Attribution (CC BY) license (<https://creativecommons.org/licenses/by/4.0/>).

Abstract: The accurate estimation of an increase in forest stand biomass has remained a challenge. Traditionally, in situ measurements are done by inventorying a number of trees and their biometric parameters such as diameter at the breast height (DBH) and height; sometimes these are complemented by carbon (C) content studies. Here we present the estimation of net primary productivity (NPP) over a two years period (2019–2020) at a 25-year-old Scots pine stand. Research was based on allometric equations made by direct biomass analysis (tree extraction) and carbon content estimations in individual components of sampled trees, combined with a series of stem diameter increments recorded by a network of band dendrometers. Site-specific allometric equations were obtained using two different approaches: using the whole tree biomass vs DBH (M1), and total dry biomass-derived as a sum of the results from individual tree components' biomass vs DBH (M2). Moreover, equations for similar forest stands from the literature were used for comparison. Gross primary productivity (GPP) estimated from the eddy-covariance measurements allowed the calculation of carbon use efficiency (CUE = NPP/GPP). The two investigated years differed in terms of the sum and patterns of precipitation distribution, with a moderately dry year of 2019 that followed the extremely dry 2018, and the relatively average year of 2020. As expected, a higher increase in biomass was recorded in 2020 compared to 2019, as determined by both allometric equations based on in situ and literature data. For the former approach, annual NPP estimates reached ca. 2.0–2.1 t C ha⁻¹ in 2019 and 2.6–2.7 t C ha⁻¹ in 2020 depending on the “in situ equations” (M1-M2) used, while literature-derived equations for the same site resulted in NPP values ca. 20–30% lower. CUE was higher in 2020, which resulted from a higher NPP total than in 2019, with lower summer and spring GPP in 2020. However, the CUE values were lower than those reported in the literature for comparable temperate forest stands. A thorough analysis of the low CUE value would require a full interpretation of interrelated physiological responses to extreme conditions.

Keywords: carbon sequestration; net primary productivity; carbon use efficiency; water deficit

1. Introduction

Carbon dioxide (CO₂) is one of the most important greenhouse gases that contributes to global warming [1]. Through photosynthetic uptake and respiratory losses, it is continu-

ally exchanged between forest ecosystems and the atmosphere. In principle, undisturbed forest ecosystems and afforested stands on non or marginal agricultural land are a significant sink of atmospheric CO₂ [2,3]. It was estimated that forests account for approximately half of the annual global net primary production (NPP) of all terrestrial ecosystems [4]. Forests contribute to the terrestrial carbon balance in two ways: as principal pools of carbon stored in plant biomass due to photosynthesis, and through the release of CO₂ via ecosystem respiration [5]. These carbon pools are composed of living and dead biomass both above and below ground (AGB and BGB, respectively), such as dead wood, litter, and soil organic matter [6]. The productivity of any forest ecosystem corresponds to its carbon sequestration potential [7] and depends mainly on the age and species of trees, as well as the habitat and meteorological conditions. It has been assumed that the recent increase in the tropospheric concentration of ozone (O₃) has reduced terrestrial carbon uptake compared to the preindustrial era [8]. This is mainly caused by O₃ molecules penetrating the leaves through the stomata, hence damaging the photosynthetic apparatus. In addition to O₃ damage, the productivity of forest ecosystems can be severely limited by water scarcity [9]. Carbon sequestration (stock) estimation is essential to understand the overall storage efficiency of a forest ecosystem [6]. For example, Kumar et al. [10] showed that dominant species in Uttarakhand Himalaya, India, and the overlying soils are important contributors to the total carbon stocks. These factors play a crucial role in carbon sequestration, which will further help mitigate GHG emissions. Another study recommends that in addition to conserving forests for climate change mitigation, carbon sequestration potential extends to trees outside of forests as well, hence non-forested lands should also be protected [11]. Furthermore, estimation of stem volume and tree biomass is very important for planning sustainable forest resource use, and for research on the energy and nutrient flow in the ecosystems [12].

Estimates of forest ecosystem productivity are often expressed as gross or net primary productivity (GPP and NPP, respectively). GPP is defined as a balance between the total amount of carbon fixed by the ecosystem through photosynthesis and carbon loss through photorespiration [13]; NPP is the share of GPP used for new biomass growth [14]. Thus, NPP is theoretically defined as the difference between GPP and autotrophic respiration (R_a) [15]. Studies of ground-based NPP are often based on litterfall and AGB accumulation measurements, and are therefore not closely related to the concept of NPP as a balance between GPP and R_a [15,16]. In practice, NPP is often estimated as the sum of biomass production components [16,17], which can be done using literature or site-specific allometric equations. To estimate tree biomass, it is recommended to use allometric relationships based on tree parameters such as diameter at the breast height (DBH) and tree height [14]. Many allometric equations can be found in the literature, for example in the study by Zianis et al. [12]. These are also often derived for individual species [18]. One important indicator of ecosystem function that can be estimated with known NPP and GPP is carbon use efficiency (CUE = GPP/NPP). CUE is commonly defined as the ratio of carbon sequestered by plants from the atmosphere and carbon allocated to growth [19], which also indirectly informs about the share of carbon respired by plants due to R_a [7]. Earlier studies have used various methods to estimate biomass increment, carbon storage and CUE [14,19–22], for example biometric in situ measurements and eddy covariance observations for NPP estimation of Pedunculate Oak Forest in Croatia [23]. Similarly, temporal variability of the NPP-GPP ratio in a temperate beech forest has been estimated at both seasonal and interannual time scales [24]. Further concepts and methods of measuring NPP in forests have been described earlier [16].

The main aim of this study was to present the differences in NPP between the two years that varied in terms of water availability: a dry year (2019) that followed extreme droughts at the study area in 2018, and a moderate year (2020). It was hypothesized that water conditions have a significant impact on the amount of carbon absorbed by trees, and thus biomass production. The relationship between changes in GPP and NPP over the two studied years was also explored.

2. Materials and Methods

2.1. Site Description

This research was conducted at the eddy covariance (EC) study site established in May 2018 near Mezyk (ME) village in north-western Poland (52°50' N, 16°15' E). The forest was planted after a fire in 1992. It is an even-aged monoculture dominated by Scots pine (*Pinus sylvestris* L.) with approximately 1% admixture of silver birch (*Betula pendula* Roth).

In order to identify the stand structure at the study area, three square experimental plots were established, each with an area of approximately 1089 m² (33 × 33 m) (Figure 1). The number of trees (Scots pine) was counted at each plot, and tree DBH was measured. The sum from all three plots was extrapolated to obtain the total number of trees per 1 ha, considering the contribution of roads, free spaces and birch plantations. The stand density was estimated to be 4262 trees ha⁻¹. The average tree height in this area was 10.49 m (standard deviation of 0.99 m; median distribution = 10.15 m) [25]. The average diameter at breast height (DBH) was 9.5 cm. Based on three soil pedons, the soil type was determined to be Brunic Arenosoil.



Figure 1. Photomap showing the distribution of the experimental plots at which the number of trees and DBH were measured (yellow squares). Five groups were established within the white square; each group had five trees with dendrometers installed. The flux tower is located near the center of the right edge of the white square. Blue stripes represent treeless areas or birch plantations (for the purpose of fire protection). Source: google maps.

2.2. Eddy Covariance and Meteorological Measurements

The EC system was composed of an open-path analyzer (IRGA, model LI-7500DS, LI-COR Inc., Nebraska, NE, USA) combined with a three-dimensional (3D) anemometer (model WindMaster Pro, Gill Instruments, Hampshire, UK) and smart flux systems. This was installed at the top of a 22 m-high flux tower, to measure the fluxes of trace gases (CO₂ and H₂O) exchange with the atmosphere. These measurements have been carried out since May 2018. Basic meteorological factors were continuously recorded, including four components of the surface radiation balance (model CNR4 Kipp&Zonen Niderland, Delf, Netherlands), air temperature (T_a) and air humidity measured at the top of the tower and at 2 m above the ground (Rotronik, Bassersdorf, Germany), as well as bulk precipitation (P)-tipping bucket rain gauge (model 52202-L, R. M. Young Company, Michigan, MI, USA). Soil temperature and soil water content (SWC) were measured at a depth of 2 cm in mineral soil (under the organic layer) using TDT Soil Moisture (SDI-12) sensors (Acclima, Meridian, Idaho, USA) with five replicates. In addition, the soil temperature was measured at five different profiles randomly placed around the EC tower, each at 2 and 5 cm deep. Since

there were gaps in the P records collected here, continuous P measurements were obtained from the Miały rainfall station of the Institute of Meteorology and Water Management (IMiGW) network, located 2 km from ME. Daily observations were used instead of in situ measurements for the whole study period.

2.3. Dendrometer Measurements and Tree Circumference Increment Calculations

Within the main research area (white square, Figure 1), five groups of five Scots pine trees were chosen for continuous dendrometric measurements. A band dendrometer (model DR26E dendrometric increase sensors, EMS Brno, Brno Czech Republic) was installed at the breast height (130 cm from the soil surface) of each of these 25 selected trees. The recorded circumference increment data was sent to the datalogger (Datalogger GreyBox N2N, EMS Brno, Brno, Czech Republic) at a frequency of two minutes, and averaged to half-hourly values, corresponding to a measurement resolution of 0.002 m. The so-called “average tree” growth within the studied ecosystem was obtained by averaging DBH increments from all 25 dendrometers. Dendrometric phases were then determined based on the course of DBH increment within the entire investigation period. The beginning of wood growth in a particular year was set as the end of the growth phase in the previous year, considering the maximum winter contraction. Calculations and data analyses were performed with R software (R version 4.0.2, The R Foundation for Statistical Computing) [26].

2.4. Biomass Inventory of the Individual Parts of the Model Trees

The biomass of five sample trees was determined by an inventory carried out at the turn of spring and summer 2018 [25]. For this purpose, a sample area of 0.03 ha was established. Of the 114 trees within this area, five model trees were selected and extracted. Their DBH represented the average values for the main research plot (Table 1). The DBH measurement was made by the forest cluster. Sectional measurements were taken on approximately 1 m sections of the tree trunk (Figure 2). The stem was then pruned, and the separated branches were divided into two categories: main branches, and fine branches with needles. The root system was also excavated for each of these five model trees. The main roots (at least 2 mm thick) were cleaned and the trunks were collected.

Table 1. Dry Biomass (DB) of the above- (AGB) and belowground (BGB) components of the five model trees (kg).

| No. | DBH | Stem with Bark | Bark | Main Branches | Fine Branches | Needles | Fine Roots | Main Roots | Total (Whole Tree) | AGB (% DB) | BGB (% DB) |
|---------|------|----------------|------|---------------|---------------|---------|------------|------------|--------------------|------------|------------|
| 1 | 8.0 | 12.9 | 1.7 | 2.3 | 1.5 | 1.2 | 0.95 | 2.8 | 23.43 | 84.0 | 16.0 |
| 2 | 9.8 | 17.5 | 2.3 | 4.3 | 3.2 | 2.8 | 0.94 | 4.3 | 35.32 | 85.1 | 14.9 |
| 3 | 11.7 | 23.5 | 3.1 | 6.1 | 2.9 | 2.5 | 0.98 | 4.6 | 43.61 | 87.3 | 12.7 |
| 4 | 12.5 | 28.4 | 4.3 | 12.7 | 4.2 | 3.1 | 1.02 | 8.2 | 61.89 | 85.0 | 15.0 |
| 5 | 13.3 | 29.9 | 4.6 | 6.0 | 3.5 | 2.8 | 1.01 | 7.9 | 53.13 | 88.2 | 11.8 |
| Average | 11.1 | 22.4 | 3.2 | 6.3 | 3.1 | 2.5 | 0.98 | 5.6 | 43.47 | 85.9 | 14.1 |

The contribution of components such as deadwood (above and below ground) and undergrowth in the total stand biomass was estimated separately at four sample areas (50 m² each). Two smaller circular areas (approximately 0.2 m²) were set up within these areas (established by tossing a hula hoop), and a single sampling was performed by collecting plants from these small areas. All herbaceous plants, bryophytes, and woody plants up to 0.5 m high were collected and cut at the ground with shears. Samples of fine roots were collected from the center of each area using a cylindrical root collector (volume 1387 cm³, diameter 4.7 cm, height 20 cm) inserted to a depth of 0–20 cm and 20–40 cm. Dead aboveground wood biomass consisted of standing deadwood, living and dead thick branches (>7 cm in diameter at the thicker end). For the belowground dead wood estimation, stems or trunks of torn, broken and felled trees were included. Dry mass was also determined for each tree separately by drying individual tree parts at 65 °C. The

results of biomass estimations of the five model trees are presented in Table 1. Carbon content in the dry biomass was calculated as the average of the samples from the trees' components. The highest value was characteristic for stem and bark, and the lowest for fine roots, resulting in an average of 50% carbon content in dry biomass. NPP was calculated as 50% of the total dry biomass. Within the main study area (1 ha), other forest ecosystem elements such as deadwood (both above and below ground) and undergrowth (herbaceous plants, bryophytes, woody plants up to 0.5 m high) constituted approximately 6.3% of the total dry biomass.

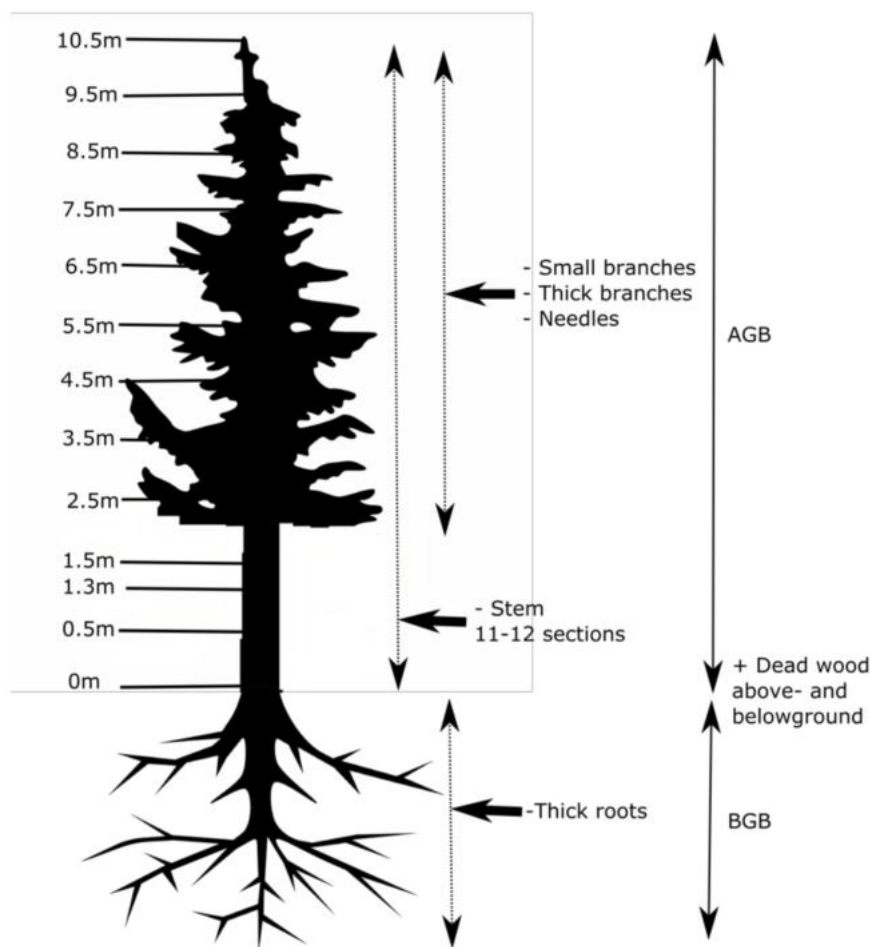


Figure 2. Scheme of tree components used for in situ biomass investigation of five model trees collected from the main research area. AGB—Above Ground Biomass, BGB—Below Ground Biomass.

2.5. In Situ Allometric Equations—The Relationship between Biomass of Tree Components and Their DBH

The total dry biomass of individual trees was correlated with their DBH in order to obtain site-specific allometric equations (Figure 3). Fitted non-linear regression parameters suggest that total dry biomass is highly correlated with DBH—the coefficient of determination exceeded 0.9. A power-type regression was used, since this function type best fits the data. The approach of relating total biomass of the tree to its DBH will hereinafter be referred to as the “site-specific method M1”.

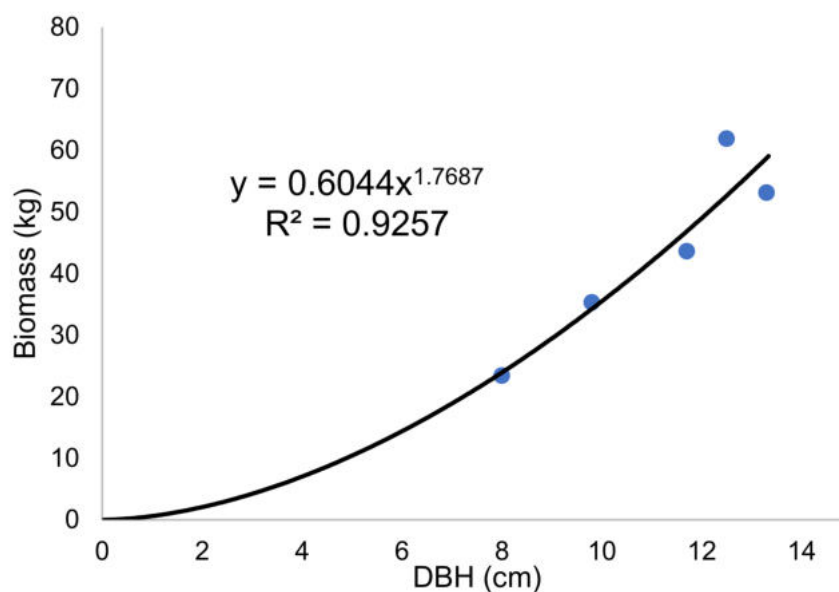


Figure 3. In situ allometric equation derived as the relationship between total dry biomass and diameter at breast height (DBH) of five model trees.

To estimate the biomass of the different tree components, particular functions can be fitted. However, Picard et al. (2012) suggested that these should be used together (equation matrix) rather than separately (simple sum) when calculating total tree biomass [27]. In our work, the parameters were obtained for individual components based on direct in situ measurements; these were summed to derive the whole tree biomass. Stem increment of the average tree determined from dendrometer measurements was used to relate the biomass of individual tree components to DBH. The resulting set of empirical equations is presented below (Equation (1)), hereinafter referred to as the “site-specific method M2”.

$$\text{Total dry biomass} = \sum \begin{array}{l} 0.3932 \text{ DBH}^{1.7298} - a \\ 0.0122 \text{ DBH}^{2.5525} - b \\ 0.0586 \text{ DBH}^{1.635} - c \\ 0.0537 \text{ DBH}^{1.5844} - d \\ 0.0381 \text{ DBH}^{2.0549} - e \\ 0.014 \text{ DBH} + 0.8245 - f \end{array} \quad \begin{array}{l} [R^2 = 0.99] \\ [R^2 = 0.72] \\ [R^2 = 0.75] \\ [R^2 = 0.70] \\ [R^2 = 0.87] \\ [R^2 = 0.67] \end{array} \quad (1)$$

where DBH—diameter at breast height, a —stem + bark biomass, b —thick branches biomass, c —needles biomass, d —thick roots biomass, f —small roots biomass. The coefficient of determination (R^2) for the obtained equations is given in square brackets.

In addition, we compared the results obtained from in situ allometric equations with those from Wegiel and Polowy [1], which were determined to be decent empirical estimations for comparison. Their research area was located about 50 km northwest of the Mezyk site, and their equations were derived for 82-year-old Scots pine. The climatic and meteorological conditions of both ecosystems are very similar.

2.6. Eddy Covariance Data Processing

Raw net ecosystem exchange (NEE) fluxes were calculated using commercial EddyPro software (version 7.0.1, Lincoln, NE, USA) with default settings. According to this mode, several processing steps were applied: despiking, amplitude resolution, drop-outs, absolute limits, skewness and kurtosis, discontinuities analysis. The following corrections were then made: angle of attack, since a Gill anemometer was used, double rotation correction, the time delay due to the separation of measuring instruments, block averaging and density correction (WPL). Basic filtering included stationarity test according to Mauder and Foken, [28], and thus only data with “0” flag were used here for further computation.

Fluxes measured during low turbulent conditions were removed by using friction velocity threshold as a sufficient turbulence parameter [29–31]. For this purpose, the measurement period was arbitrarily divided into monthly sub-periods. Friction velocity threshold (u^*_{th}) was calculated for each month and the data was filtered in these periods according to the given u^*_{th} value. Outliers were then removed, assuming monthly integration periods and two standard deviations value as a criterion. The “anomalize” package for R was used for this purpose [32]. The rate of concentration change (i.e., the storage flux) of CO_2 and H_2O (ΔSCO_2 and ΔSH_2O , respectively) in the air column below the EC system was also calculated in the EddyPro software [33]. Briefly, storage fluxes are obtained as the difference between the average concentration in the beginning and in the end of a specific averaging period (most often 30 min, as also in our study). This yielded similar results to those obtained with the concentration profile approach [34]. Both ΔSCO_2 and ΔSH_2O values were accounted for in the final fluxes calculations [35]. Finally, NEE fluxes gap-filling and partitioning into GPP and ecosystem respiration (R_{eco}) was performed using the “REddyProc” package [30] in the R environment [26], following the Reichstein night-time approach of using the air temperature measured under a canopy at 2 m above ground for the R_{eco} fluxes estimation [31,36–39]. In addition, water fluxes (given as evapotranspiration, ET) obtained by the EC method were calculated and gap-filled according to the same methodology as for the carbon fluxes, also using the REddyProc package [30].

The assimilation of atmospheric CO_2 is undoubtedly correlated with wood growth. However, due to the complexity of distinguishing irreversible seasonal wood growth from the increase in tree volume that results from reversible swelling and contraction of the stem, it was very difficult to determine this relationship, especially over a period of less than one year. The occurrence of the periodic reversible shrinkage or expansion of DBH mainly resulted from changes in the water content of plant tissue, and not from the actual increase in biomass. Nevertheless, there are various concepts regarding tree growth during periods of reversible contraction in response to water stress conditions. One such example is a concept of “zero growth” during periods of stem shrinkage, which utilizes a water-related growth threshold [40]. During a dry period, the stem may increase in size as a result of water-related swelling of stem tissues [41,42]. For example, a slight increase after longer periods of water shortage was observed in two deciduous and two evergreen trees species in one dry and two wetter sites in Switzerland; this increase was interpreted as activity during periods of stem swelling and shrinkage [40]. Therefore, due to these difficulties, we have presented the annual stem increment and the total biomass growth for both years.

2.7. Carbon Use Efficiency (CUE) and Definition of Vegetation Period

CUE ($CUE = NPP/GPP$) was calculated using the results obtained both by biometric and EC measurements. GPP obtained from the EC system has been summarized for each study year starting from the point when the annual cumulative value of net ecosystem productivity (NEP) was no longer negative relative to the maximum value of the previous year. The end of this range was defined when the positive annual growth of NEP ended and the cumulative values began to decline, suggesting the overall advantage of emissions over CO_2 absorption. This period will be referred hereinafter to the “vegetation period”, in order to differentiate this from the wood growth period (B) when the carbon absorbed during photosynthesis was turned into the growth of tree biomass.

For clarity, all described calculations and the final combination of results from dendrometric, biometric and EC measurements are presented in the diagram below (Figure 4).

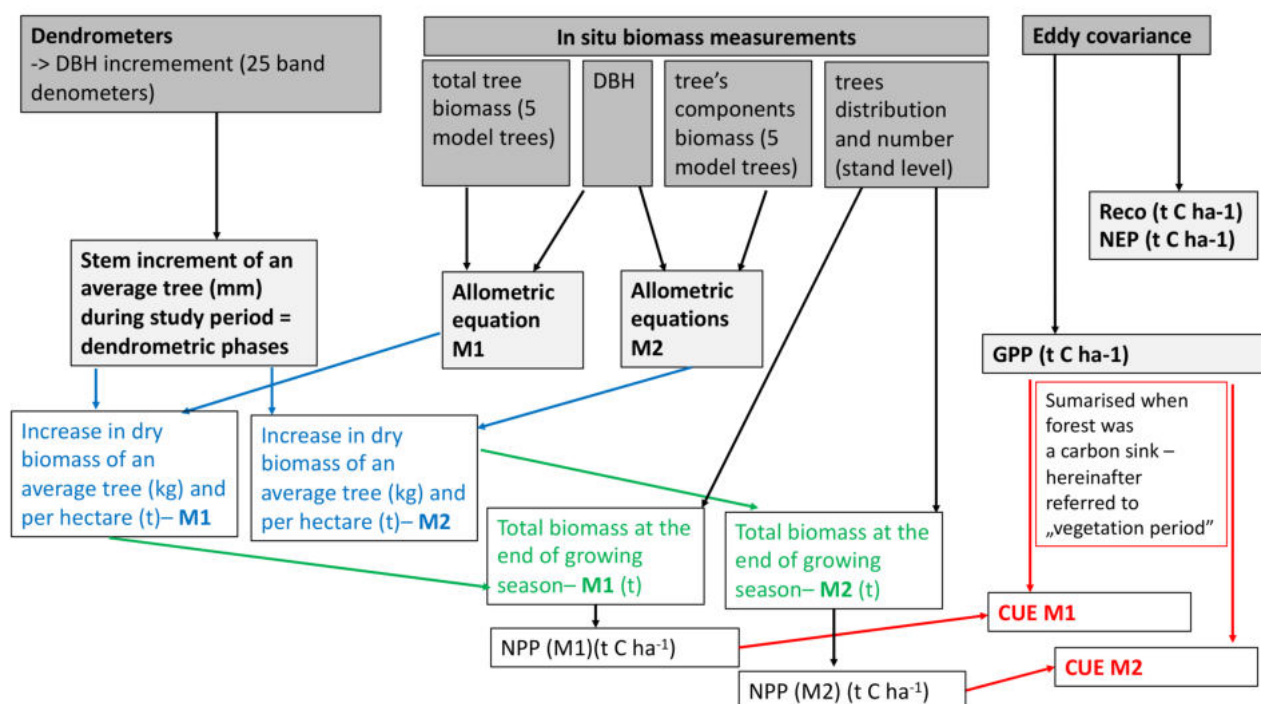


Figure 4. Schematic of data analysis and calculation combining results from dendrometric, biometric and EC measurements for obtaining net primary productivity (NPP), gross primary productivity (GPP) and carbon use efficiency (CUE).

2.8. Drought Conditions Estimates

To present the characteristics of individual months in terms of drought occurrence over the study period (2019–2020), the SPEI Global Drought Monitor database was used [43]. Standardized precipitation evapotranspiration index (SPEI) is a multiscale drought index that combines precipitation and temperature data based on normalization of water balance estimation [44]. Detailed methodology for calculating and applying this indicator is presented in the literature [44–46]. In addition, complete description of the used data and metadata can be found online [<https://spei.csic.es/home.html> access on 1 February 2021].

3. Results

3.1. Drought Occurrence Detected by SPEI Index Monitoring

SPEI index values over a three-month time scale were used here, since it is assumed that such scale allows effective assessment of meteorological drought intensity. The reference period ranges from 1950 to 2020, and the values of this index since 1981 are shown in Figure 5. Lower negative results indicate more severe drought in a given month. Extreme droughts are characterized by SPEI values of less than -2 . Such conditions occurred at ME study area in August 2019, as well as in July and August 2018. It should be noted that even though there were several dry months during both study years, fewer severe drought events occurred in 2020 than in 2019 (Figure 5).

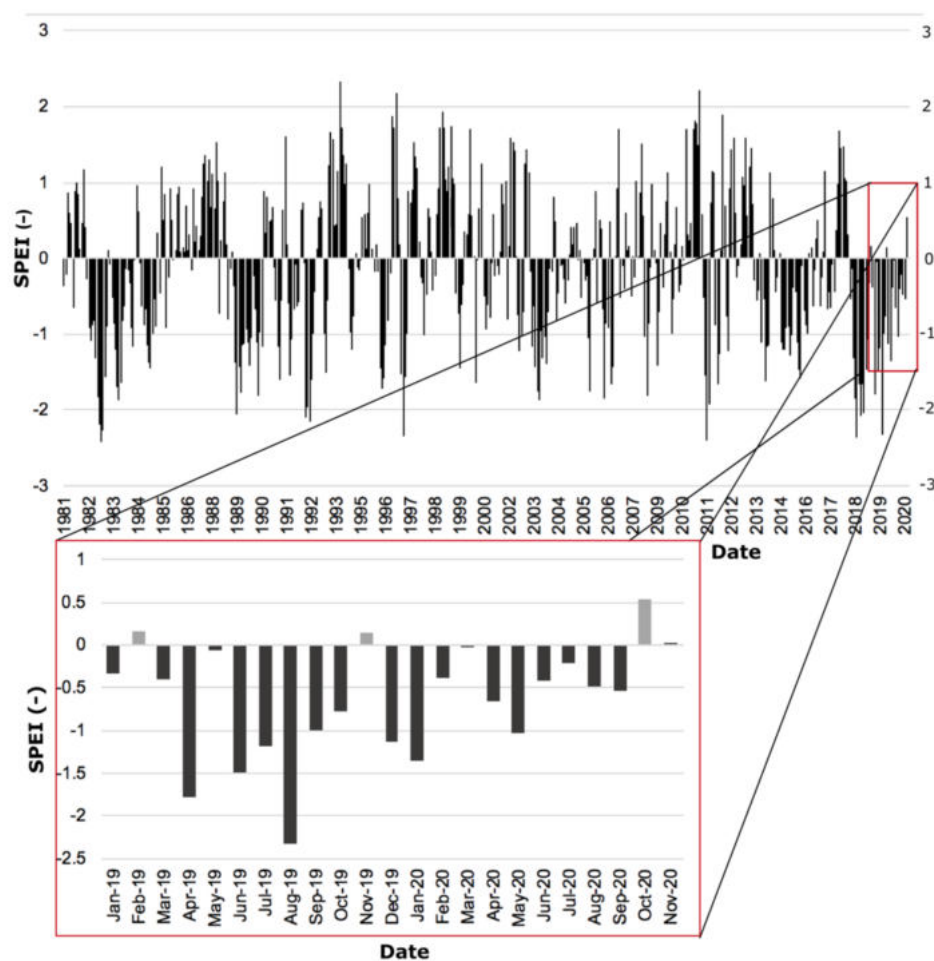


Figure 5. SPEI (standardized precipitation evapotranspiration index) values estimated over a three month scale during the period of 1981–2020 (**upper panel**), and for individual months during 2019–2020 (**bottom panel**). Reference period: 1950–2020, based on SPEI Global Drought Monitor database [43].

3.2. Meteorological Conditions and CO_2 and H_2O Fluxes Courses

The highest monthly precipitation for 2019 was recorded in September (more than 100 mm), and the lowest in April and June (both less than 20 mm). In 2020, the drought conditions in April were even more severe, as the sum of P for that month did not exceed 10 mm. On the other hand, precipitation conditions during the summer season of 2020—which is important for tree growth and development—were generally much more favorable than in the previous year (Table 2). In 2020, the highest monthly precipitation total was recorded in July, and amounted to slightly less than 100 mm. In general, 2019 was drier and warmer than 2020. However, annual GPP totals were quite similar, while ET reached significantly higher values in 2020, particularly during the summer (Table 2). The ratio between annual totals of R_{eco} and GPP were similar between the years (0.75 and 0.76 in 2019 and 2020, respectively). Thus, the difference between GPP and R_{eco} , which in principle constitutes net primary productivity (NEP), was only slightly higher in 2019. Compared to 2019, 2020 was characterized by lower mean T_{air} , vapor pressure deficit VPD, global radiation (R_g), and higher mean SWC. Aside from spring, higher R_{eco} totals were measured in 2020 on the seasonal scale. ET sums for spring and summer, as well as annually, were also higher in 2020 than the previous year. Even though ET totals in autumn were almost equal in both years, precipitation totals were substantially higher in autumn of 2019 than in 2020 (Table 2). In spite of the higher T_{air} , VPD and R_g in autumn 2020, the SWC was almost the same as in 2019. Regardless of the season, GPP totals were higher with higher average

T_{air} and higher SWC. Even though increased precipitation was recorded in spring and autumn of 2019, this did not correspond to increasing SWC. As such, SWC in spring of 2019 was lower than in 2020. It should be noted that in spring and summer (i.e., the most important periods for plant growth), photosynthesis rates (GPP) were higher in 2019. This likely resulted from the higher average temperatures and slightly higher radiation than summer, even with lower soil water content (Table 2).

Table 2. Annual and seasonal (spring: March–May, summer: June–August, and autumn: September–November) precipitation totals (P), mean vapor pressure deficit (VPD), mean global radiation (R_g), mean soil water content (SWC), and totals of gross primary productivity (GPP), ecosystem respiration (R_{eco}) and evapotranspiration (ET) during the period 2019–2020 at the ME site.

| YEAR | P (mm) | T _{air} (°C) | VPD (kPa) | R _g (Wm ⁻²) | SWC (%) | GPP (gCm ⁻²) | R _{eco} (gCm ⁻²) | ET (mm) |
|-------------|--------|-----------------------|-----------|------------------------------------|---------|--------------------------|---------------------------------------|---------|
| 2019 | 509 | 9.87 | 0.37 | 127.7 | 6.7 | 1724 | 1284 | 479 |
| 2020 | 624 | 9.73 | 0.33 | 127.2 | 8.6 | 1727 | 1316 | 493 |
| Spring 2019 | 116 | 9.32 | 0.49 | 165.3 | 7.7 | 536 | 301 | 129 |
| Spring 2020 | 98 | 7.97 | 0.39 | 191.4 | 9.9 | 511 | 259 | 140 |
| Summer 2019 | 70 | 18.48 | 0.76 | 238.4 | 5.1 | 776 | 527 | 168 |
| Summer 2020 | 232 | 17.45 | 0.58 | 209.7 | 5.5 | 765 | 575 | 181 |
| Autumn 2019 | 191 | 9.64 | 0.12 | 71.8 | 7.1 | 314 | 330 | 112 |
| Autumn 2020 | 132 | 10.32 | 0.25 | 75.8 | 7.0 | 317 | 352 | 100 |

3.3. Identification of Specific Periods during Wood Growth

In order to determine the individual dendrometric phases, the stem increment for both studied years was followed. In order to distinguish growth processes from reversible water-related processes and to avoid the disturbing effects of rapid freezing-induced changes in stem diameter during winter, the starting point for annual radial growth of the stem was set as the previous year's culmination [47]. The point of the maximum winter contraction (MWC) occurred at a similar time in both years (21 April 2019 and 23 April 2020) (Figure 6a). From that moment, rapid relaxation began and DBH increased simultaneously. However, in order to quantify the actual increase, the biomass growth was estimated from the beginning of seasonal growth after rehydration—i.e., 1 May and 2 May for 2019 and 2020, respectively, until the end of the growing period when DBH stopped increasing. In early October 2019, the end of the seasonal increase in biomass was recorded (tree circumferential growth), while the DBH growth continued in 2020 until mid-October (Figure 6a). Thus, the total period of actual wood growth (B) was 14 days longer in the second year. During winter, the change in DBH was caused by reversible trunk variations. The beginning of the seasonal biomass growth was then assessed from the cessation of growth in the previous year (P0 point). By applying the methodology described in the Materials and Methods section (Figure 4) and recognizing B period range for the average tree, NPP was calculated for both years. (Figure 6b).

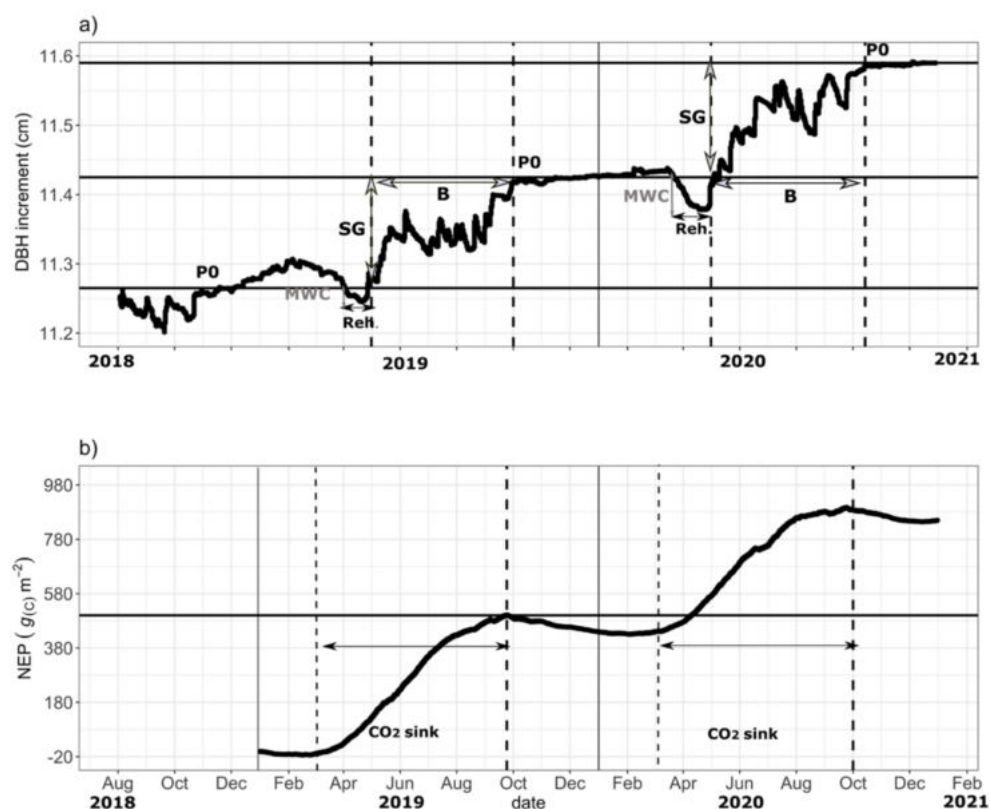


Figure 6. Specific moments and periods of tree growth based on: (a) dendrometers and (b) eddy covariance measurements. SG—Stem increment over the year, related to seasonal growth, MWC—maximum winter stem contraction, B—wood growth period, P0—the zero-point of the current year that corresponds to the respective culmination point of the past year, NEP—net ecosystem productivity, CO₂ sink—ecosystem productivity over the year.

Differences in the course of DBH growth between the years are visible, especially in summer—August in particular—when dry conditions prevailed in 2019 year (Figure 6a). According to the theory of zero growth during periods of stem shrinkage, the increase in biomass was significantly limited in the most optimal period in terms of productivity [40], since any potential growth-induced expansion is associated with the time after tree water deficit-induced reversible stem shrinkage has completely ceased. In 2019, the increase in DBH was on average 0.14 mm per tree, while in 2020 it was 0.16 mm, so the difference was over two hundredths of a millimeter. Nevertheless, considering there is over 4200 trees per hectare in our study area, even a small change in DBH increment over a year can translate into an increase in carbon accumulation in the biomass by as much as 0.6 tons per hectare (Figure 6; Table 3).

3.4. Stand Biomass and CUE Estimations

As shown above, the total increase in biomass was determined starting from the point after the rehydration period (Figure 6a). EC-derived GPP for the vegetation period ranged from the beginning of March to the end of September for both years (Figure 6b.). The estimates of NPP and GPP allowed the calculation of the CUE values. It should be pointed out that GPP summarized for the vegetation period represents the total CO₂ amount absorbed from the atmosphere which could be then potentially be built into the tree's tissues as carbon (C).

Table 3. Results of the dry biomass estimations including above- and belowground biomass for two site-specific allometric equations M1 (one equation for the whole tree) and M2 (separate formulas for tree components), based on dendrometers and in situ biometric measurements, including deadwood and understory (NPP) as well as NEP and GPP values derived from the eddy covariance observations. B—wood growth period.

| Year | 2019 | | 2020 | |
|--|-----------------|-----------------|-----------------|-----------------|
| | M1 | M2 | M1 | M2 |
| Total stem increment of an average tree (cm)—dendrometers | 0.142 ± 0.01 | - | 0.164 ± 0.01 | - |
| Total increase in dry biomass of an average tree (kg) | 0.942 ± 0.070 | 0.978 ± 0.072 | 1.206 ± 0.070 | 1.255 ± 0.073 |
| Total biomass of the stand at the end of growing seasons (t ha ⁻¹) | 203.387 ± 0.295 | 204.017 ± 0.306 | 208.861 ± 0.298 | 209.714 ± 0.310 |
| Total increase in dry biomass of the stand (t ha ⁻¹) | 4.273 ± 0.295 | 4.439 ± 0.306 | 5.473 ± 0.298 | 5.697 ± 0.310 |
| Total NPP (t C ha ⁻¹) | 2.137 ± 0.148 | 2.220 ± 0.153 | 2.737 ± 0.149 | 2.849 ± 0.155 |
| GPP total during vegetation period (t C ha ⁻¹) | | 14.70 | | 14.49 |
| NEP total during vegetation period (t C ha ⁻¹) | | 5.00 | | 4.50 |
| CUE for vegetation period | 0.15 | 0.15 | 0.19 | 0.20 |
| GPP total during B (t C ha ⁻¹) | | 11.79 | | 11.74 |
| NEP total during B (t C ha ⁻¹) | | 3.70 | | 3.19 |
| CUE for B | 0.18 | 0.19 | 0.23 | 0.24 |

Using the first method of the allometric equation with the general formula (M1), an absolute increase in dry biomass of 0.9 kg per average tree was estimated in 2019, and 1.2 kg in 2020 (Table 3). Considering the number of trees estimated at our study site (4262 per hectare), the total increase in dry biomass was approximately 4.3/4.4 t C ha⁻¹ in 2019, and 5.5/5.7 t C ha⁻¹ in 2020 (calculated by M1/M2 method, respectively). Consequently, NPP was approximately 2.1/2.2 t C ha⁻¹ in 2019, and 2.7/2.8 t C ha⁻¹ in 2020. A possible uncertainty was also given, considering an error that could occur when determining the phases of the biomass increase (± 0.01 cm for initial increment measurement; Table 3). This also reveals how the 0.01 cm of the average DBH increment for each tree translates into the estimation of the total forest biomass during the year (the difference of 0.01 mm, depending on the method, gives an error of ca. 0.3 kg of the total dry biomass of the stand unit area).

The total amount of absorbed CO₂ (GPP) during the vegetation period was higher in 2019 than in 2020 (Table 3). However, the sum of respired CO₂ (R_{eco}) during the same period was slightly higher in 2020 (10 t C ha⁻¹) than in 2019 (9.7 t C ha⁻¹). Hence, the difference between GPP and R_{eco}, which essentially constitute Net Ecosystem Productivity (NEP), was higher in 2019. Nevertheless, CUE, which is a key indicator of how much absorbed CO₂ was fixed and converted into fresh wood growth, was higher in 2020. CUE has been calculated both for the vegetation period (different periods for total annual NPP and total annual GPP) and the wood growth period (B) (Figure 6; Table 3). It was found that CUE for the vegetation period remained fairly low in both years, although it was higher in 2020; depending on the method, it was estimated to be 0.19/0.20 (M1/M2). In 2019, it was estimated to be 0.15 using both methods. For the B period, CUE values were 0.18/0.19 and 0.23/0.24 in 2019 and 2020, respectively (Table 3).

4. Discussion

4.1. NPP Biometric Estimates

Forests absorb carbon dioxide in the process of photosynthesis. Part of it is fixed in plant biomass (carbon sequestration), while some returns back to the atmosphere through ecosystem respiration. In this study, biometric measurements and derived site-specific allometric equations (M1/M2 method) showed that, on average, 2.0/2.1 t C ha⁻¹ was sequestered in wood tissues of a 25-year-old Scots pine stand (annual NPP totals) in dry 2019. In the following year, characterized by moderate water availability, these values

were 2.6/2.7 t C ha⁻¹ (Table 3). Among various forest types, boreal forests are the least productive (the lowest annual NPP totals) in comparison to temperate and especially tropical forests. The results from the global studies conducted by Xu et al. suggest that, on average, less than 10 tons of carbon per hectare is assimilated in boreal forests in the form of new woody tissue, while more than 12 tons of carbon per hectare is sequestered in temperate forest ecosystems [48]. On the other hand, Xu et al. [48] have shown that across biomes, the highest NPP is found in middle-aged forests (mean = 6.5 t C ha⁻¹), while young forests showed the lowest NPP (average = approx. 4 t C ha⁻¹) [48]. The respective results presented in our study indicate annual NPP totals several times lower than the average for boreal forests, and roughly two times lower than the average for young forests, even though the research was conducted at a Scots pine stand located in a temperate climatic zone. This surprising outcome is likely related to the young age of the stand, and further to the extreme meteorological conditions that occurred in the year 2019 (extreme drought) and slow recovery in 2020, in which the impact of the previous year's conditions was still noticeable. Another reason for these lower values could be the differences in methodology between cited study presented above, which covers various species of the climatic zones, while our study concerns only one dominant tree species. Drake et al. [17] reported NPP values twice as high as those found at the ME site—roughly 4 t C ha⁻¹ year⁻¹ for forests of loblolly pine older than 20 years. These authors also report the highest NPP for trees younger than 20 years (assuming NPP as the sum of wood, foliar, and fine roots production), concluding that for this pine species, NPP generally decreases with age after reaching this maximum [17]. There has been broad discussion in the literature addressing the question of the decrease in NPP with forest age. This revealed, inter alia, that the decline in GPP—rather than an increase in Ra—was the cause of NPP decrease as pine trees aged [17]. Sapwood respiration, which is an important component of Ra, also decreases with age. The decrease in pine GPP was driven by the age-related decrease in canopy conductance, which is in line with the hydraulic limitation hypothesis of Ryan et al. [17,49]. Hence, it is expected that in the future, stand biomass growth that was currently estimated for the Mezyk site will most probably decrease. Further studies are needed to show at what age exactly NPP reaches its maximum for this temperate Scots pine stand, and what meteorological conditions will be conducive to this.

4.2. Differences between Meteorological Conditions in 2019 and 2020 and Their Impact on NPP and GPP, and CUE Values

It has been suggested that carbon use efficiency decreases with forest age [19]. In our study, CUE increased in 2020 compared to the previous year, which comes from only slightly higher annual total of GPP with generally higher NPP. This can be explained by more favorable environmental conditions—higher average soil water content and higher precipitation totals, both annually and in the summer—which led not only to a higher NPP/GPP ratio, but also to higher total ET fluxes. Stomata minimize the amount of transpired water per given gross primary productivity (GPP) rate under scarce water conditions, which has a theoretical basis in photosynthesis and air humidity control on stomatal conductance [50]. Therefore, by reducing water loss during drought conditions while maintaining photosynthesis at a fairly stable level for as long as possible, drought conditions have a greater impact on the annual variation in ET totals than GPP. ET sums were lower both in spring and summer of 2019 (Table 3.), when dry conditions were more severe. The differences in meteorological conditions between 2019 and 2020 resulted in only slight changes in photosynthesis and transpiration fluxes. Considering their influence on NPP, the impact was significant—almost 1 t C ha⁻¹ more in woody biomass in 2020 compared to dry 2019. The drought that occurred in 2019, especially in June and August, has particularly important consequences. Since the highest GPP values were observed in summer months (in 2020 constituting 52.8% of the total vegetation period GPP, and 44.3% of its annual total), their contribution was crucial on the annual basis. Thus, significant reduction due to drought can lead to the decrease in summer contribution to both vegetation period and annual GPP totals. Nevertheless, in 2019, especially with a very

dry August, the share of GPP in relation to the entire year and the vegetation period was not less than in 2020 (52.8% and 45%, respectively).

The average annual CUE from across a range of forest ecosystems has been estimated as approximately 0.5, which means that, on average, half of the carbon absorbed in the photosynthesis process is allocated to the growth of wood tissue [51–53]. Nevertheless, reported CUE ranges from 0.2 to 0.8 depending on species, environmental, age and methodology [19,51,53,54]. According to the study of different-aged pine stands (6-, 19-, 34-, and 69-years-old) in southern Ontario, Canada, CUE varies greatly with age. Annual mean CUE during 2005–2008 amounted to 0.61, 0.33, 0.50, 0.43, respectively [2]. This research considered different climatic conditions of a 30-year norm, where the year 2005 was identified as hot and dry, 2006 as hot and wet, 2007 as warm and dry, and 2008 as a nearly average year. In another study conducted in a managed forest (afforestation) with predominantly *Pinus halepensis* species (Yatir Forest, Israel), annual CUE ranged from 0.38 to 0.42, depending on the method used [51]. Thus, it can be concluded that in relation to similar ecosystem types (temperate pine forest), the CUE values presented in our study are quite low.

It is worth emphasizing that wood growth is even more drought sensitive than photosynthesis itself [24,55,56]. Nevertheless, when severe drought occurs, the photosynthesis rate slows due to stomata enclosure, and biomass growth is also reduced [57]. In the research by Campioli et al. conducted at a temperate beech forest, it was shown that annual GPP totals were significantly lower in years when drought occurred, compared to wetter years; a corresponding significant decrease in NPP was also seen [24]. Hence, in dry years the annual NPP/GPP ratio was still quite high (40–44%). The data shows that the reduction in annual net primary productivity in our study is related to the occurrence of conditions distant from the comfort zone (in this case, the occurrence of drought). This can be explained by the adaptation process in which forest ecosystems adjust their optimal productivity to the climatic conditions of the region that used to be close to the average [2]. In addition, Peichl et al. [2] observed a negative relationship between NPP and air temperature, which is opposite to the common understanding of the NPP climate response in forests [58]. Such effect also seems true for our research, where a lower NPP total occurred in the warmer year. However, this was more likely caused by drought and/or heat stress, which are generally limiting conditions of NPP in warmer years [59]. Importantly, our results are based on only two years of data (one of which being extreme climate conditions), making them less reliable in supporting the findings of Peichl et al. [2]. Moreover, summer of 2020 was cooler, such that the total GPP sum was lower than in the previous year. A higher total NPP is recorded in years characterized by dry conditions—for example in the research by Campoli et al., who found a relatively high NPP during the extremely dry 2003, which is even more difficult to explain [24]. One possibility is interannual growth buffers such as C reserves and buds preformed in the previous year, especially if it was climatically medium or wet. This was not the case in our study, since 2019 followed a very dry year, which probably also influenced the presented biomass growth results. The average value of the SPEI index from March to October in 2018 amounted to -1.64 . Extreme drought was evident in June (SPEI = -2.36) and August (SPEI = -2.09). Furthermore, extreme conditions such as drought often hinder thorough analysis and interpretation, as well as different physiological responses of plants to the existing conditions. Plants adopt a special “strategy” as they partition resources among different organs for optimal functioning. This helps to maximize life span, seed production, and growth rate under particular environmental conditions [60]. It was found that in a tropical forest, the lowest CUE (0.35) occurred in undisturbed forest patches, while slight forest disturbance had a positive effect on CUE increase (0.62) [7]. Moreover, the authors of this study suggest that monocultures had a higher CUE than mixed forest stands. In our research, the difference in NPP resulted in approximately $0.600 \text{ t C ha}^{-1}$. Applying the literature-derived method (excluding dead branches) yielded in $0.566 \text{ t C ha}^{-1}$ for the ME site [1]. The literature-derived absolute sums of biomass and NPP were approximately 20–30% lower than those calculated by constructing equations based on in situ data, which amounted to 1.7 C ha^{-1} for 2019 and

1.9 C ha⁻¹ for 2020. It was thus concluded that in biomass research, site-specific equations are more likely to give robust results. The literature-based solution resulted in very low CUE, which amounted to roughly 0.13 for 2019 and 0.15 for 2020.

4.3. Difficulties in Calculating NPP as a Part of GPP Using Different Approaches

The use of allometric relationships between stem diameter (DBH) and tree biomass can lead to systematic errors in aboveground NPP estimates [14]. It has also been suggested that the use of inadequate allometric equations and uncertainty in the estimates of fine-grained litter production potentially introduces significant errors in biometric estimates of NPP [2,61–63]. Several reports have showed that discrepancies between biometric and EC measurements on an annual basis may be caused by the time-lag between carbon assimilated in photosynthesis and its allocation represented by stem growth [64]. Nevertheless, relative annual changes of NEP were found to be comparable between the two estimation methods, even when there were differences in its absolute values [65–67]. In our research, lower productivity in spring and summer (GPP) was associated with less severe drought events in 2020, although Reco increased in the summer and autumn of this year and was thus higher than in 2019. In general, the highest respiration fluxes were found to be in the summer, apparently caused not only by high temperatures but also higher overall plant activity (leaves and fine-roots are present and active, growth is occurring, etc.) [31]. The total EC-derived sum of NEP from March to October was higher in 2019 by 0.5 t C ha⁻¹ than in 2020 (Table 3). Higher NPP values were estimated for the same period in 2020 with biometric methods. Thus, the results obtained in our study suggest that higher NPP values estimated with biometric equations are associated with lower GPP and higher CUE. These may occur together with a lower NEP derived from EC measurements in the same season (Table 3). Notably, it is assumed that if the share of GPP used for respiration changes depending on soil conditions, NPP should also vary according to the ratio of NPP to GPP. Collati and Prentice attempted to answer the question posed by Waring et al. [52] 20 years earlier, and investigated if NPP of forests is a constant fraction of GPP. Their results provided evidence to reject the hypothesis of a universal or constant ratio of NPP to GPP, which in fact changes under disturbances, ageing and changes in biomass accumulation with changing climate, soil fertility and management practices. These have all been indicated to influence the ratio of NPP to GPP, likely in a non-mutually exclusive manner [68]. However, this approach was already implemented as a simplified concept in a large number of ecosystem models. In our research, such variation was also true: very similar GPP values estimated for different years under varying conditions did not change proportionally to NPP totals in the studied period. On the contrary, they indicated greater wood growth in a moderately wet year with higher soil water content during spring and summer.

It is often considered that low CUE results do not reflect a significant underestimation of NPP, but are more likely related to the overestimation of GPP, since CO₂ fluxes measured by the EC method are prone to uncertainties. Different conclusions have been reached when using the open path (OP) analyzers as compared to closed path (CP) analyzers. For instance, Richardson et al. compared random CO₂ fluxes using concurrent CP and OP measurements above soybean and maize crop [69]. The authors found differences in random flux uncertainty to be negligible during the day, while at night the random uncertainty of the OP system exceeded that of the CP systems by up to 20%. On the contrary, another study suggested very small differences in the random flux uncertainty between CP and OP systems [70]. Some of the latest results from Bog Lake Peatland flux tower (US-MBP on AMERIFLUX) suggest that during the growing season, the OP system measured larger net daytime CO₂ uptake than the CP sensor did, while the OP and CP CO₂ fluxes tended to converge at night [71]. A specific difficulty in the methodology used here was the appropriate estimation of the end of period for the stem diameter increment in 2018, which was the reference point for the start of the biomass growth in 2019. Interpreting data from band dendrometers becomes difficult due to reverse contractions and swelling of

the stem, especially in winter. It has been found that the effects of freezing temperatures on plant functions differ greatly from those caused by low, but non-freezing, temperatures [72]. Severe dehydration can be caused by the formation of extracellular ice under freezing conditions, so that the plant retains its ability to cope with these conditions [73]. As a consequence of hardening the plant in response to cold, the lipid composition [74], membrane structure [75] and sugar concentration [76] vary greatly, and some specific metabolites, including proteins that prevent freezing, accumulate [72,77]. This, among other issues, caused the visible swelling of the stem that was observed in January 2019, which was not related to wood growth.

5. Conclusions

Our study of a 25-year-old temperate Scots pine monoculture in north-western Poland has led to several conclusions:

Using five sampled trees at the Mezyk research area, the combination of biomass measurements, continuous dendrometric measurements, and recognition of the stand structure allowed site-specific allometric equations to be derived. Absolute values of wood biomass growth in 2019 and 2020 were also calculated, which were more robust than literature-derived equations.

The drought in spring and summer 2019 was preceded by even more severe drought in 2018. As a result of this extreme water conditions, the NPP in this young Scot pine monoculture was about 0.6 t C ha^{-1} lower than in moderately wet 2020.

The higher temperatures in spring and summer led to higher GPP in these seasons in 2019, despite the lower precipitation and soil water content. On an annual basis, GPP totals were comparable between the years. Slight changes in GPP sums during vegetation periods of the study period did not correspond to proportional variation in NPP total sums, which were considerably higher in the wetter year.

The thermal and humidity conditions that occurred in 2020 were more favorable than in 2019. This resulted in higher R_{eco} and NPP sums, despite the lower GPP and NEP in 2020, which resulted in higher efficiency in the use of carbon assimilated due to photosynthesis for new wood production (CUE).

Author Contributions: Conceptualization: P.D. and K.Z.; methodology: P.D.; formal analysis: J.O., S.M., T.V., M.U.; resources: J.O., S.M.; data curation: P.D., M.U.; writing—original draft preparation: P.D.; writing—review and editing: K.Z., M.U., T.V.; visualization: P.D.; supervision: M.U.; project administration: J.O.; funding acquisition: J.O., S.M. All authors have read and agreed to the published version of the manuscript.

Funding: This research was supported by funding from General Directorate of the State Forests, Warsaw, Poland (project LAS, No OR-2717/27/11).

Data Availability Statement: Data available on request. The data presented in this study are available on request from the corresponding author. The data are not publicly available due to the unfinished repository, however, the authors are willing to share it.

Acknowledgments: We would like to express our gratitude to soil scientist team from the Department of Ecology and Silviculture, Faculty of Forestry, University of Agriculture in Krakow, for their fieldwork, expertise and preliminary data analysis, and to the Tyumen region government in accordance with the Program of the World-Class West Siberian Interregional Scientific and Educational Center (National Project “Nauka”). The authors would like to thank Jacquelin DeFaveri from Language Centre at University of Helsinki for their help with revising the language.

Conflicts of Interest: The authors declare no conflict of interest. The funders had no role in the design of the study, the collection, analyses, and interpretation of data, the writing of the manuscript, or in the decision to publish the results.

References

1. Wegiel, A.; Polowy, K. Aboveground carbon content and storage in mature scots pine stands of different densities. *Forests* **2020**, *11*, 240. [[CrossRef](#)]
2. Peichl, M.; Brodeur, J.J.; Khomik, M.; Arain, M.A. Biometric and eddy-covariance based estimates of carbon fluxes in an age-sequence of temperate pine forests. *Agric. For. Meteorol.* **2010**, *150*, 952–965. [[CrossRef](#)]
3. Dixon, R.K.; Solomon, A.M.; Brown, S.; Houghton, R.A.; Trexler, M.C.; Wisniewski, J. Carbon Pools and Flux of Global Forest Ecosystems. *Science* **1994**, *263*, 185–190. [[CrossRef](#)]
4. Denman, K.L.; Brasseur, G.; Chidthaisong, A.; Ciais, P.; Cox, P.M.; Dickinson, R.E.; Hauglustaine, D.; Heinze, C.; Holland, E.; Jacob, D.; et al. Couplings Between Changes in the Climate System and Biogeochemistry. In *Climate Change 2007: The Physical Science Basis. Contribution of Working Group I to the Fourth Assessment Report of the Intergovernmental Panel on Climate Change*; Solomon, S., Qin, D., Manning, M., Chen, Z., Marquis, M., Averyt, K.B., Tignor, M., Miller, H.L., Eds.; Cambridge University Press: Cambridge, UK; New York, NY, USA, 2007; pp. 501–568.
5. Urban, J.; Čermák, J.; Ceulemans, R. Above- and below-ground biomass, surface and volume, and stored water in a mature Scots pine stand. *Eur. J. For. Res.* **2015**, *134*, 61–74. [[CrossRef](#)]
6. Manickam, V.; Krishna, I.V.M.; Shanti, S.K.; Radhika, R.; Campus, B.V.; Pradesh, A. Biomass Calculations for Carbon Sequestration in Forest Ecosystem. *J. Energy Chem. Eng.* **2014**, *2*, 30–38.
7. Kunert, N.; El-Madany, T.S.; Aparecido, L.M.T.; Wolf, S.; Potvin, C. Understanding the controls over forest carbon use efficiency on small spatial scales: Effects of forest disturbance and tree diversity. *Agric. For. Meteorol.* **2019**, *269–270*, 136–144. [[CrossRef](#)]
8. Juráň, S.; Grace, J.; Urban, O. Temporal Changes in Ozone Concentrations and Their Impact on Vegetation. *Atmosphere* **2021**, *12*, 82. [[CrossRef](#)]
9. Bréda, N.; Huc, R.; Granier, A.; Dreyer, E. Temperate forest trees and stands under severe drought: A review of ecophysiological responses, adaptation processes and long-term consequences. *Ann. For. Sci.* **2006**, *63*, 625–644. [[CrossRef](#)]
10. Kumar, A.; Kumar, M. Estimation of Biomass and Soil Carbon Stock in the Hydroelectric Catchment of India and its Implementation to Climate Change. *J. Sustain. For.* **2020**, *39*, 1–16. [[CrossRef](#)]
11. Rai, P.; Vineeta; Shukla, G.; Manohar K, A.; Bhat, J.A.; Kumar, A.; Kumar, M.; Cabral-Pinto, M.; Chakravarty, S. Carbon storage of single tree and mixed tree dominant species stands in a reserve forest—Case study of the eastern sub-himalayan region of india. *Land* **2021**, *10*, 435. [[CrossRef](#)]
12. Zianis, D.; Muukkonen, P.; Mäkipää, R.; Mencuccini, M. *Biomass and Stem Volume Equations for Tree Species in Europe*; The Finnish Society of Forest Science: Helsinki, Finland; The Finnish Forest Research Institute: Helsinki, Finland, 2005; Volume 4, ISBN 9514019830.
13. Wohlfahrt, G.; Gu, L. The many meanings of gross photosynthesis and their implication for photosynthesis research from leaf to globe. *Plant Cell Environ.* **2015**, *38*, 2500–2507. [[CrossRef](#)] [[PubMed](#)]
14. Chambers, J.Q.; dos Santos, J.; Ribeiro, R.; Higuchi, N. Tree damage, allometric relationships, and aboveground net primary production in a tropical forest. *For. Ecol. Manag.* **2001**, *152*, 73–84. [[CrossRef](#)]
15. Chapin, F.S.; Woodwell, G.M.; Randerson, J.T.; Rastetter, E.B.; Lovett, G.M.; Baldocchi, D.D.; Clark, D.A.; Harmon, M.E.; Schimel, D.S.; Valentini, R.; et al. Reconciling carbon-cycle concepts, terminology, and methods. *Ecosystems* **2006**, *9*, 1041–1050. [[CrossRef](#)]
16. Clark, D.A.; Brown, S.; Kicklighter, D.W.; Chambers, J.Q.; Thomlinson, J.R.; Ni, J. Measuring net primary production in forests: Concepts and field methods. *Ecol. Appl.* **2001**, *11*, 356–370. [[CrossRef](#)]
17. Drake, J.E.; Davis, S.C.; Raetz, L.M.; Delucia, E.H. Mechanisms of age-related changes in forest production: The influence of physiological and successional changes. *Glob. Chang. Biol.* **2011**, *17*, 1522–1535. [[CrossRef](#)]
18. Bruchwald, A. New Empirical Formulae for Determination of Volume of Scots Pine Stands. *Folia For. Pol. Ser.* **1996**, *A 38*, 5–10.
19. DeLucia, E.H.; Drake, J.E.; Thomas, R.B.; Gonzalez-Meler, M. Forest carbon use efficiency: Is respiration a constant fraction of gross primary production? *Glob. Chang. Biol.* **2007**, *13*, 1157–1167. [[CrossRef](#)]
20. Zanutelli, D.; Montagnani, L.; Manca, G.; Tagliavini, M. Net primary productivity, allocation pattern and carbon use efficiency in an apple orchard assessed by integrating eddy covariance, biometric and continuous soil chamber measurements. *Biogeosciences* **2013**, *10*, 3089–3108. [[CrossRef](#)]
21. Law, B.E.; Sun, O.J.; Campbell, J.; Van Tuyl, S.; Thornton, P.E. Changes in carbon storage and fluxes in a chronosequence of ponderosa pine. *Glob. Chang. Biol.* **2003**, *9*, 510–524. [[CrossRef](#)]
22. Doughty, C.E.; Goldsmith, G.R.; Raab, N.; Girardin, C.A.J.; Farfan-Amezquita, F.; Huaraca-Huasco, W.; Silva-Espejo, J.E.; Araujo-Murakami, A.; da Costa, A.C.L.; Rocha, W.; et al. What controls variation in carbon use efficiency among Amazonian tropical forests? *Biotropica* **2018**, *50*, 16–25. [[CrossRef](#)]
23. Anić, M.; Ostrogović Sever, M.Z.; Alberti, G.; Balenović, I.; Paladinić, E.; Peressotti, A.; Tijan, G.; Večenaj, Ž.; Vuletić, D.; Marjanović, H. Eddy covariance vs. biometric based estimates of net primary productivity of Pedunculate Oak (*Quercus robur* L.) forest in Croatia during ten years. *Forests* **2018**, *9*, 764. [[CrossRef](#)]
24. Campioli, M.; Gielen, B.; Göckede, M.; Papale, D.; Bouriaud, O.; Granier, A. Temporal variability of the NPP-GPP ratio at seasonal and interannual time scales in a temperate beech forest. *Biogeosciences* **2011**, *8*, 2481–2492. [[CrossRef](#)]
25. Małek, S.; Pająk, M.; Wosó, B.; Jasik, M. Zapas węgla w biomase drzewostanów sosnowych o różnym wieku wokół stacji pomiarowych: Tuczno, Mezyk, Tlen1 i Tlen2. In *Rola Lasu w Pochłanianiu Dwutlenku Węgla z Atmosfery*; Olejnik, J., Małek, S., Eds.; Wydawnictwo Uniwersytetu Przyrodniczego w Poznaniu: Poznań, Poland, 2020; pp. 123–134, ISBN 978-83-7160-971-8.

26. R Core Team. *R: A Language and Environment for Statistical Computing*; R Core Team: Vienna, Austria, 2020.
27. Picard, N.; Saint-André, L.; Henry, M. *Manual for Building Tree Volume and Biomass Allometric Equations: From Field Measurement to Prediction*; Food and Agricultural Organization of the United Nations, Rome, and Centre de Coopération Internationale en Recherche Agronomique pour le Développement: Montpellier, France, 2012; ISBN 9789251073476.
28. Mauder, M.; Foken, T. Impact of post-field data processing on eddy covariance flux estimates and energy balance closure. *Meteorol. Zeitschrift* **2006**, *15*, 597–609. [[CrossRef](#)]
29. Barr, A.G.; Richardson, A.D.; Hollinger, D.Y.; Papale, D.; Arain, M.A.; Black, T.A.; Bohrer, G.; Dragoni, D.; Fischer, M.L.; Gu, L.; et al. Use of change-point detection for friction–velocity threshold evaluation in eddy-covariance studies. *Agric. For. Meteorol.* **2013**, *171–172*, 31–45. [[CrossRef](#)]
30. Wutzler, T.; Lucas-Moffat, A.; Migliavacca, M.; Knauer, J.; Sickel, K.; Šigut, L.; Menzer, O.; Reichstein, M. Basic and extensible post-processing of eddy covariance flux data with REddyProc. *Biogeosciences* **2018**, *15*, 5015–5030. [[CrossRef](#)]
31. Reichstein, M.; Falge, E.; Baldocchi, D.; Papale, D.; Aubinet, M.; Berbigier, P.; Bernhofer, C.; Buchmann, N.; Gilmanov, T.; Granier, A.A.; et al. On the separation of net ecosystem exchange into assimilation and ecosystem respiration: Review and improved algorithm. *Glob. Chang. Biol.* **2005**, *11*, 1424–1439. [[CrossRef](#)]
32. Dancho, M.; Vaughan, D. anomalize: Tidy Anomaly Detection. 2020. Available online: <https://github.com/business-science/anomalize> (accessed on 29 June 2021).
33. LI COR, I. EddyPro®Software, Lincoln, Nebraska. 2019. Available online: <https://www.licor.com/env/support/EddyPro/software.html> (accessed on 29 June 2021).
34. Morgenstern, K.; Black, T.A.; Humphreys, E.R.; Griffis, T.J.; Drewitt, G.B.; Cai, T.; Nesic, Z.; Spittlehouse, D.L.; Livingston, N.J. Sensitivity and uncertainty of the carbon balance of a Pacific Northwest Douglas-fir forest during an El Niño/La Niña cycle. *Agric. For. Meteorol.* **2004**, *123*, 201–219. [[CrossRef](#)]
35. Ziemblińska, K.; Urbaniak, M.; Chojnicki, B.H.; Black, T.A.; Niu, S.; Olejnik, J. Net ecosystem productivity and its environmental controls in a mature Scots pine stand in north-western Poland. *Agric. For. Meteorol.* **2016**, *228–229*, 60–72. [[CrossRef](#)]
36. Falge, E.M.; Clement, R.J.; Baldocchi, D.D.; Dolman, H.; Burba, G.G.; Anthoni, P.; Aubinet, M.; Olson, R.; Bernhofer, C.; Ceulemans, R.; et al. Gap filling strategies for defensible annual sums of net ecosystem exchange. *Agric. For. Meteorol.* **2001**, *107*, 43–69. [[CrossRef](#)]
37. Gilmanov, T.G.; Johnson, D.A.; Saliendra, N.Z. Growing season CO₂ fluxes in a sagebrush-steppe ecosystem in Idaho: Bowen ratio/energy balance measurements and modeling. *Basic Appl. Ecol.* **2003**, *4*, 167–183. [[CrossRef](#)]
38. Körner, C. Leaf diffusive conductances in the major vegetation types of the globe. In *Ecophysiology of Photosynthesis*; Schulze, E.-D., Caldwell, M.M., Eds.; Springer: Berlin/Heidelberg, Germany, 1995; pp. 463–490, ISBN 9788578110796.
39. Lasslop, G.; Reichstein, M.; Papale, D.; Richardson, A.D.; Aarneth, A.; Barr, A.; Stoy, P.; Wohlfart, G. Separation of net ecosystem exchange into assimilation and respiration using a light response curve approach: Critical issues and global evaluation. *Glob. Chang. Biol.* **2010**, *16*, 187–208. [[CrossRef](#)]
40. Zweifel, R.; Haeni, M.; Buchmann, N.; Eugster, W. Are trees able to grow in periods of stem shrinkage? *New Phytol.* **2016**, *211*, 839–849. [[CrossRef](#)]
41. Hinckley, T.M.; Bruckerhoff, D.N. The effects of drought on water relations and stem shrinkage of *Quercus alba*. *Can. J. Bot.* **1975**, *53*, 62–72. [[CrossRef](#)]
42. Zweifel, R.; Zimmermann, L.; Newbery, D.M. Modeling tree water deficit from microclimate: An approach to quantifying drought stress. *Tree Physiol.* **2005**, *25*, 147–156. [[CrossRef](#)]
43. Beguería, S.; Latorre, B.; Reig, F.; Vicente-Serrano, S.M. SPEI Global Drought Monitor. Available online: <https://spei.csic.es/map/maps.html#months=1%23month=10%23year=2020> (accessed on 6 January 2020).
44. Vicente-Serrano, S.M.; Beguería, S.; López-Moreno, J.I. A multiscalar drought index sensitive to global warming: The standardized precipitation evapotranspiration index. *J. Clim.* **2010**, *23*, 1696–1718. [[CrossRef](#)]
45. Beguería, S.; Vicente-Serrano, S.M.; Reig, F.; Latorre, B. Standardized precipitation evapotranspiration index (SPEI) revisited: Parameter fitting, evapotranspiration models, tools, datasets and drought monitoring. *Int. J. Climatol.* **2014**, *34*, 3001–3023. [[CrossRef](#)]
46. Beguería, S.; Vicente-Serrano, S.M.; Angulo-Martínez, M. A multiscalar global drought dataset: The SPEI base: A new gridded product for the analysis of drought variability and impacts. *Bull. Am. Meteorol. Soc.* **2010**, *91*, 1351–1356. [[CrossRef](#)]
47. Zweifel, R.; Eugster, W.; Etzold, S.; Dobbertin, M.; Buchmann, N.; Häsler, R. Link between continuous stem radius changes and net ecosystem productivity of a subalpine Norway spruce forest in the Swiss Alps. *New Phytol.* **2010**, *187*, 819–830. [[CrossRef](#)]
48. Xu, B.; Yang, Y.; Li, P.; Shen, H.; Fang, J. Global patterns of ecosystem carbon flux in forests: A biometric data-based synthesis. *Glob. Biogeochem. Cycles* **2014**, *28*, 962–973. [[CrossRef](#)]
49. Ryan, M.G.; Phillips, N.; Bond, B.J. The hydraulic limitation hypothesis revisited. *Plant Cell Environ.* **2006**, *29*, 367–381. [[CrossRef](#)] [[PubMed](#)]
50. Ball, J.T.; Woodrow, I.E.; Berry, J.A. *A Model Predicting Stomatal Conductance and Its Contribution to the Control of Photosynthesis under Different Environmental Conditions*; Biggins, J., Ed.; Springer: Amsterdam, The Netherlands, 1987.
51. Maseyk, K.; Grünzweig, J.M.; Rotenberg, E.; Yakir, D. Respiration acclimation contributes to high carbon-use efficiency in a seasonally dry pine forest. *Glob. Chang. Biol.* **2008**, *14*, 1553–1567. [[CrossRef](#)]

52. Waring, R.H.; Landsberg, J.J.; Williams, M. Net primary production of forests: A constant fraction of gross primary production? *Tree Physiol.* **1998**, *18*, 129–134. [[CrossRef](#)]
53. Gifford, R.M. Plant respiration in productivity models: Conceptualisation, representation and issues for global terrestrial carbon-cycle research. *Funct. Plant Biol.* **2003**, *30*, 171–186. [[CrossRef](#)]
54. Thornley, J.H.M.; Cannell, M.G.R. Modelling the components of plant respiration: Representation and realism. *Ann. Bot.* **2000**, *85*, 55–67. [[CrossRef](#)]
55. Cannell, M.G.R.; Dewar, R.C. Carbon Allocation in Trees: A Review of Concepts for Modelling. *Adv. Ecol. Res.* **1994**, *25*, 59–104.
56. Leuschner, C.; Backes, K.; Hertel, D.; Schipka, F.; Schmitt, U.; Terborg, O.; Runge, M. Drought responses at leaf, stem and fine root levels of competitive *Fagus sylvatica* L. and *Quercus petraea* (Matt.) Liebl. trees in dry and wet years. *For. Ecol. Manag.* **2001**, *149*, 33–46. [[CrossRef](#)]
57. Granier, A.; Reichstein, M.; Bréda, N.; Janssens, I.A.; Falge, E.; Ciais, P.; Grünwald, T.; Aubinet, M.; Berbigier, P.; Bernhofer, C.; et al. Evidence for soil water control on carbon and water dynamics in European forests during the extremely dry year: 2003. *Agric. For. Meteorol.* **2007**, *143*, 123–145. [[CrossRef](#)]
58. Luyssaert, S.; Inglima, I.; Jung, M.; Richardson, A.D.; Reichstein, M.; Papale, D.; Piao, S.L.; Schulze, E.-D.; Wingate, L.; Matteucci, G.; et al. CO₂ balance of boreal, temperate, and tropical forests derived from a global database. *Glob. Chang. Biol.* **2007**, *13*, 2509–2537. [[CrossRef](#)]
59. Ciais, P.; Reichstein, M.; Viovy, N.; Granier, A.; Ogée, J.; Allard, V.; Aubinet, M.; Buchmann, N.; Bernhofer, C.; Carrara, A.; et al. Europe-wide reduction in primary productivity caused by the heat and drought in 2003. *Nature* **2005**, *437*, 529–533. [[CrossRef](#)] [[PubMed](#)]
60. Lacointe, A. Carbon allocation among tree organs: A review of basic processes and representation in functional-structural tree models. *Ann. For. Sci.* **2000**, *57*, 521–533. [[CrossRef](#)]
61. Curtis, P.S.; Hanson, P.J.; Bolstad, P.; Barford, C.; Randolph, J.; Schmid, H.; Wilson, K.B. Biometric and eddy-covariance based estimates of annual carbon storage in five eastern North American deciduous forests. *Agric. For. Meteorol.* **2002**, *113*, 3–19. [[CrossRef](#)]
62. Ketterings, Q.M.; Coe, R.; Van Noordwijk, M.; Ambagau, Y.; Palm, C.A. Reducing uncertainty in the use of allometric biomass equations for predicting above-ground tree biomass in mixed secondary forests. *For. Ecol. Manag.* **2001**, *146*, 199–209. [[CrossRef](#)]
63. Black, K.; Bolger, T.; Davis, P.; Nieuwenhuis, M.; Reidy, B.; Saiz, G.; Tobin, B.; Osborne, B. Inventory and eddy covariance-based estimates of annual carbon sequestration in a Sitka spruce (*Picea sitchensis* (Bong.) Carr.) forest ecosystem. *Eur. J. For. Res.* **2005**, *126*, 167–178. [[CrossRef](#)]
64. Gough, C.M.; Vogel, C.S.; Schmid, H.P.; Su, H.B.; Curtis, P.S. Multi-year convergence of biometric and meteorological estimates of forest carbon storage. *Agric. For. Meteorol.* **2008**, *148*, 158–170. [[CrossRef](#)]
65. Ehman, J.L.; Schmid, H.P.; Grimmond, C.S.B.; Randolph, J.C.; Hanson, P.J.; Wayson, C.A.; Cropley, F.D. An initial intercomparison of micrometeorological and ecological inventory estimates of carbon exchange in a mid-latitude deciduous forest. *Glob. Chang. Biol.* **2002**, *8*, 575–589. [[CrossRef](#)]
66. Ohtsuka, T.; Saigusa, N.; Koizumi, H. On linking multiyear biometric measurements of tree growth with eddy covariance-based net ecosystem production. *Glob. Chang. Biol.* **2009**, *15*, 1015–1024. [[CrossRef](#)]
67. Keith, H.; Leuning, R.; Jacobsen, K.L.; Cleugh, H.A.; van Gorsel, E.; Raison, R.J.; Medlyn, B.E.; Winters, A.; Keitel, C. Multiple measurements constrain estimates of net carbon exchange by a Eucalyptus forest. *Agric. For. Meteorol.* **2009**, *149*, 535–558. [[CrossRef](#)]
68. Collalti, A.; Prentice, I.C. Is NPP proportional to GPP? Waring’s hypothesis 20 years on. *Tree Physiol.* **2019**, *39*, 1473–1483. [[CrossRef](#)]
69. Richardson, A.D.; Hollinger, D.Y.; Burba, G.G.; Davis, K.J.; Flanagan, L.B.; Katul, G.G.; William Munger, J.; Ricciuto, D.M.; Stoy, P.C.; Suyker, A.E.; et al. A multi-site analysis of random error in tower-based measurements of carbon and energy fluxes. *Agric. For. Meteorol.* **2006**, *136*, 1–18. [[CrossRef](#)]
70. Haslwanter, A.; Hammerle, A.; Wohlfahrt, G. Open-path vs. closed-path eddy covariance measurements of the net ecosystem carbon dioxide and water vapour exchange: A long-term perspective. *Agric. For. Meteorol.* **2009**, *149*, 291–302. [[CrossRef](#)] [[PubMed](#)]
71. Deventer, M.J.; Roman, T.; Bogoev, I.; Kolka, R.K.; Erickson, M.; Lee, X.; Baker, J.M.; Millet, D.B.; Griffis, T.J. Biases in open-path carbon dioxide flux measurements: Roles of instrument surface heat exchange and analyzer temperature sensitivity. *Agric. For. Meteorol.* **2021**, *296*. [[CrossRef](#)]
72. Tanaka, A. Photosynthetic activity in winter needles of the evergreen tree *Taxus cuspidata* at low temperatures. *Tree Physiol.* **2007**, *27*, 641–648. [[CrossRef](#)]
73. Goldstein, G.; Nobel, P.S. Water relations and low-temperature acclimation for cactus species varying in freezing tolerance. *Plant Physiol.* **1994**, *104*, 675–681. [[CrossRef](#)]
74. Uemura, M.; Steponkus, P.L. A contrast of the plasma membrane lipid composition of oat and rye leaves in relation to freezing tolerance. *Plant Physiol.* **1994**, *104*, 479–496. [[CrossRef](#)]
75. Steponkus, P.L.; Uemura, M.; Joseph, R.A.; Gilmour, S.J.; Thomashow, M.F. Mode of action of the COR15a gene on the freezing tolerance of *Arabidopsis thaliana*. *Proc. Natl. Acad. Sci. USA* **1998**, *95*, 14570–14575. [[CrossRef](#)] [[PubMed](#)]

-
76. Hare, P.D.; Cress, W.A.; Van Staden, J. Dissecting the roles of osmolyte accumulation during stress. *Plant Cell Environ.* **1998**, *21*, 535–553. [[CrossRef](#)]
 77. Thomashow, M.F. PLANT COLD ACCLIMATION: Freezing Tolerance Genes and Regulatory Mechanisms. *Annu. Rev. Plant Physiol. Plant Mol. Biol.* **1999**, *50*, 571–599. [[CrossRef](#)] [[PubMed](#)]

6.3. Publikacja #3

Scots pine responses to drought investigated with eddy covariance and sap flow methods



Scots pine responses to drought investigated with eddy covariance and sap flow methods

Paulina Dukat^{1,3} · Klaudia Ziemblińska¹ · Matti Räsänen² · Timo Vesala^{2,3} · Janusz Olejnik¹ · Marek Urbaniak¹

Received: 12 May 2022 / Revised: 4 February 2023 / Accepted: 28 February 2023
© The Author(s) 2023

Abstract

Scots pine, as one of the dominant European tree species in the temperate zone, is experiencing intensified water deficits, especially in north-western and central Poland, where it suffers from frequent droughts and generally low precipitation. This work investigates drought impact on forest functioning, by analysing ecosystem transpiration under normal as well as dry conditions. Therefore, eddy covariance (EC) and sap flow measurements (using the thermal heat balance, THB, method) were combined to estimate transpiration (T) in two different-aged Scots pine (*Pinus sylvestris*) stands in north-western Poland: Mezyk (ME; 26 years old) and Tuczno (TU; 67 years old). Transpiration (T) estimates regarding EC measurements were derived from gross primary productivity (GPP) fluxes and vapour pressure deficit (VPD) dependence, considering their common relationship with stomatal activity. In 2019, the year following severe drought in Poland and Europe in general, total annual transpiration estimated based on sap flow measurements (T_{SF}) was significantly lower than EC-derived transpiration (T_{EC}) at both sites. The total ratio of T_{SF}/T_{EC} for the growing season (March–August) was 0.64 and 0.41 at ME and TU, respectively. We thus speculate that the understory, which was more abundant in TU than in ME, and which could only be observed by the EC system, may be responsible for the observed discrepancies. Bigger differences between T_{SF} and T_{EC} occurred under dry and wet conditions, while both were fairly similar under moderate conditions. The analysis of the relationships between T_{SF} and soil water content (SWC) at depth of 10 cm revealed that there is a thresholds (SWC ~ 3.5%) at which T_{SF} starts to decrease sharply, presumably due to stomatal closure. However, the decrease in GPP fluxes at the same time was less pronounced, indicating the impact of additional non-stomatal factor on water conductivity. We generally conclude that care should be taken if the conclusion of the occurrence of drought stress of some plants is derived from a bulk evapotranspiration flux, as it is commonly done with EC measurements averaging over the whole ecosystem. Our results also support the notion that non-stomatal water losses are an important element during extreme dry conditions, and that these may appear not only when stomata are already closed.

Keywords Heat balance method · Eddy covariance · Transpiration · Scots pine · Water balance · Drought stress · Temperate forest

Communicated by Ruediger Grote.

✉ Paulina Dukat
paulina.dukat@helsinki.fi

¹ Meteorology Lab, Department of Construction and Geoengineering, Faculty of Environmental Engineering and Mechanical Engineering, Poznan University of Life Sciences, Piątkowska 94, 60-649 Poznań, Poland

² Faculty of Science, Physics, Institute for Atmospheric and Earth System Research, University of Helsinki, Helsinki, Finland

³ Faculty of Agriculture and Forestry, Forest Sciences, Institute for Atmospheric and Earth System Research, University of Helsinki, Helsinki, Finland

Introduction

With intensified climate change caused by the growing human impact on the environment, as well as the increasing severity of droughts in Europe, it is important to address and understand the major role that forest ecosystems play in the global carbon and water cycling. Ecosystem disturbances originating from human activities (e.g. harvesting, land cover changes) and natural causes (e.g. drought, wild-fires, windstorms) significantly affect hydrological processes at any ecosystem by impacting vegetation dynamics (Wang et al. 2018). It is commonly known that stomata play a dominant role in regulating the amount of water transpired (T) by

vegetation (Jarvis and McNaughton 1986; Pieruschka et al. 2010). On a global scale, the transpiration fraction of evapotranspiration (ET) is estimated to be 56–74% (median = 65%, mean = 64%) (Good et al. 2015). It has been previously reported that T/ET varies among different types of vegetation which is though the highest in forests (Moran et al. 2009; Hu et al. 2018). It was also found that the average T/ET in temperate coniferous forests is $55 \pm 15\%$ s.d. (standard deviation), while for boreal forests it is ca. $65 \pm 18\%$ s.d. (Schlesinger and Jasechko 2014).

Understanding the relationship between T , ET and precipitation (P) allows proper planning and implementation of water management in terms of ecosystem efficiency and water protection (Aiken and Klocke 2012). However, estimating the transpiration flux at the ecosystem level is difficult due to inter-species differences as well as variability between trees of the same species. Therefore, a mechanistic understanding is needed to estimate the transpiration flux of individual trees. Also, specific environmental conditions can affect the strategy of plants to maintain the highest photosynthesis rate at the expense of the lowest water loss. It is particularly important to identify when/in which conditions such strategy begins to affect plants' health, as this can eventually lead to tree mortality. It is projected that drought-related tree mortality will most probably increase in the future on the global scale, yet the knowledge required to accurately predict forest functioning under drought stress and the occurrence of tree mortality itself is still limited (Plaut et al. 2012; Trugman et al. 2021). Therefore, any research aiming at understanding water scarcity impact on forests functioning helps to improve the estimates and future predictions related to drought resistance.

The general impact of drought can be described as a strong influence on water and carbon fluxes, and consequently the productivity of all terrestrial ecosystems (Granier et al. 2007). For these reasons, thorough analysis of water cycling, its individual components and its interactions with the carbon cycle in ecosystems is crucial for understanding the factors controlling these processes. One of the most crucial links in water cycle of land ecosystems is the soil, because it is the first element of soil–tree–atmosphere continuum. Water deficit in the soil can thus affect several stages along that continuum substantially (Bréda et al. 2006). Besides, drought stress alters both soil–root and leaf–atmosphere exchange, which further threatens the integrity of the liquid phase continuum from soil to leaves. It has been shown on the example of urban trees that an increase in drought stress and susceptibility to drought can lead to the development of embolism, suggesting a stress-induced deterioration in hydraulic conductivity (Savi et al. 2015). Drought stress reduces the exchange of both water and CO_2 fluxes and consequently limits tree growth. It comes from the fact that water availability is one of the most

important drivers for both processes (Levesque et al. 2017). It is assumed that under drought-related stress conditions, the rate of water and carbon exchange with the atmosphere should decrease. The suggested underlying mechanism of that reduction is the closing reaction of stomata which has evolved to protect against excessive dehydration and physiological damage to plants (Oren et al. 1999).

Partitioning ET into T and E is challenging, but can be done using various methods including: eddy covariance (EC) observations, chamber measurements, isotopes analysis, lysimeters and sap flow systems (Kool et al. 2014; Sulman et al. 2016; Anderson et al. 2017; Rafi et al. 2019). The ET partitioning utilizing EC point measurements, which are nowadays available from numerous sites, can be done indirectly by the use of empirical relationships or estimated from above- and below-canopy systems working simultaneously (Paul-Limoges et al. 2020). Nevertheless, at many flux tower sites the measurement setup is located only above the tree canopy.

In this work, in addition to direct sap flow measurements at several trees, the transpiration of the entire forest ecosystems was obtained by partitioning ET fluxes (T_{EC}) derived from one above-canopy EC system, using the relationship between gross primary productivity (GPP) and vapour pressure deficit (VPD) (after Berkelhammer et al. 2016). It is well known that the higher the VPD, the higher the transpiration at the leaf level (Yong et al. 1997; Broughton et al. 2021). Simultaneously, stomata regulates transpiration via adjusting closing/opening range to avoid a decrease in water potential (Oren et al. 1999). The interplay of these are described by stomatal optimization theories that maximize carbon gain for a given amount of water loss in the rooting system per unit leaf area. The assumption of optimizing stomatal control makes T proportional to $GPP \times VPD^{0.5}$ (Katul et al. 2009). In addition, the method assumes that the T can be approximated by ET during ideal conditions for transpiration (Stoy et al. 2019). The $T=ET$ line is determined from half-hour eddy covariance data by regressing the minimum ET values defined as the 5th percentile of ET values in each $GPP \times VPD^{0.5}$ bin. A linear regression of these minimum ET values defines the $T=ET$ line, and any point below this line has T/ET equal to 1 by definition. Due to stochastic nature of half-hour values of eddy covariance, some data points are below the $T=ET$ line (Berkelhammer et al. 2016). Moreover, many water use efficiency (WUE)-derived methods for ET partitioning are based on these same assumptions (Berkelhammer et al. 2016; Zhou et al. 2016; Boese et al. 2017; Stoy et al. 2019).

In this paper, we estimated ET and T fluxes in two managed Scots pine stands of different age classes (young and mature) located in north-western Poland by combining EC and sap flow measurements during the year 2019, with the main focus on the influence of drought

conditions. We thus follow the rationale of previous studies (Zhou et al. 2016; Nelson et al. 2018) that focus on T/ET mainly for across-site comparisons and land surface model development, suggesting that T/ET ratio is likely more useful than absolute T and ET values. Since sap flow measurements were only available in 2019, comparisons of both water fluxes (T_{SF} and T_{EC}) were only available over such a short term. Reliable estimates of T , especially during dry conditions, are very important for recognition and diagnosis of forest ecosystem status. In general, it is difficult to identify the ideal reference method because each has its advantages and disadvantages. Our dataset allowed for an insight into ecosystem as well as tree-scale transpiration utilizing robust upscaling method (based on 20 sensors per site). Moreover, the investigated areas were recently exposed to prolonged and repetitive droughts. In general, the entire region is one of the poorest in Europe regarding freshwater supplies with a large fraction of a Scots pine forests being managed. Thus, the investigation of how Scots pine trees are adjusting to these harsh conditions, especially in relation to tree hydraulics coupled with carbon exchange, is important at the national scale.

The main aim of this study is to determine differences between the stand transpiration (T) calculated using the EC-derived water vapour fluxes and upscaled sap flow data. Specifically, we determine the suitability of the two methods to detect changes in T in drought conditions. The purpose of using two different-aged ecosystems with a similar species composition and soil conditions was to explore whether the established relationships are age- and stand-structure dependent. The hypothesis is that T estimated from the upscaled sap flow measurements (T_{SF}) is technically and methodologically more sensitive to changes caused by drought compared to EC-derived transpiration (T_{EC}) obtained from directly measured ecosystem-scale evapotranspiration (ET) and is thus better suited to detect drought-induced effects on trees. On the other hand, the relationship between low soil water content reflecting drought conditions and an increase in vapour pressure deficit (e.g. Grossiord et al. 2020) should result in T_{EC} to be sensitive to drought similarly to T_{SF} obtained at tree scale. Low values of soil water content (SWC) were used as an indicator of drought on a daily scale for each site individually. It was also investigated how GPP changes with soil water conditions, since it is included in T_{EC} calculation and coupled with T_{SF} via stomata activity. Finally, we discussed the possible role of understory (shrubs and other hardwood species) transpiration in its total stand value, which is only included in T_{EC} , not in T_{SF} . Thus, the discrepancies between T_{SF} and T_{EC} were used as a rough estimate of understory transpiration.

Material and methods

Site description

This research was conducted at two EC study sites. The first site, Mezyk (ME), is located in north-western Poland (52°50'N 16°15'E). This 26-year-old forest was established after a fire in 1992 and is currently dominated by Scots pine (*Pinus sylvestris*) and approximately 1% admixture of silver birch (*Betula pendula*). The understory (i.e. other hardwood species and shrubs) is very poorly developed, mainly due to the young age of the ecosystem and the fact that it was established in a postfire area. It has been estimated that within the 1-hectare area, other forest ecosystem elements such as dead wood (both above- and belowground), herbaceous plants, bryophytes and woody plants up to 0.5 m high together constitute approximately 6.3% of the total dry biomass. The estimated tree density within the 500 m footprint of the EC system is about 4260 trees per hectare. The average tree height is approximately 10 m, and the average diameter at the breast height (DBH) is 9.5 cm. The organic layer was about 2 cm; along the top soil layer up to 2 m where profile measurements were performed, the dominating granulometric soil type was loose sand. The second site, Tuczno (TU), is located 50 km north of ME (53°11'N, 16°05'E) in a mature, 67-year-old Scots pine forest. The main tree species composition at TU is very similar to that at ME—Scots pine accounts for 99% of the tree species composition, with an admixture of birch (*Betula pendula* Roth). The understory is dominated by beech (*Fagus sylvatica* L.) and hornbeam (*Carpinus betulus* L.) (Ziemlińska et al. 2016a). Other abundant species of the forest floor include sea buckthorn (*Pleurozium schreberi*), fern (*Dryopteris carthusiana*), red raspberry (*Rubus idaeus*) and two grass species (*Deschampsia flexuosa* and *Calamagrostis epigejos*). The approximate tree density is 600 trees per hectare, and the average height and DBH are approximately 28.5 m and 31.2 cm, respectively. The soil profile was similar to ME, where loose sand is the main soil type up to 2 m, with the organic layer reaching 4 cm, composed mainly of freshly fallen pine needles and branches. According to the classification in the World Reference Base for Soil Resources (2006), the soil at both study areas is classified as a Brunic Arenosol (Dystric; (WRB-IUSS 2007). Similar soil properties at both sites allowed for a reliable comparison considering soil water conditions. At both sites the soil was highly permeable, as evidenced by the grain size composition and fluvio-glacial origins (related to the North Polish Glaciations). The soil fluvio-glacial origin and a thick layer of permeable sands caused the groundwater to be deep (> 10 m). Basic characteristics of the investigated sites are summarized in Table 1.

Table 1 Stand characteristics for Tuczno (TU) and Mezyk (ME) Scots pine forest sites (as for the year 2019)

| | ME | TU |
|---|------------------|--------------------------|
| Dominant tree species (%) | Scots Pine (99%) | Scots Pine (99%) |
| Stand age | 26 | 67 |
| Canopy height (m) | 11 | 29 |
| Stand density (trees h ⁻¹) | 4260 | 600 |
| Average tree DBH (cm) | 9.5 | 31.2 |
| Stand basal area (m ² ha ⁻¹) | 30 | 47 |
| Features | postfire | planted on former meadow |
| Soil type | Brunic Arenosol | Brunic Arenosol |

Table 2 Annual means/totals of basic meteorological elements and soil water content for TU site during the period 2012–2019. P—annual precipitation sum, ET—annual evapotranspiration sum, SWC—mean soil water content, T_a—mean air temperature, T_{soil}—mean soil temperature

| Year | P (mm) | ET (mm) | SWC (%) | T _a (°C) | T _{soil} (°C) |
|------|--------|---------|---------|---------------------|------------------------|
| 2012 | 783 | 611 | 10.0 | 7.7 | 11.0 |
| 2013 | 721 | 559 | 8.6 | 8.6 | 8.9 |
| 2014 | 647 | 499 | 7.4 | 9.9 | 10.1 |
| 2015 | 569 | 453 | 5.7 | 9.8 | 9.7 |
| 2016 | 700 | 536 | 8.9 | 9.2 | 9.5 |
| 2017 | 1075 | 545 | 13.3 | 8.9 | 9.3 |
| 2018 | 533 | 433 | 7.0 | 11.2 | 10.0 |
| 2019 | 563 | 517 | 6.7 | 11.8 | 11.3 |

Eddy covariance (EC) and sap flow measurements

Eddy covariance and meteorological measurements

Measurements of the CO₂ and H₂O exchange between forest and the atmosphere have been carried out at ME by an EC system installed at the top of a 22-m-high flux tower since May 2018. The EC system includes a three-dimensional (3D) sonic anemometer (model WindMaster Pro, Gill Instruments, Hampshire, UK) and an open-path infrared gas analyser IRGA (model 7500DS, LI-COR Inc., Nebraska, USA). Continuous meteorological measurements were simultaneously performed, including radiation balance components, air temperature (*T_a*), air humidity, precipitation (*P*) as well as soil water content (SWC) and temperature. Both soil temperature and volumetric water content were measured at a depth of 10 cm in the mineral soil using Digital TDT sensors (Acclima, USA). All measurements were averaged to 30 min. The data collected from the uppermost layer were used as a proxy for sub-daily and daily soil water status as well as drought stress intercomparison between the two stands, as the sites have the same soil type to at least 2 m depth. It does not represent the all water available for trees at deeper layers. The same measurements were performed at TU at a 38-m-high steel scaffold flux tower (2 m × 2 m) since 2008. The EC system comprised a 3D non-orthogonal sonic anemometer (model CSAT3, Campbell Scientific Inc. (CSI), UK) and an IRGA (model LI-7500, LI-COR Inc., Nebraska, USA). The instruments were positioned 39 m above the ground until January 2019 and then moved to 44 m due to tree growth. A detailed description of the TU station's meteorological equipment can be found in the study of (Ziemblińska et al. 2016b). At the TU site, temperature probes (model T-107, CSI, USA) were installed at 2, 5, 10, 30 and 50 cm below the soil surface. Volumetric water content was measured directly beside the temperature sensors at depths of 10, 30 and 50 cm using CS-616 sensors (CSI, USA). The measurements of SWC in two separate

profiles show that the values obtained at 10 cm depth have the greatest diurnal variability in response to changing meteorological conditions and drought occurrence (Fig s2. supplementary materials). Moreover, this supports the argument that although water deficit exists in the shallow soil layer (especial during April and June), more water is still available in the deeper soil layers. Also, because measurements were performed only down to 130 cm depth, most probably pine trees could still benefit from water below that threshold. The magnitude of the SWC measured between 10 and 130 cm in profile 2 was 5%, and thus, the variability of the SWC between different soil levels was not large. Since there were technical problems with the rain gauge at both sites, daily precipitation records were replaced by those collected at the Mialy precipitation station (ca. 2 km from the ME site) and Człopa precipitation station (ca. 10 km from TU) of the National Institute of Meteorology and Water Management (IMGW-PIB 2021). We used EC and meteorological measurements at the ME site from 2019 only, while the measurements from TU were used from the data range between 2012 and 2019.

Meteorological conditions and climate classification

In reference to the widely used Köppen–Geiger climate classification, the climate at the research area was characterized as Cfb (warm temperate, fully humid with warm summer (Kottek et al. 2006)). Monthly precipitation totals measured at the Człopa meteorological station, averaged for the period 2012–2019 station (Fig. s1, Supplementary materials), show characteristic annual course—with low values especially in spring (average ~ < 40 mm), and the highest precipitation in summer (> 80 mm in July) and most of the winter months (December, January > 60 mm). Average annual precipitation reached almost 700 mm, with a maximum in 2017 when the annual P sum was 1075 mm (Table 2). In 2018, the annual P sum reached the lowest value of all investigated years.

As for the thermal conditions, the highest average monthly temperature was measured in July and August ($> 18\text{ }^{\circ}\text{C}$), while the lowest in January (monthly average $< -2\text{ }^{\circ}\text{C}$) (Fig. s1, Supplementary materials). In 2018 and 2019, the annual average air temperature reached the highest values among all eight analysed years. During the investigated period, significant droughts occurred not only in Poland but also in other European countries, particularly in 2015, 2018 and 2019 (Ionita et al. 2017; Boergens et al. 2020). Consequently, soil water content in 2018 and 2019 was the lowest compared to the previous years, except for the very dry year of 2015.

As for ME site in 2019, when measurements at both sites were performed simultaneously, some meteorological conditions, such as T_a and global solar radiation (R_g), were fairly similar to those observed at TU on an annual scale, since they are both located in the same climatic region. However, there were noticeable differences regarding P and ET annual totals which were lower in ME than for TU, reaching 449 and 563 mm, respectively. Average annual daily mean value of SWC was 7.6% at ME and 6.7% at TU, while the average annual T_{soil} at the 10 cm depth was 9.7 and 11.3 $^{\circ}\text{C}$, respectively.

In order to detect and compare drought conditions in the investigated areas, the Standardised Precipitation and Evapotranspiration Index (SPEI) over a 3-month period was calculated (Vicente-Serrano et al. 2010). Long-term data used to calculate historical background values were retrieved from the Global Drought Monitor database (Beguería et al. 2020). It is assumed that values of SPEI below 0 indicate transition to drier conditions, values below -1.5 indicate severe drought, and those below -2 reflect extreme drought. The index together with SWC at the uppermost soil depth is used to characterize the drought conditions (Fig. s6, supplementary materials). Daily precipitation and SWC variations recorded in 2019 as well as SPEI values are compared for both sites in the Results section.

EC data processing

The forest within the flux footprint of the towers can be considered homogeneous from the perspective of aerodynamic properties. At the both sites the 80% flux footprint extends c. 500 m away from the tower (Kormann and Meixner 2001). Although the measurement height is higher at TU, the footprint is the same as in the ME site because the TU forest is also taller (aerodynamic displacement height is higher). Due to the asymmetric type of anemometer used at TU, the data recorded from wind directions that were disturbed by the instrument construction were omitted, resulting in the exclusion of 27% of data over the four years. The raw data obtained from the EC system were used to calculate covariances of the vertical wind speed (w) component and the quantity of interest: T_a , water vapour (H_2O) and carbon

dioxide (CO_2), to finally derive turbulent sensible heat (H), water vapour (which is ET) and CO_2 (F_C) fluxes. The rate of change in CO_2 and ET (ΔS_{CO_2} , ΔS_{ET}) in the air column below the EC system (i.e. the storage flux) was calculated during the first step of the data processing in EddyPro software version 7.0.1 (LI-COR; Inc. 2019). Storage fluxes are commonly obtained as a product of the estimation of air density, height of EC measurement, and the rate of CO_2 or water vapour concentration change at EC measurement height (using the difference between the average concentration at the beginning and end of the corresponding 30 min single-point EC measurement period). However, it has been shown that this storage flux calculation yields similar results to those obtained with the profile approach used in similarly tall vegetation (Morgenstern et al. 2004). Both ΔS_{CO_2} and ΔS_{ET} values were accounted for in the final fluxes calculations.

During data processing, the following corrections were applied: the double rotation calculation, tilt correction, WPL correction, covariance maximization and analytic correction of high-pass and low-pass filtering effects (Webb et al. 1980; Moncrieff et al. 1997, 2004; Burba et al. 2012). Final datasets of carbon and water fluxes include quality control and gap-filling procedures. Additionally, all fluxes recorded during precipitation events at both sites were excluded. To filter out fluxes measured under insufficient turbulence conditions, friction velocity (u^*) threshold (u^*_{th}) was used, as obtained from the breakpoint detection method (Barr et al. 2013; Wutzler et al. 2018), performed with the ReddyPro package (Wutzler et al. 2018) in R software (R Core Team 2020). The gap filling of carbon and water fluxes as well as NEE fluxes partitioning into GPP and ecosystem respiration (R_{eco}) was also performed using the ReddyPro package. The partitioning was done following the Reichstein night-time approach (Körner 1995; Falge et al. 2001; Gilmanov et al. 2003; Reichstein et al. 2005; Lasslop et al. 2010). Ecosystem respiration was estimated according to Lloyd and Taylor's (1994) regression model, to fit the ecosystem respiration (R_{eco}) as a function of soil (T_s) or air temperature (T_a) (Lloyd and Taylor 1994). In this work, the soil temperature was used in the partitioning procedure.

The gross primary productivity GPP is estimated by:

$$\text{GPP} = R_{\text{eco}} - \text{NEE} \quad (1)$$

where R_{eco} is the total ecosystem respiration and NEE is the net ecosystem exchange.

Sap flow measurements

At both ME and TU site, three test plots with an area of 1080 m^2 were chosen randomly within the 20–70% flux footprint domain, mainly to the west of the tower (within

approximately 100 m from the tower, Fig. 1), since this was the prevailing wind direction at both sites. At each site, 25 “model trees” were selected (Fig. 1), all equipped with sap flow sensors. Sap flow has been measured at both sites since October 2018. The EMS 81 sap flow system used here consists of sensors and SDI12 modules produced by EMS Brno (Czech Republic). Each sap flow sensor (SF 81) consists of stainless-steel electrodes inserted into the slots, which assure that sap flow values are nearly independent on the radial profile of sap flow density (Kučera 2018). The greatest advantage of this approach is the direct heating of a relatively large volume of xylem, which ensures high accuracy of the sap flow estimation. High electrical resistance of some trees’ tissue (not related to their age) caused poor quality of measurements in six samples at both sites (mainly due to internal stem damages (drying, cracks cavitations, etc.); these were excluded. Also, the measurements for the thinnest trees in ME had low quality and were thus excluded from the further analysis—the instruments used here have been designed for trees with a circumference greater than 40 cm. One sap flow sensor per tree was installed (north side) at DBH level (Fig. 2).

Due to difficulties of sap flow and eddy covariance observations during winter (Foken et al. 2012; Kittler et al. 2017; Frank and Massman 2020), transpiration data were only analysed during the growing season (from March to the end of August; in the case of ME, to the end of September, because there was no downtime in the operation of the equipment). The gaps in transpiration were filled with the MDS (marginal distribution sampling) method using ReddyPro.

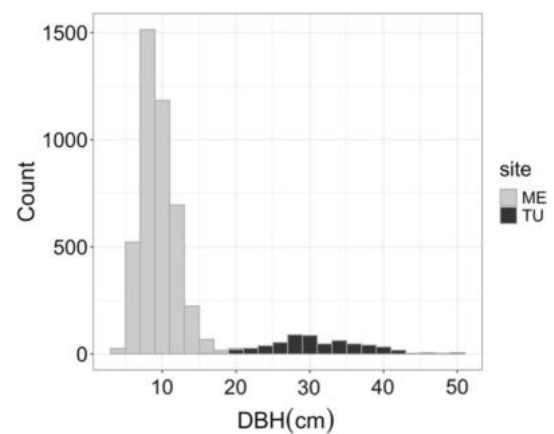


Fig. 2 Tree diameter at breast height (DBH) distributions at ME and TU sites measured in 2019. ME—grey bars; TU—black bars. (Color figure online)

There are several techniques for sap flow measurements, including the tissue heat balance (THB) method (Čermák et al. 1973; Čermák and Deml 1974; Čermák et al. 1976, 2004; Kučera 1977; Kucera et al. 1977). The “balance family” of sap flow measurements (including mainly the THB method) are the only methods that directly measure sap flow rate (Flo et al. 2019). In the THB method, thermal balance is calculated for a given heated space. According to its assumptions, the input energy is divided between conductive heat losses and warming of the flowing water (Čermák et al. 2004). The amount of water passing through the measuring

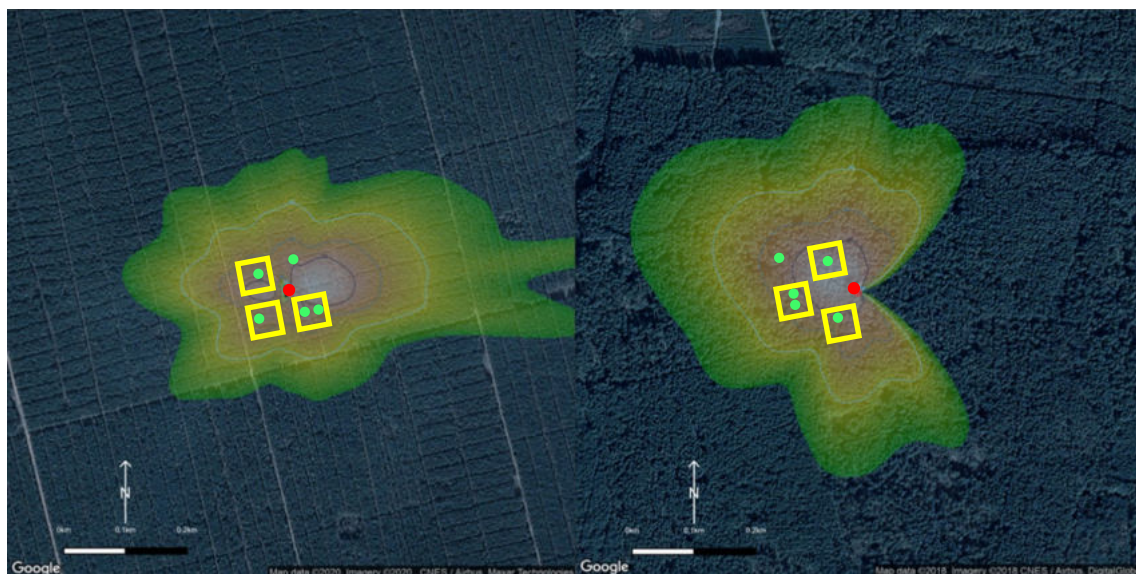


Fig. 1 Location of the three selected test plots (1080 m²; yellow rectangles) within the footprint of the EC system (calculated for unstable conditions by the approach described by (Kormann and Meixner 2001)). Diameter and number of trees were directly measured at ME

(left) and TU (right) sites. Green circles indicate a group of 5 sap flow sensors; red dots represent the location of the EC flux towers. Colour scale represents the areal contribution of the flux (in %) from the footprint area. (Color figure online)

point in the stem is calculated based on the electric power input consumption and the increase in temperature of water flowing through the area that is heated (Kučera and Urban 2012). Whole tree sap flow (Q_{tree} —kg time⁻¹) was derived by multiplying Q by the tree circumference, after the bark and phloem layer was excluded (Szatniewska et al. 2022). The phloem layer was measured during the equipment installation.

As mentioned earlier, thermal methods for measuring sap flow are based on heat loss detected by the sensor. Therefore, when tree sap flow data are processed, the zero transfer value (“baseline”) must be determined, which varies depending on the sensor and the time of year (Oishi et al. 2016). When performing this procedure, the possibility of nocturnal sap flow appearance should also be taken into consideration, since night sap flux is thought to be driven by atmospheric evaporative demand (Forster 2014). In our work, raw sap flow data were post-processed by applying the automated baseline subtraction based on the Exponential Feedback Weighting method (Kučera et al. 2020) developed for mini32 software (EMS 2020a). This method considers the nocturnal sap flow and removes outliers due to natural temperature gradients. It has been found that the best results were computed by the 5-day weighting average (Kučera et al. 2020), and thus, the same averaging interval was applied here.

Upscaling model tree sap flow values to the stand level

We applied the diameter class technique for sap flow results upscaling, which is based on the assumption that sap flow rates depends only on the DBH (Čermák and Kučera 1987, 1990) (Fig. 3b).

For the purpose of upscaling sap flow from the tree to stand level, a histogram of the DBH distribution was created for the sampled areas (Fig. 1), then proportionally upscaled to 1 ha (Fig. 2). The reliability of this procedure is supported by the homogeneity of both forests’ structure.

An exponential function was fitted to the relationship between sap flow rates and DBH (Cristiano et al. 2015). Differences in physiology of 27-year-old and 67-year-old trees raised doubts about using one common relationship for both sites, since trees of the similar size but different age can have different features related to water transport. Thus, upscaling was done with parameters specified separately for each ecosystem. Specifically, the $Q_{tree} \sim DBH$ original exponential relationships were fitted for a 7-day window from 05.05.2019 to 15.05.2019, as the average daily sap flow quickly reached high values in May, with the highest observed in June. It is suggested that regression parameters for such relationships should be calculated over a few days when soil water content is roughly constant and VPD is

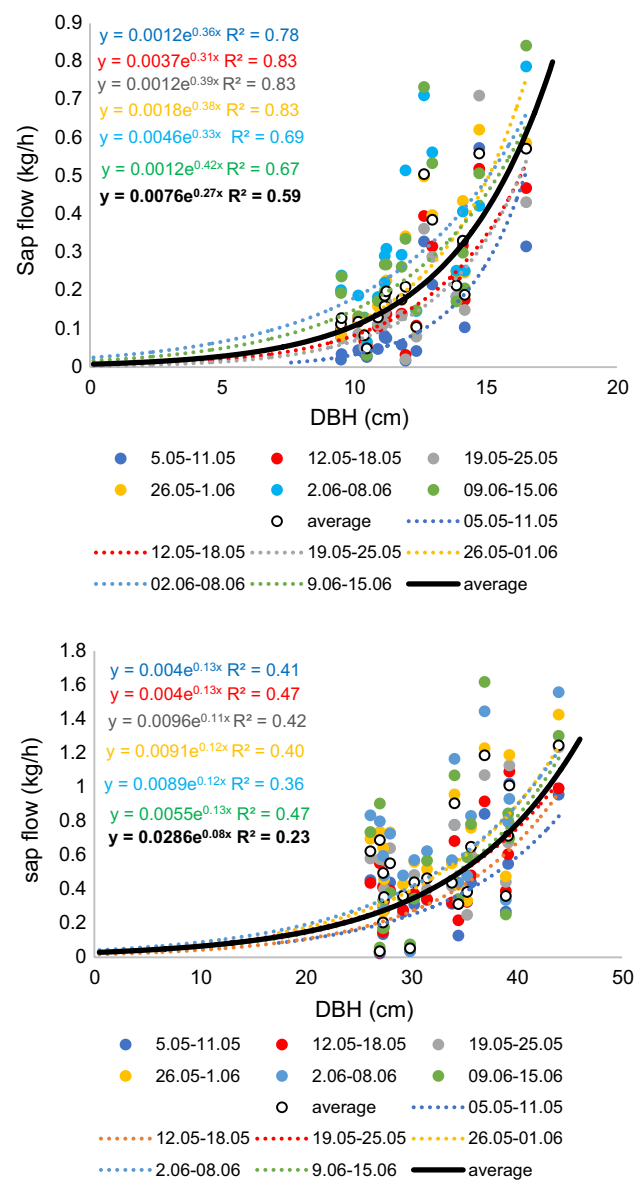


Fig. 3 Relationship between daily averages of sap flow rates (Q [kg/h]) and diameter at the breast height (DBH) used for upscaling the tree-level transpiration to stand-level transpiration (TSF)

relatively high—conditions that characterize high evaporative demand.

Average daily sap flow (kg h⁻¹tree⁻¹) for individual DBH classes was first calculated based on regression parameters obtained from the exponential relationship for sample trees between these two factors (Fig. 3). Then, the values of the daily average tree sap flow [kg/h] for individual DBH classes were multiplied by the number of trees in a given class and total average daily sap flow of all DBH classes were aggregated for the unit stand area (1 ha). Total daily sap flow per ha was finally divided by the sum of the average daily sap flow of the sample trees in

the same period—this ensured that despite different maximum sap flow rates during different periods, the obtained sap flow rescaling factor from the sample trees to the stand transpiration (SC) was very similar regardless the calculation period.

The final stand transpiration expressed in kg m^{-2} (or mm m^{-2}) was obtained with the following calculation:

$$\text{TSF} = \frac{\sum_{i=1}^n (Q_{\text{tree}_i}) \times F_s}{A} \quad (3)$$

where A (m^2) is stand area, Q_{tree} is sap flow rate (kg/h), and F_s is the scaling factor. If the investigated stand is not homogeneous, different species must be analysed separately, similar to the situation when different canopy layers occur.

ET Partitioning

The method used for EC-derived ET partitioning was based on the assumption that ET is linearly related to $\text{GPP} \times \text{VPD}^{0.5}$ only when T is the dominant term in ET. To estimate the T/ET value for each 30 min period, the product of $\text{GPP} \times \text{VPD}^{0.5}$ was plotted against ET (for 2019 at the ME site; for 2012–2019 at the TU site; Fig. s3—supplementary materials), and the minimum value of ET was then selected as the 5th percentile for each equal-sized $\text{GPP} \times \text{VPD}^{0.5}$ bin (after Berkelhammer et al. 2016). Fifty bins of equal numbers of points were implemented for both sites. The number of points in each bin differed between sites due to the larger dataset in TU. The linear regression determined for these bins gives the ET value for which $T = \text{ET}$. Similarly, for the points below the regression line, it was also assumed that $T = \text{ET}$ (Räsänen et al. 2022). ET partitioning was done for EC datasets after excluding night-time data, as well as observations during precipitation events and when relative humidity was greater than 80%.

To determine the water loss per carbon gain for the forest stand, we calculated the daily water use efficiency (WUE) as GPP/T_{SF} (unit: $\text{g C}/(\text{kg H}_2\text{O m}^2 \text{ per day})$). This way a better understanding of water use efficiency of Scots pine trees, which are the main scope here, can be achieved than with the use of ET flux that includes also other components like evaporation from the soil and interception which were not directly measured. Since both forests are composed in 99% of one tree species for which transpiration was upscaled from sap flow measurements, thus it was assumed that T_{SF} should represent stand-level tree transpiration fairly well. We also assumed here that GPP represents only dominant pine trees since the contribution of other minor tree species—mainly birches, understory and soil vegetation, is negligible. Additionally, we calculated the canopy stomatal conductance from the upscaled foliage transpiration T_{SF} (in

$\text{kg/m}^2 \text{ s}$) by dividing each estimate by corresponding VPD value converted to units kg/m^3 .

Results

Annual relationships between the components of the water balance at Tuczno 2012–2019

The data collected during 2012–2019 period at the Tuczno site were used to investigate what are the interannual differences between the annual totals and proportions of water balance components (Table 3). These components and their interrelation were then calculated for the 2019 growing season when data from both measurement methods were available for both sites at a higher time resolution. Annual T_{EC} total was the highest in 2012 (421 mm) and 2013 (407), when annual P sum > 700 mm. In the wettest year of 2017, T_{EC} constituted only 33% of the annual P sum, while in the driest 2018 and 2019, it was noticeably higher (61% and 60%, respectively). Even though the lowest annual cumulative ET was recorded in 2018, the calculated T_{EC} was the lowest in 2015. Still, the ratio of T_{EC}/ET was the lowest for dry 2019 year which was only 0.65.

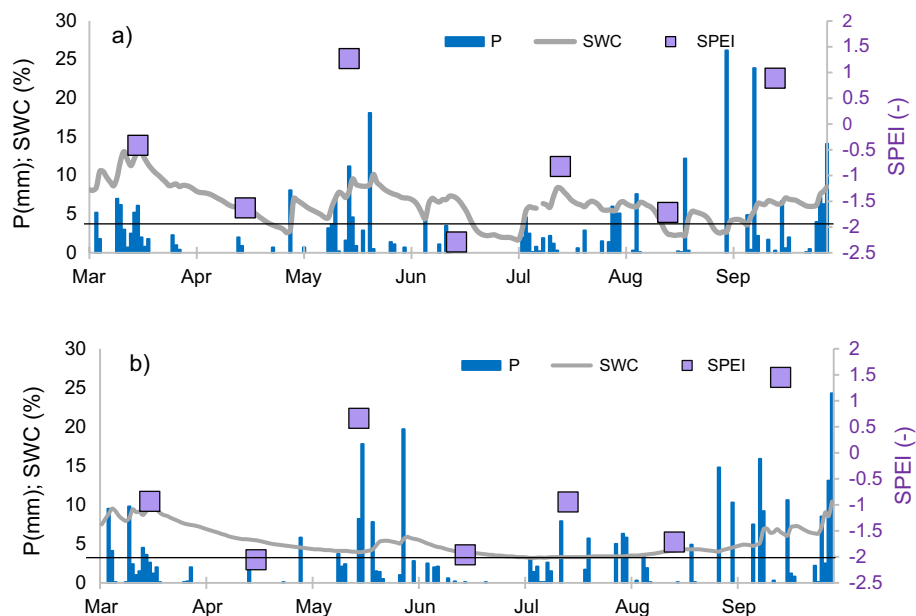
Drought conditions in 2019 indicated by SPEI, daily sums of precipitation and mean daily SWC

We compared T derived with the two different methods throughout the growing season of 2019, when a full set of measurements (sap flow and EC) were available at both study sites. The growing season T_{EC} total at ME was 304 mm, and its share in precipitation was 60%, similar to the value calculated at TU. In order to compare water conditions at the two investigated sites during the growing season of 2019, daily precipitation and soil moisture patterns are presented in Fig. 4. Slight differences related to precipitation distribution reflect the local conditions

Table 3 Annual EC-derived: transpiration total (T_{EC}) and the ratios of evapotranspiration to precipitation (ET/P), T_{EC}/P and T_{EC}/ET at the TU site during 2012–2019

| Year | ET/P (mm) | T_{EC} (mm) | T_{EC}/P | T_{EC}/ET |
|------|-----------|----------------------|-------------------|---------------------------|
| 2012 | 0.78 | 421 | 0.54 | 0.69 |
| 2013 | 0.77 | 407 | 0.56 | 0.73 |
| 2014 | 0.77 | 353 | 0.55 | 0.71 |
| 2015 | 0.80 | 297 | 0.52 | 0.66 |
| 2016 | 0.77 | 363 | 0.51 | 0.68 |
| 2017 | 0.51 | 359 | 0.33 | 0.66 |
| 2018 | 0.81 | 327 | 0.61 | 0.76 |
| 2019 | 0.92 | 338 | 0.60 | 0.65 |

Fig. 4 Daily precipitation totals (P) and mean daily soil water content (SWC—depth of 10 cm) at ME **a** and TU **b** during the growing season of 2019, on the background of monthly values of the SPEI index. SPEI below -2 (marked with a black horizontal line) indicates extreme drought conditions. (Color figure online)



characterizing the TU site, where more frequent thunderstorms during the summer season occurred—these result in strong, local, convective precipitation in summer. In terms of meteorological drought, two periods (April and June) were identified at both sites, due to the prolonged rainless/dry periods and the increase in or persistently high temperatures. These findings were confirmed by the results derived from drought monitoring and analysis based on SPEI index (Fig. 4). For the grids covering the area of the two investigated sites, April, June and August 2019 were identified as severe ($SPEI < -1.5$ and > -2) or extremely dry ($SPEI < = -2$) depending on the site (Fig. 4). Precipitation total in March was higher than in April, when drought has occurred. We assumed that trees benefited from this water supply which helped

maintaining their functioning (including transpiration) in the spring.

Variability of water fluxes at young (ME) and mature (TU) scots pine forest

To test the hypothesis that T estimated from the upscaled sap flow measurements (T_{SF}) is better suited to detect drought-induced effects than EC-derived T , the results of both methods were compared under different precipitation conditions, including extreme drought. During the growing season of 2019, the cumulative sum of T_{SF} was higher at TU (137 mm) than at ME (189 mm, Fig. 5), and total growing season T_{EC} amounted to 222 mm and 283 mm for ME and TU, respectively. Apart from the differences between transpiration fluxes derived with the two methods,

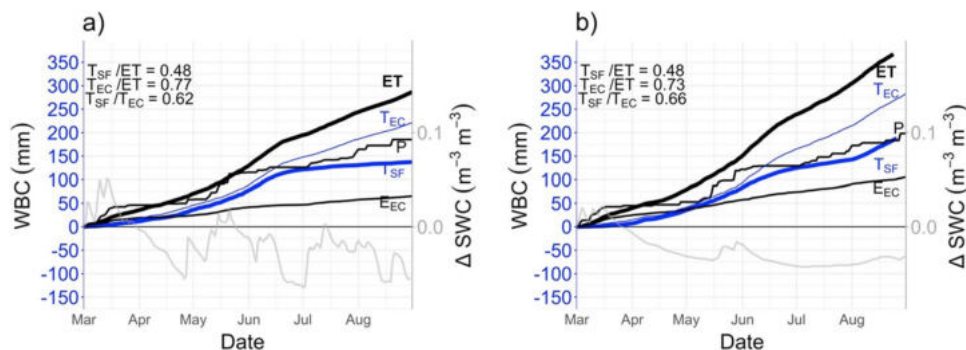


Fig. 5 Cumulative components of water balance (WBC) during the growing season of 2019 at ME **a** and TU **b**. Transpiration from sap flow (TSF), transpiration from ET partitioning (TEC), evapotranspiration (ET), evaporation from partitioning ($E_{EC} = ET - TEC$) and precip-

itation sum (P). T_{SF}/ET , T_{EC}/ET and T_{SF}/T_{EC} ratios represent total values for the growing season. Changes of daily mean SWC values are presented on the right y axis

ET sums from EC measurements also differed substantially between sites (287 mm at ME and 389 mm at TU). The calculations of the share of the T_{EC} sum from March to August (assumed growing season period) in the respective ET totals resulted in 0.77 for ME and 0.73 for TU. However, the T_{SF}/ET ratio was much lower and accounted for only 49% of ET flux at both the young and mature Scots pine stands (Fig. 4). Overall, the T_{SF}/T_{EC} was similar between sites: 0.60 and 0.65 for ME and TU, respectively. Moreover, despite the fact that precipitation totals for this period were almost equal for both sites, the total T_{SF}/P relationship was different; it reached 0.74 for ME and 0.95 for TU. Interestingly, the T_{EC} sum in both cases exceeded the precipitation sum during the growing season in 2019: at ME, the T_{EC}/P reached 1.20, while at TU it was ca. 1.43. For both sites during this period, cumulative ET strongly exceeded the value of total precipitation (Fig. 5).

In order to further explore the relationships for the entire growing season, monthly totals of transpiration (T_{EC} and T_{SF}) for both sites are shown together with precipitation during the growing season of 2019 (Fig. 6). Despite the differences in total sums of T_{SF} and T_{EC} for the growing season, there are similar patterns regarding high and low monthly sums at ME and TU, for both T fluxes. In particular, the estimated T_{EC} was higher than the T_{SF} in all months except April at TU. In May, the highest precipitation total was recorded at both sites: 58 mm at ME and 69 mm at TU. The lowest precipitation sums—ca. 10 mm or less—at both sites were recorded in April and June. In July, T_{SF} reached one of the lowest values at ME and TU.

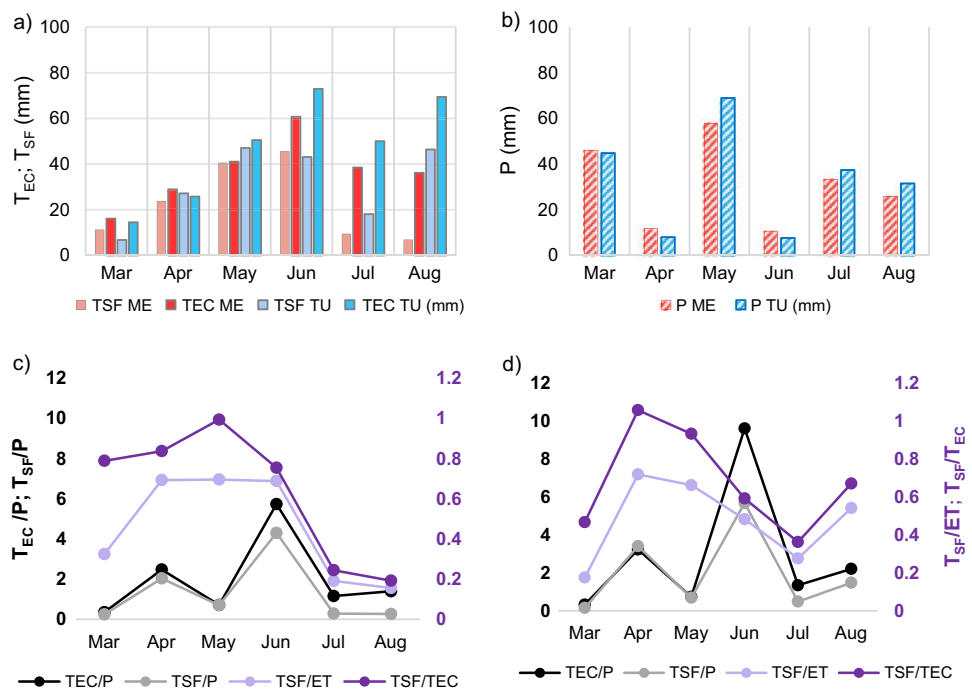
Also, at ME site, the sap flow sum reached its lowest value in August, in contrast to the TU site. Highest monthly T_{SF} was observed in June and May for ME and TU, respectively. T_{EC} was the highest for both sites in June.

It was also shown that in specific months, precipitation sums exceeded both T_{EC} and T_{SF} similarly at both sites. T_{EC} exceeded precipitation in almost all months, excluding March and May when P sums were higher than transpiration. T_{SF} was higher than monthly P only in April and June, when drought was detected at both sites by SPEI index. At ME, the share of T_{SF} in ET was the highest in May, when it reached 0.70, with very similar values in the preceding and following month. At this site, T_{SF}/ET was the lowest in the summer months of July and August (below 0.20; Fig. 6c). At the mature pine stand (TU), the highest T_{SF}/ET was detected in April (0.72) and May (0.66); the lowest (ca 0.12) was observed in March (Fig. 6c, d). The highest T_{SF}/T_{EC} ratio was calculated in April and May at TU (Fig. 6d), while at ME the highest was in May (Fig. 6c)—it reached 0.99, which means that T_{SF} and T_{EC} sums were nearly identical in this month. The lowest values of monthly T_{SF}/T_{EC} at ME were found in July and August, while at TU it occurred in July when T_{SF}/T_{EC} was less than 0.25.

Comparison of daily transpiration fluxes estimated by sap flow (TSF) and eddy covariance (TEC) methods

Since soil water content measurements were used to indicate drought occurrence on a daily time scale, transpiration fluxes

Fig. 6 Monthly sums of EC-derived evapotranspiration (ET), transpiration from sap flow (TSF), transpiration from ET partitioning (TEC) and precipitation (P), as well as the ratios of TEC/P, TSF/P, TSF/ET and TSF/TEC for the growing season of 2019 at ME **a** and **c**, and TU **b** and **d**, respectively



were related to changing SWC conditions. The estimates of daily sums of T_{EC} were compared to T_{SF} for the 2019 growing season for each site separately. When summer data with $SWC < 3.5\%$ were excluded, which was the case especially in June and August for ME and July for TU, an additional correlation between the two fluxes was derived, to exclude the influence of days with drought related to deficits of water in the soil. This was represented by an increase in R^2 to 0.73 and 0.80 at ME and TU, respectively (Fig. 7a, b). Data with precipitation events have been excluded in this analysis. The regression line slopes of the relationships between daily values of these two transpiration fluxes over the growing season have been different for each site and approach (all data together vs low SWC days excluded) and ranged from 0.70 to 0.79 (Fig. 7a, b). T_{SF} values in July (when the T_{SF}/ET was also low) indicate a reduction in tree transpiration during this time. T_{EC} was not consistent with the T_{SF} values after prolonged drought (Fig. 7a, b), which was observed mainly by the relationship between $T_{SF} \sim T_{EC}$ in June at TU, and in August for ME, when SWC reached the lowest values. It should be noted that transpiration after upscaling to the stand level from the sap flow measurements only corresponds to the transpiration from pine trees. The remaining flux from other plants in TU—young beech and hornbeam trees—was also in the range of the EC system and thus only visible in T_{EC} measurements, even though in principle both stands consist of 99% Scots pine trees (Table 1). In ME, both T_{SF} and T_{EC} were high under high SWC in May and June, and there was a good agreement between those T estimates. In TU, higher daily T_{EC} values were also observed in May, while the lowest was in April and March, similar to ME. However, lower SWC values—especially in August—were

accompanied with higher T_{SF} and T_{EC} at TU than ME. The daily T_{EC} and T_{SF} courses during the growing season of 2019 are presented in the supplementary materials (Fig. s4, supplementary materials).

The comparison of the responses of daily T_{SF} and T_{EC} fluxes to the daily mean SWC variations showed that both calculated T fluxes have similar dynamics at the same site (Fig. 8). The 9th decile of T sums daily averages was chosen as the threshold, above which values of T_{SF} and T_{EC} were considered high. The figures show that under similar SWC conditions, most of the values higher than the 9th decile for both T fluxes occurred similarly at each site. T_{SF} and T_{EC} reached the highest values, and T_{SF}/T_{EC} was closer to 1 for a SWC of 5–9% (ME) and 4–6% (TU) (Fig. 8c). Water use efficiency increases steeply below SWC values of 4%, since carbon uptake (GPP) was maintained at relatively high level (Fig. s5, supplementary materials), while the differences between T_{SF} and T_{EC} were distinct, especially at the ME site. The enhanced water use efficiency at low SWC (Fig. 8d) reflects the strategy of trees to minimize T while keeping GPP rate at a high level. When SWC was above 9%, lower transpiration and GPP values were observed. This is usually associated with evaporative demand reduction at the end or early beginning of the growing season together with lower VPD and lower radiation conditions. With low VPD values both GPP and T_{SF} decreased (Fig. 8e, f). At high values, a reduction in transpiration was observed, which was not as pronounced for GPP at ME site. At the TU site, corresponding reduction of both fluxes was observed at high VPD. Additionally, results from the ME site show the gradual increase in the conductance as a function of SWC ($< 5.5\%$)—Fig s6. Supplementary materials.

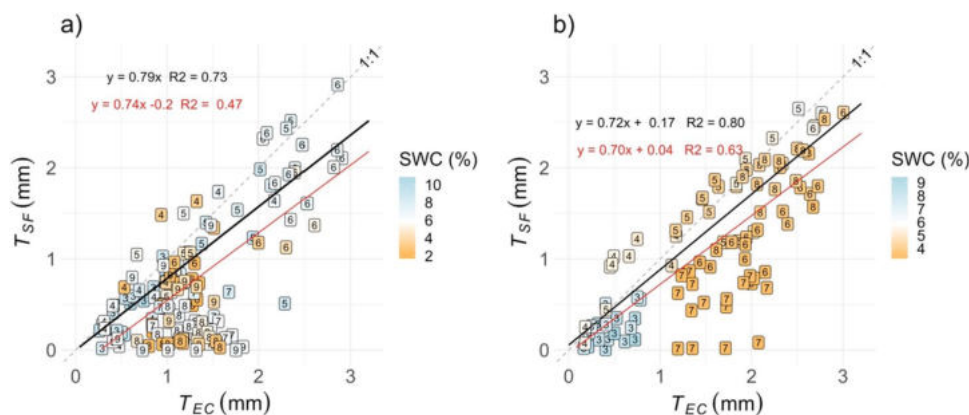


Fig. 7 The relationship between daily sums of transpiration derived from ET partitioning (T_{EC}) and transpiration from upscaled sap flow measurements (T_{SF}) at ME **a** and TU **b** during March–August 2019. Solid red lines represent linear regressions for all available water fluxes. Black solid lines represent simple linear regressions with the

exclusion of data when SWC was $< 3.5\%$ in June and July for TU site and June–August for ME site. The colour of each point indicates corresponding mean daily SWC; numbers indicate individual months; dashed lines indicate the 1:1 regression line. (Color figure online)

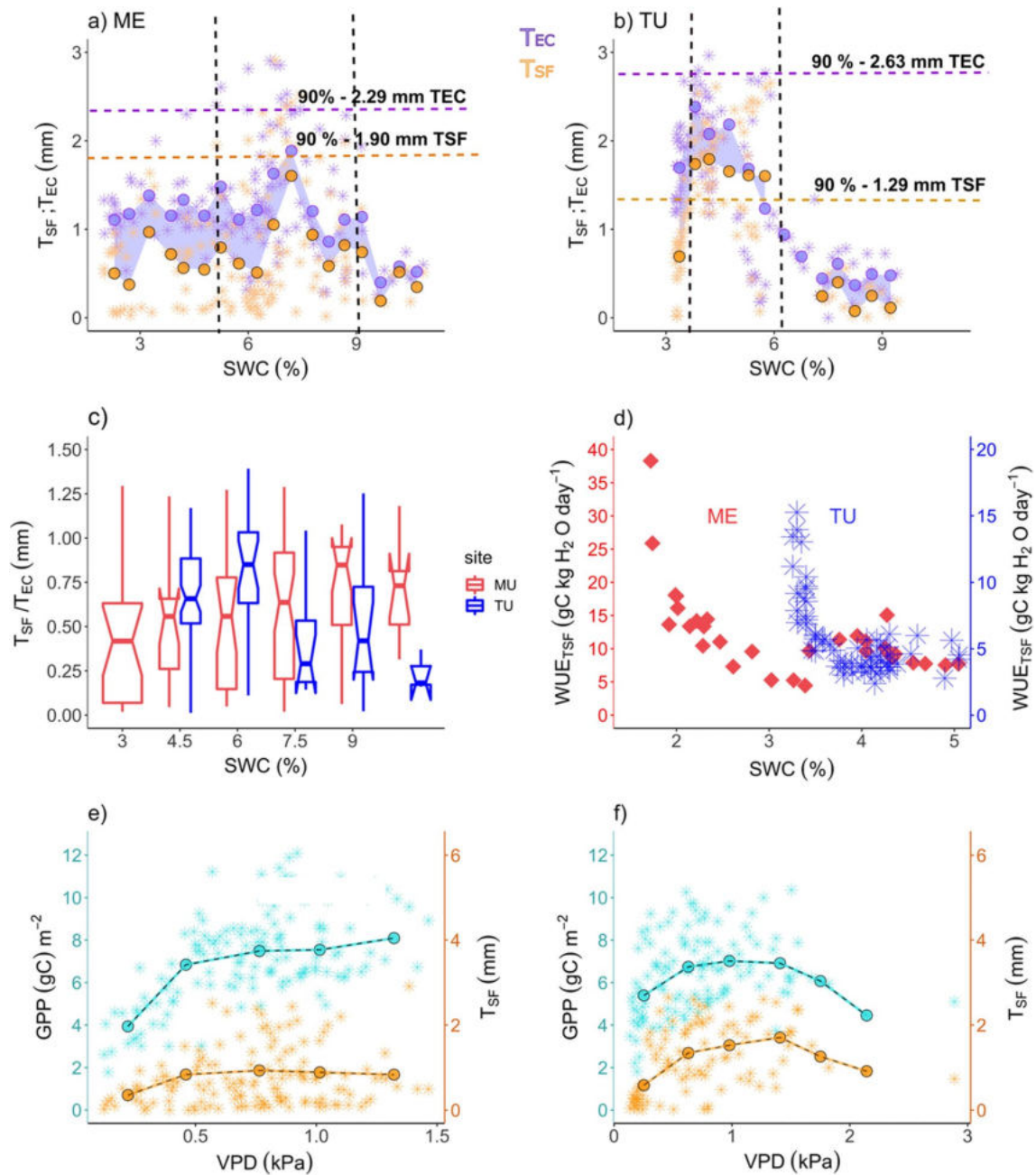


Fig. 8 Relationship between SWC and TSF (orange) and TEC (purple) at **a** ME and **b** TU. **c** boxplot presenting the relationship of TSF/TEC at different SWC levels (bin width of 1.8% of SWC), at ME (red) and TU (blue). **d** Relationship between WUE_{TSF} and SWC at ME (red) and TU (blue) for SWC < 5.5%. **e, f** Relationship between daily sums of GPP, TSF and VPD is presented for ME and TU; light-

shaded points represent all data of daily T and GPP totals; highlighted points and lines represent binned data; dashed horizontal lines **a, b** indicate the 9th decile (90%) of daily mean SWC at ME (orange) and TU (purple); vertical lines represent the intervals with daily values above the designated threshold for both sites. (Color figure online)

Discussion

Differences between water fluxes estimated for both sites

The investigated sites are located in a region that is exposed to water shortages and has experienced several rainfall anomalies in recent years (IMGiW 2020). For the studied 2019 growing season, total T_{SF} was higher at the mature stand (TU) than at the 26-year-old site (ME), which can mainly be explained by differences in the characteristics of the stand—larger trees and basal area at the TU site. Also, total T_{EC} at ME was lower than at TU, mainly due to the less understory at the ME site, as well as lower precipitation totals. Tree height, basal area and number of trees were the most distinguished differences between sites. The basal area was 1.5 times greater in Tuczno, where the sum of T_{SF} in the growing season was also greater by a factor of 1.4. As shown by Zimmermann et al. (2000), density and sapwood area in western Siberian pine were strongly correlated, which results from the exponential decrease in stem number with age (self-thinning) and the linear increase in sapwood area per tree (Zimmermann et al. 2000). Thus, transpiration was higher for stands with the higher sapwood area compared to the average transpiration of all other stands, by as much as a factor of 2. Growing season T_{SF} total at ME constituted 74% of precipitation, while at TU it was as much as 95%. In our study, the growing season T_{SF} constituted 48% of its annual value both at the ME and TU site. Despite the differences in absolute sums of ET and T_{SF} between sites, the tree transpiration has contributed similarly to ET at both sites. For T_{EC} , its share in ET was much higher than corresponding T_{SF}/ET and equal too: 77% and 73% at ME and TU, respectively. Since the decrease of T_{EC} (derived from the EC-derived ET fluxes partitioning method) during drought conditions was not as pronounced as for the stand-level T_{SF} , it seems that the EC method is not as sensitive to extreme conditions as the upscaled sap flow measurements at individual trees. Annually, T_{EC}/ET at the TU site varied throughout the study period (2012–2019), reaching the highest values in 2018—the year with the lowest annual precipitation sum. This is likely to be driven by high evaporative demand during days with sufficient water availability. The variability in transpiration rates originates from uncertain supply from soil layers deeper than 50 cm as well as transpiration from ground vegetation and tree species not considered in the investigation. Similarly, in a study that partitioned evapotranspiration derived from the EC method into transpiration and evaporation (Li et al. 2019), it was found that the T/ET and mean annual precipitation relationship was also weak and non-significant on an annual timescale

($R^2 = 0.09$, p value = 0.11). Another study based on data from sites that are part of the Fluxnet network, which only consider evergreen coniferous forests, showed that T/ET varies throughout the year, with a minimum in the winter and a maximum (reaching almost 0.8) in the summer (Nelson et al. 2020). In our study, it was found that the highest T_{EC}/ET occurred in spring: in May at both sites and additionally in April 2019 in the mature forest only. Estimated E at our sites (as a simple difference between measured ET and T_{EC}) was close to semi-arid conditions (Fig. 5) and has contributed to ET by 23% and 27% at ME and TU, respectively. It has been shown that soil E can reach up to 26% of ET under semi-arid conditions with a very water saving vegetation (Qubaja et al. 2020), while in alpine forest with ample water supply it was up to 40% (Wieser et al. 2018). Thus, despite the uncertainties related to the remaining water balance elements, not attributed to pine transpiration, our results indicate a close relation to the investigations under semi-arid conditions. The assessment of the share of transpiration in total ET is important for improving models of stomata behaviour, as well as understanding the mechanisms that control the amount of T in various environmental conditions, especially in ecosystems exposed to water deficits. We also found that even when the T_{EC}/P annually fluctuated between 0.50 and 0.60 over the years, T_{EC}/P calculated for the growing season only increased significantly in relation to its annual value. In the same year, considering the total for the growing season (March to August), values of T_{EC}/P exceeded 1, reaching 1.20 and 1.43 at ME and TU, respectively. For this period, the ET sum at both sites exceeded the value of precipitation reaching 287 mm at ME and 389 mm at TU, which was not the case for the annual ET and P totals calculated for 2012–2019 at TU. ET/P ranges annually from ca. 0.76 to 0.92 depending on the precipitation conditions, with the exception of 2017 (which was very wet), when it was only 0.51 (Table 2). The differences in the ET/P ratio for the growing season and the whole year indicate that the use and replenishment of water in the sandy soil is affected by the intra-annual precipitation pattern. ET exceeds P over the growing season whereas precipitation predominates over ET in autumn and winter. Although the summer-time ET is thus already high, it is predicted to increase further due to the increasing temperature and associated hydrological changes resulted from altering climate conditions (Okoniewska and Szuminska 2020). The high ET/P values for growing season indicate the dependence of transpiration on soil water storage. In the presented study, it was particularly noticeable in June 2019, when the SPEI index indicated extreme drought along with high transpiration, which contributed to reduced SWC over the same period. Transpiration which occurred in June under low SWC values indicates an increasing use of stem water

storage. Subsequently, the low T_{SF} values in July were measured by the sap flow method at both sites independently, indicating a similar ecosystem reaction to changing environmental conditions—mainly low values of precipitation and SWC in the preceding month. Previous research has shown that for Scots Pine, relative stored water use ranged from less than 1% up to 44% of the daily transpiration (Verbeeck et al. 2007). After exceeding a certain site- and species-specific soil moisture threshold, plants attempt to optimize the carbon uptake against transpiration by stomatal regulation (Cowan 1978; Hari et al. 1986; Katul et al. 2000; Farquhar et al. 2002; Tang et al. 2006; Beer et al. 2009). If the water consumption of the plant exceeds soil water recharge, this can cause restrictions on plant water uptake, reduction of stomatal conductance (g_o), and lead to feedback on leaf-related processes and evaporative losses (Beer et al. 2009).

Our results also revealed that on a daily timescale, transpiration was the highest with non-extreme/moderate SWC values, for both T_{SF} and T_{EC} . Moderate values of daily average soil water content (6–8%) were found to be optimal for promoting higher T_{SF} and T_{EC} at ME. The highest differences between the two methods (T_{SF} and T_{EC}) occur under SWC values lower than 3.5 and 4% for ME and TU, respectively (Fig. 7). Similarly, after exceeding the above-mentioned moderate values, differences between T_{SF} and T_{EC} increased as the soil water content increased. Low soil moisture reduces T due to stomata closure and decrease in hydraulic conductivity (Duursma et al. 2008). High soil moisture is often associated with conditions of decreasing vapour pressure deficit and radiation during days with precipitation, which reduce evaporative demand, also causing reduction of T . Similar non-extreme values of soil moisture (~10%) have been found to be optimal for higher daily sap flow sums, for example, in high-elevation five-needle pines. Nevertheless, it was suggested that the differences in species' characteristics (like leaf area index, tree age and density, root characteristics) are possible factors underlying the different response of T to soil water content changes (Ji et al. 2016; Jiao et al. 2019). Moreover, there are some studies showing that finding a clear relationship between T and SWC is difficult for many forests (Kumagai et al. 2014; Ghimire et al. 2014; Jiao et al. 2019). One of the main reasons for this is the distribution of roots which are sensitive to heterogeneously distributed soil water both in time and space (Kume et al. 2007; Brito et al. 2015). Furthermore, it is difficult to separate the relative influence of soil water from other cross-correlating environmental factors (e.g. VPD).

The dependencies between available water for plants and high vapour pressure deficit (Grossiord et al. 2020) should cause a decline in T_{EC} , obtained at the ecosystem scale. It is thus sensitive to drought, similar to T_{SF} obtained by measurements performed at the tree scale. Some relationships

regarding sap flow measurements, especially the decrease in tree transpiration (T_{SF}) at very low SWC values, were not as pronounced in results obtained for water fluxes derived from EC observations (Figs. 6, 7). Our findings concerning lower T_{SF} under drought stress conditions are consistent with the recognized role of stomata in protecting hydraulic function of the xylem by regulating transpiration rates in order to keep the water potential in this tissue below critical thresholds (Oren et al. 1999). If plants respond by reducing transpiration, ET is also reduced, and thus, soil moisture is conserved (Massmann et al. 2019). This is especially important during prolonged periods with no precipitation (as in April and June in this study). In principle, under such condition's evaporation should be low, and the main part of ET should be transpiration which is likely to be reduced to prevent tree from excessive water loss. We also can assume that roots have access to deeper soil layers where water content was higher and which was not covered by measurements. Daily T_{EC} was generally higher than T_{SF} , especially when the SWC values were lower than 3.5% (Figs. 6, 7c). It should be emphasized that the soils had very similar properties at both sites (same soil type). The different dynamics of SWC may arise from a different interception caused by the specific structure and stand density at the sites, as well as the different thickness of the organic layer between sites.

Transpiration of understory trees and ground vegetation—which, for technical reasons, is neglected in the methodology of upscaled sap flow measurements, is one of the most possible explanations for the observed discrepancies between T_{SF} and T_{EC} . This applies especially to the case of the older, more structurally complex pine stand at TU, where beech and hornbeam saplings as well as some shrubs are present. Understory contributes to overall transpiration and can thus decrease the evaporative share of the dominant species' transpiration. Research on the influence of understory removal on water, soil micro-climate, growth and physiology of dominant Scots pine trees showed that stomata closure occurred during dry periods in the control plot with retained understory, whereas the trees without understory were able to maintain a certain stomatal aperture—roughly 50% more open than the control trees (Giuggiola et al. 2018). However, T_{EC} was the closest to T_{SF} as long as there were appropriate conditions for high tree transpiration, i.e. stable water supply in soil (Fig. 7). Nevertheless, understory may not experience the same stress and can also have more anisohydric strategies than pines (e.g. birches). This may allow for relatively high understory transpiration under dry conditions. Finally, the low T_{SF} contribution to measured ET may be influenced by non-stomatal loss of water, which becomes more important when stomata are closed but which may have a moderate significance in general. Thus, we conclude that drought stress of plants should not be derived solely with an integrated method such as EC. Our results also support the

notion that non-stomatal water losses are important during extreme dry conditions.

Sources of uncertainties

After analysing the components of forest water balance with a focus on transpiration, some factors that influenced the obtained results were identified. We assumed that under stress conditions, direct upscaled sap flow measurements are technically and methodologically more sensitive to drought than the EC method. It has been shown that measuring sap flow in trees (sap fluxes) provides better estimates of water use at the stand level than those derived by other methods (Renninger and Schäfer 2012).

We chose to partition ET based on water use efficiency since flux partitioning does not require additional instrumentation aside from the commonly used eddy covariance, which has become the standard in many sites worldwide. Transpiration regulated by the stomata quickly responds to changes in VPD; therefore, T_{EC} was estimated at a resolution of every 30 min (Zhou et al. 2014, 2015). However, there are multiple sources of uncertainty in the estimation of the ET–GPP relationship itself (Sulman et al. 2016; Anderson et al. 2017). ET/VPD is a proxy for canopy conductance if the canopy is well coupled to the atmosphere, and if boundary layer resistance is low and leaf temperature is similar to air temperature (Beer et al. 2009). Another important aspect is the possibility of reliable estimation of the share of T in ET using the method based on water use efficiency ($ET \sim GPP * VPD^{0.5}$) in conditions of drought, as done here, since the accuracy of the linear relation during drought is unclear. The assumption whether T/ET approaches 1 during favourable conditions for transpiration has been reasonable assumption in ecosystem with higher LAI while rare in dry ecosystems (Stoy et al. 2019). Interestingly, previous research has shown that WUE values did not vary much under severe soil drought during summer in a boreal Scots pine forest in Finland (Gao et al. 2017). This would indicate that the transpiration of the boreal Scots pine forest was not disturbed by the drought event at the analysed site, although the stomatal conductance of plants decreased. T_{EC} based on ecosystem-scale ET measurements from the high tower includes information on not only main tree species (Scots pine) but also the understory, if present. As mentioned above, the thorough inventory of the studied Scots pine forest resulted in the conclusion that there is no significant understory in the younger forest (ME), while a much richer composition of small trees and shrubs are present in the older ecosystem (TU). However, we do not have quantitative information on the composition and biomass of other hardwood trees and shrubs at the TU site.

Potential sources of error for eddy covariance measurements may also result from the fact that the open-path gas analyser (OP) was used. Often, the OP system accuracy is compared to enclosed-path (CP) gas analysers. The different design of both instruments and data processing is a potential source of bias for ongoing global flux synthesis activities (Haslwanter et al. 2009). For water flux measurements, open-path systems minimize spectral attenuation and therefore also require smaller correction factors than sensors with an inlet tube (Polonik et al. 2019). Gas analysers with heated tubes have been found to be less effective (losses of H₂O) under conditions of relative humidity over 60%. On the other hand, in a study by Haslwanter et al. (2009), the CP system had a tendency to underestimate H₂O fluxes in comparison to the OP system during high air temperature conditions, high wind speed, large global radiation, sun angles and low relative humidity (Haslwanter et al. 2009). However, open-path analysers do not work sufficiently under sub-optimal conditions such as during rain, fog and exposure to aerosols and dirt and therefore must be cleaned frequently to avoid signal weakening (Polonik et al. 2019). There is an increasing amount of evidence suggesting that observations of trace gases fluxes from open-path analysers can be influenced by errors related to the heating of open-path instruments (Novick et al. 2013).

Overall, the greatest analytical difficulty was mainly related to upscaling the results obtained from the sap flow sensors to estimate stand transpiration within the area covered by the EC footprint. Upscaling the point measurements to the stand or catchment level remains challenging and causes some uncertainties (Rabbel et al. 2018). The obtained results were also affected by differences between the stands and the limits of the upscaling method. Utilized exponential relationship between DBH and Q has described the relationship between the average sap flow and DBH within the range of measured samples relatively well, as it was presented in the literature (Cristiano et al. 2015). However, the occurrence of trees with DBH out of the measured range would increase the uncertainty and result in greater bias, especially for younger ecosystem, where trees with DBH out of range may constitute a great share of all trees. It has been suggested that the discrepancies in upscaled ET flux from the sap flux could also result from the systematic underestimation of sap flux by the actual sensors (Wilson et al. 2001; thermal dissipation probes, operated at the constant power principle (Granier 1987)). Therefore, more research is needed to explore the possibility of accurately upscaling tree- or leaf-level T estimates before confidently including the influence of species composition at the stand- or catchment-scale T (Ford et al. 2007). It is particularly demanding to accurately recognize the number of trees “seen” by the EC system (accurate footprint) that represent the characteristics of the overall research area. In this study, we measured the

number of trees and their DBH only on a few sample plots; therefore, our measurements might not reliably represent the actual stand tree distribution.

Additionally, the wounding effect is a known issue that can cause sap flux measurements to become unreliable. According to Maranon-Jimenez et al. (2018), the wounding effect showed a progressive development up to 22 weeks after sensor installation in living stems (Marañón-Jiménez et al. 2018). The same research also revealed that faster and more efficient wound compartmentalization occurs in early growing season installation, when physiological mechanisms involved in defence and prevention of pathogen infections are very active. Higher temperatures can also enhance this effect. In our experiment, we installed sensors in late autumn 2018, to generate the most reliable measurements for the upcoming growing season. According to the literature, the wounding effect develops with time. As such, it is recommended to change the sensors position in the stem after every growing season. Point measurements like the heat dissipation method (HD) are more prone to the wounding effect than tissue heat balance (THB).

Other water balance components such as undergrowth transpiration, canopy interception and runoff were not directly measured, and hence, their importance is difficult to estimate. It is frequently assumed that interception is already accounted for in ET flux (Soubie et al. 2016; Gu et al. 2018). Since the T_{EC} was determined here based on the ET fluxes after excluding the precipitation events, it was assumed that the T_{EC} does not contain interception. Nevertheless, this issue is a potential source of uncertainty, since the lens of the EC open-path gas analyser can dry faster after rain compared to the canopy. Using data that have been observed after short periods of rain, when the canopy was still wet, can thus lead to biased interpretation if it is assumed that the canopy is already dry. Thus, methodology of calculating interception using ET measurements from EC, combined with simplified assumptions, can produce potential failure to close the water balance. Evaporation (E) flux was higher at TU than at ME, presumably because of the higher total precipitation and number of low intensity rain events (Paschalis et al. 2018). It has been shown that such conditions typically result in an increase in rainfall interception loss. Also, E from exposed soil increase after precipitation. Furthermore, wet canopy surface simultaneously enhances evaporation and hampers transpiration due to blockage of the leaf stomates (Gash 1979; Paschalis et al. 2018).

Conclusions

Our study of transpiration fluxes in two Scots pine stands of different age classes (young and mature) located in north-western Poland was focused mainly on comparing EC and

sap flow measurements under drought conditions, and finding key drivers of these processes. Our results yielded the following conclusions:

- (1) For the growing season of 2019, total T_{EC} exceeded precipitation sums for both sites, while T_{SF} did not. Calculated as total for year T_{EC} did not exceed precipitation (for TU site). This means that ecosystem is using winter precipitation stored in soil and stems to survive during prolonged droughts in summer and most likely plants have access to water retained in deep soil layers (up to 2 m or deeper), which was not directly measured.
- (2) T_{SF} and T_{EC} had similar seasonal variability, daily and monthly courses and dynamics in response to environmental conditions for both sites. This confirms that both observations reflect the same flux, although the scale and scope of measurement have been different (ecosystem vs. tree level). T_{EC} includes information on transpiration of other species and understory as well. Thus, we can conclude that for managed forests, where one species is clearly dominant, upscaled sap flow measurements can be sufficient to properly diagnose the forest life status (in case that all tree size classes are well represented). In contrary, upscaling of sap flow measurements for forests with a significant amount of other hardwood species and ground vegetation, that are not considered in sap flow measurements, is challenging and consequently the sap flow measurement solely is not suitable for forest drought stress recognition.
- (3) It was found that with adequate water availability (5–8% for MU and ca. 4–6% for TU), T_{SF} and T_{EC} were high, and both methods give similar total values for the entire growing season. For lower SWCs, GPP was still relatively high, and discrepancies between T_{SF} and T_{EC} increased for both young and mature forest. Transpiration which occurred in June under low SWC values indicates an increasing use of stem water storage. High WUE with low SWC values within days of drought indicates that both ecosystems have reduced their water loss per carbon gain. Also, under low SWC values in the summer (ca. 3.5%), T_{SF} strongly decreased at both sites. Thus, it was evident that functioning of Scots pines at the investigated sites has reflected the strategy of trees to increase their water use efficiency under dry conditions to a surprisingly high level.
- (4) The sensitivity of T to dry conditions was similar at both sites/stands, but larger reductions were observed in T_{SF} relative to T_{EC} and in ET in July and August, when SWC was extremely low. This also shows that for assessing drought-induced effects on trees at the stand scale, transpiration from upscaled sap flow measurements seems more useful than EC-derived transpiration.

Supplementary Information The online version contains supplementary material available at <https://doi.org/10.1007/s10342-023-01549-w>.

Acknowledgements Research at both sites was supported by funding from States Forest National Forest Holding in Poland (project LAS, No OR-2717/27/11 and LAS IV 31/2021/B). The authors would like to thank Jacquelin DeFaveri from Language Centre at University of Helsinki for their help with revising the language. The work was done in collaboration with the University of Helsinki in the framework of the project 342930 “The Hidden Role of Gases in Trees” by Academy of Finland as well as SMARTLAND (grant number 318645) “Environmental sensing of ecosystem services for developing climate smart landscape to improve food security in East Africa”.

Author Contributions DP has written the original draft and was responsible for manuscript conceptualization, DP and RM have been responsible for methodology used in the manuscript, DP and UM were responsible for data curation, ZK, RM, UM, and VT commented and edited the manuscript, DP has prepared all figures (work visualization), UM, VT, ZK, and RM have supervised writing the manuscript, and OJ has been responsible for project administration and funding acquisition. All authors were involved in the manuscript preparation and revision.

Declarations

Competing interests The authors declare no competing interests.

Open Access This article is licensed under a Creative Commons Attribution 4.0 International License, which permits use, sharing, adaptation, distribution and reproduction in any medium or format, as long as you give appropriate credit to the original author(s) and the source, provide a link to the Creative Commons licence, and indicate if changes were made. The images or other third party material in this article are included in the article's Creative Commons licence, unless indicated otherwise in a credit line to the material. If material is not included in the article's Creative Commons licence and your intended use is not permitted by statutory regulation or exceeds the permitted use, you will need to obtain permission directly from the copyright holder. To view a copy of this licence, visit <http://creativecommons.org/licenses/by/4.0/>.

References

- Aiken RM, Klocke NL (2012) Inferring transpiration control from sap flow heat gauges and the penman-monteith equation. *Transac ASABE* 55(2):543–549. <https://doi.org/10.13031/2013.41389>
- Anderson RG, Zhang X, Skaggs TH (2017) Measurement and partitioning of evapotranspiration for application to vadose zone studies. *Vadose Zo J* 16:1–9. <https://doi.org/10.2136/vzj2017.08.0155>
- Barr AG, Richardson AD, Hollinger DY et al (2013) Use of change-point detection for friction-velocity threshold evaluation in eddy-covariance studies. *Agric For Meteorol* 171–172:31–45. <https://doi.org/10.1016/j.agrformet.2012.11.023>
- Beer C, Ciais P, Reichstein M et al (2009) Temporal and among-site variability of inherent water use efficiency at the ecosystem level. *Global Biogeochem Cycles* 23:1–13. <https://doi.org/10.1029/2008GB003233>
- Beguieria S, Latorre B, Reig F, Vicente-Serrano SM (2020) SPEI Global Drought Monitor. <https://spei.csic.es/map/maps.html#months=1%23month=10%23year=2020>. Accessed 6 Jan 2020
- Berkelhammer M, Noone DC, Wong TE et al (2016) Convergent approaches to determine an ecosystem's transpiration fraction. *Global Biogeochem Cycles* 30:933–951. <https://doi.org/10.1002/2016GB005392>
- Boergens E, Güntner A, Dobsław H, Dahle C (2020) Quantifying the central European droughts in 2018 and 2019 With GRACE follow-on. *Geophys Res Lett.* <https://doi.org/10.1029/2020GL087285>
- Boese S, Jung M, Carvalhais N, Reichstein M (2017) The importance of radiation for semiempirical water-use efficiency models. *Biogeosciences* 14:3015–3026. <https://doi.org/10.5194/bg-14-3015-2017>
- Bréda N, Huc R, Granier A, Dreyer E (2006) Temperate forest trees and stands under severe drought: a review of ecophysiological responses, adaptation processes and long-term consequences. *Ann For Sci* 63:625–644. <https://doi.org/10.1051/forest:2006042>
- Brito P, Lorenzo JR, González-Rodríguez AM et al (2015) Canopy transpiration of a semi arid pinus canariensis forest at a tree-line ecotone in two hydrologically contrasting years. *Agric For Meteorol* 201:120–127. <https://doi.org/10.1016/j.agrformet.2014.11.008>
- Broughton KJ, Payton P, Tan DKY et al (2021) Effect of vapour pressure deficit on gas exchange of field-grown cotton. *J Cott Res.* <https://doi.org/10.1186/s42397-021-00105-4>
- Burba G, Schmidt A, Scott RL et al (2012) Calculating CO₂ and H₂O eddy covariance fluxes from an enclosed gas analyzer using an instantaneous mixing ratio. *Glob Chang Biol* 18:385–399
- Čermák J, Deml M, Penka M (1973) A new method of sap flow rate determination in trees. *Biol Plant* 15:171–178
- Čermák J, Kučera J (1990) Scaling up transpiration data between trees, stands and watersheds. *Silva Carelica* 15:101–120
- Čermák J, Kučera J, Penka M (1976) Improvement of the method of sap flow rate determination in adult trees based on heat balance with direct electric heating of xylem. *Biol Plant* 18:105–110
- Čermák J, Kučera J, Nadezhdina N (2004) Sap flow measurements with some thermodynamic methods, flow integration within trees and scaling up from sample trees to entire forest stands. *Trees Struct Funct* 18:529–546. <https://doi.org/10.1007/s00468-004-0339-6>
- Čermák J, Deml M (1974) Method of water transport measurements in woody species, especially in adult trees (in Czech). Patent (Certification of authorship)
- Čermák J, Kučera J (1987) Transpiration of fully grown trees and stands of spruce (*Picea abies* L. Karst) estimated by the tree trunk heat balance method. In: Swanson R, Bernier P, Woodward P (eds) *Forest hydrology and watershed measurements*, 167th edn. Proceedings of the Vancouver, Wallingford, UK, pp 311–317
- Cowan IR (1978) Stomatal behaviour and environment. *Advances in botanical research* volume 4. Elsevier, pp 117–228. [https://doi.org/10.1016/S0065-2296\(08\)60370-5](https://doi.org/10.1016/S0065-2296(08)60370-5)
- Cristiano PM, Campanello PI, Bucci SJ et al (2015) Evapotranspiration of subtropical forests and tree plantations: a comparative analysis at different temporal and spatial scales. *Agric For Meteorol* 203:96–106. <https://doi.org/10.1016/j.agrformet.2015.01.007>
- Duursma RA, Kolari P, Perämäki M et al (2008) Predicting the decline in daily maximum transpiration rate of two pine stands during drought based on constant minimum leaf water potential and plant hydraulic conductance. *Tree Physiol* 28:265–276. <https://doi.org/10.1093/treephys/28.2.265>
- Falge EM, Clement RJ, Baldocchi DD et al (2001) Gap filling strategies for defensible annual sums of net ecosystem exchange. *Agric For Meteorol* 107:43–69
- Farquhar GD, Buckley TN, Miller JM (2002) Optimal stomatal control in relation to leaf area and nitrogen content. *Silva Fenn* 36:625–637
- Flo V, Martínez-Vilalta J, Steppe K et al (2019) A synthesis of bias and uncertainty in sap flow methods. *Agric for Meteorol* 271:362–374. <https://doi.org/10.1016/j.agrformet.2019.03.012>

- Foken T, Leuning R, Oncley SR, Mauder M (2012) Corrections and Data Quality Control. In: Eddy Covariance. Springer Netherlands, Dordrecht, pp 85–131
- Ford CR, Hubbard RM, Kloeppel BD, Vose JM (2007) A comparison of sap flux-based evapotranspiration estimates with catchment-scale water balance. *Agric for Meteorol* 145:176–185. <https://doi.org/10.1016/j.agrformet.2007.04.010>
- Forster MA (2014) How significant is nocturnal sap flow? *Tree Physiol* 34:757–765. <https://doi.org/10.1093/treephys/tpu051>
- Frank JM, Massman WJ (2020) A new perspective on the open-path infrared gas analyzer self-heating correction. *Agric For Meteorol* 290:107986. <https://doi.org/10.1016/j.agrformet.2020.107986>
- Gao Y, Markkanen T, Aurela M et al (2017) Response of water use efficiency to summer drought in a boreal Scots pine forest in Finland. *Biogeosciences* 14:4409–4422. <https://doi.org/10.5194/bg-14-4409-2017>
- Gash JHC (1979) An analytical model of rainfall interception by forests. *Q J Royal Met Soc* 105(443):43–55. <https://doi.org/10.1002/qj.49710544304>
- Ghimire CP, Lubczynski MW, Bruijnzeel LA, Chavarro-Rincón D (2014) Transpiration and canopy conductance of two contrasting forest types in the Lesser Himalaya of Central Nepal. *Agric For Meteorol* 197:76–90. <https://doi.org/10.1016/j.agrformet.2014.05.012>
- Gilmanov TG, Johnson DA, Saliendra NZ (2003) Growing season CO₂ fluxes in a sagebrush-steppe ecosystem in Idaho: Bowen ratio/energy balance measurements and modeling. *Basic Appl Ecol* 4:167–183. <https://doi.org/10.1078/1439-1791-00144>
- Giuggiola A, Zweifel R, Feichtinger LM et al (2018) Competition for water in a xeric forest ecosystem—effects of understory removal on soil micro-climate, growth and physiology of dominant Scots pine trees. *For Ecol Manage* 409:241–249. <https://doi.org/10.1016/j.foreco.2017.11.002>
- Good SP, Noone D, Bowen G (2015) Hydrologic connectivity constrains partitioning of global terrestrial water fluxes. *Science* 349(6244):175–177. <https://doi.org/10.1126/science.aaa5931>
- Granier A (1987) Evaluation of transpiration in a Douglass-fir stand by means of sap flow measurements. *Tree Physiol* 3:309–320
- Granier A, Reichstein M, Bréda N et al (2007) Evidence for soil water control on carbon and water dynamics in European forests during the extremely dry year: 2003. *Agric for Meteorol* 143:123–145. <https://doi.org/10.1016/j.agrformet.2006.12.004>
- Grossiord C, Buckley TN, Cernusak LA et al (2020) Plant responses to rising vapor pressure deficit. *New Phytol* 226:1550–1566. <https://doi.org/10.1111/nph.16485>
- Gu C, Ma J, Zhu G et al (2018) Partitioning evapotranspiration using an optimized satellite-based ET model across biomes. *Agric for Meteorol* 259:355–363. <https://doi.org/10.1016/j.agrformet.2018.05.023>
- Hari P, Makela A, Korpilahti E, Holmberg M (1986) Optimal control of gas exchange. *Tree Physiol* 2:169–175. <https://doi.org/10.1093/treephys/2.1-2-3.169>
- Haslwanter A, Hammerle A, Wohlfahrt G (2009) Open-path vs. closed-path eddy covariance measurements of the net ecosystem carbon dioxide and water vapour exchange: a long-term perspective. *Agric for Meteorol* 149:291–302. <https://doi.org/10.1016/j.agrformet.2008.08.011>
- Hu H, Chen L, Liu H et al (2018) Comparison of the vegetation effect on ET partitioning based on eddy covariance method at five different sites of Northern China. *Remote Sens*. <https://doi.org/10.3390/rs10111755>
- IMGiW (2020) Biuletyn monitoringu klimatu Polski. <https://klimat.imgw.pl/pl/biuletyn-monitoring/>. Accessed 6 Nov 2020
- IMGW-PIB (2021) Dane publiczne. In: IMGW-PIB. <https://danepubliczne.imgw.pl>
- Ionita M, Tallaksen LM, Kingston DG et al (2017) The European 2015 drought from a climatological perspective. *Hydrol Earth Syst Sci* 21:1397–1419. <https://doi.org/10.5194/hess-21-1397-2017>
- Jarvis PG, McNaughton KG (1986) Stomatal control of transpiration: scaling up from leaf to region. *Adv Ecol Res* 15:1–49. [https://doi.org/10.1016/S0065-2504\(08\)60119-1](https://doi.org/10.1016/S0065-2504(08)60119-1)
- Ji X, Zhao W, Kang E et al (2016) Transpiration from three dominant shrub species in a desert-oasis ecotone of arid regions of North-western China. *Hydrol Process* 30:4841–4854. <https://doi.org/10.1002/hyp.10937>
- Jiao L, Lu N, Fang W et al (2019) Determining the independent impact of soil water on forest transpiration: a case study of a black locust plantation in the Loess Plateau, China. *J Hydrol* 572:671–681. <https://doi.org/10.1016/j.jhydrol.2019.03.045>
- Katul GG, Ellsworth DS, Lai CT (2000) Modelling assimilation and intercellular CO₂ from measured conductance: a synthesis of approaches. *Plant Cell Environ* 23:1313–1328. <https://doi.org/10.1046/j.1365-3040.2000.00641.x>
- Katul GG, Palmroth S, Oren R (2009) Leaf stomatal responses to vapour pressure deficit under current and CO₂-enriched atmosphere explained by the economics of gas exchange. *Plant Cell Environ* 8:968–979
- Kittler F, Eugster W, Foken T et al (2017) High-quality eddy-covariance CO₂ budgets under cold climate conditions. *J Geophys Res Biogeosciences* 122:2064–2084. <https://doi.org/10.1002/2017JG003830>
- Kool D, Agam N, Lazarovitch N et al (2014) A review of approaches for evapotranspiration partitioning. *Agric for Meteorol* 184:56–70. <https://doi.org/10.1016/j.agrformet.2013.09.003>
- Kormann R, Meixner FX (2001) An analytical footprint model for non-neutral stratification. *Bound Layer Meteorol* 99:207–224
- Körner C (1995) Leaf diffusive conductances in the major vegetation types of the globe. In: Schulze E-D C (ed) *Ecophysiology of photosynthesis*. Springer Verlag, Berlin, pp 463–490
- Kottek M, Grieser J, Beck C et al (2006) World map of the Köppen-Geiger climate classification updated. *Meteorol Zeitschrift* 15:259–263. <https://doi.org/10.1127/0941-2948/2006/0130>
- Kucera J, Cermák J, Penka M (1977) Improved thermal method of continual recording the transpiration flow rate dynamics. *Biol Plant* 19:413–420
- Kučera J (1977) A system for water flux measurements in plants (in Czech)
- Kučera J–EMS (2018) Sap flow system EMS 81 user manual
- Kučera J, Urban J (2012) History of the development of the trunk heat balance method in last forty years. *Acta Hort* 951:87–94. <https://doi.org/10.17660/ActaHortic.2012.951.9>
- Kučera J, Vaníček R, Urban J (2020) Automated exponential feedback weighting method for subtraction of heat losses from sap flow measured by the trunk heat balance method. *Acta Hort* 1300:81–88
- Kumagai T, Tateishi M, Miyazawa Y et al (2014) Estimation of annual forest evapotranspiration from a coniferous plantation watershed in Japan (1): Water use components in Japanese cedar stands. *J Hydrol* 508:66–76. <https://doi.org/10.1016/j.jhydrol.2013.10.047>
- Kume T, Takizawa H, Yoshifuji N et al (2007) Impact of soil drought on sap flow and water status of evergreen trees in a tropical monsoon forest in northern Thailand. *For Ecol Manage* 238:220–230. <https://doi.org/10.1016/j.foreco.2006.10.019>
- Lasslop G, Reichstein M, Papale D et al (2010) Separation of net ecosystem exchange into assimilation and respiration using a light response curve approach: critical issues and global evaluation. *Glob Chang Biol* 16:187–208. <https://doi.org/10.1111/j.1365-2486.2009.02041.x>
- Levesque M, Andreu-Hayles L, Pederson N (2017) Water availability drives gas exchange and growth of trees in northeastern US, not

- elevated CO₂ and reduced acid deposition. *Sci Rep.* <https://doi.org/10.1038/srep46158>
- Li X, Gentine P, Lin C et al (2019) A simple and objective method to partition evapotranspiration into transpiration and evaporation at eddy-covariance sites. *Agric for Meteorol* 265:171–182. <https://doi.org/10.1016/j.agrformet.2018.11.017>
- LI-COR; Inc (2019) EddyPro® Software
- Lloyd J, Taylor J (1994) On the temperature dependence of soil respiration. *Funct Ecol* 8(3):315–323
- Marañón-Jiménez S, Van Den Bulcke J, Piayda A et al (2018) X-ray computed microtomography characterizes the wound effect that causes sap flow underestimation by thermal dissipation sensors. *Tree Physiol* 38:288–302. <https://doi.org/10.1093/treephys/txp103>
- Massmann A, Gentine P, Lin C (2019) When does vapor pressure deficit drive or reduce evapotranspiration? *J Adv Model Earth Syst* 11:3305–3320. <https://doi.org/10.1029/2019MS001790>
- Moncrieff JB, Massheder JM, De Bruin H et al (1997) A system to measure surface fluxes of momentum, sensible heat, water vapour and carbon dioxide. *J Hydrol* 188–189:589–611. [https://doi.org/10.1016/S0022-1694\(96\)03194-0](https://doi.org/10.1016/S0022-1694(96)03194-0)
- Moncrieff JB, Clement R, Finnigan J, Meyers T (2004) Averaging, detrending and filtering of eddy covariance time series. In: Lee X, Massman WJ, Law BE (eds) *Dordrecht handbook of micrometeorology: a guide for surface flux measurements*. Kluwer Academic, pp 7–31
- Moran MS, Scott RL, Keefer TO et al (2009) Partitioning evapotranspiration in semiarid grassland and shrubland ecosystems using time series of soil surface temperature. *Agric for Meteorol* 149:59–72. <https://doi.org/10.1016/j.agrformet.2008.07.004>
- Morgenstern K, Black TA, Humphreys ER et al (2004) Sensitivity and uncertainty of the carbon balance of a Pacific Northwest Douglas-fir forest during an El Niño/La Niña cycle. *Agric for Meteorol* 123:201–219. <https://doi.org/10.1016/j.agrformet.2003.12.003>
- Nelson JA, Carvalhais N, Cuntz M et al (2018) Coupling water and carbon fluxes to constrain estimates of transpiration: the TEA algorithm. *J Geophys Res Biogeosciences* 123:3617–3632. <https://doi.org/10.1029/2018JG004727>
- Nelson JA, Pérez-Priego O, Zhou S et al (2020) Ecosystem transpiration and evaporation: Insights from three water flux partitioning methods across FLUXNET sites. *Glob Chang Biol* 26:6916–6930. <https://doi.org/10.1111/gcb.15314>
- Novick KA, Walker J, Chan WS et al (2013) Eddy covariance measurements with a new fast-response, enclosed-path analyzer: spectral characteristics and cross-system comparisons. *Agric for Meteorol* 181:17–32. <https://doi.org/10.1016/j.agrformet.2013.06.020>
- Oishi AC, Hawthorne DA, Oren R (2016) Baseline: An open-source, interactive tool for processing sap flux data from thermal dissipation probes. *SoftwareX* 5:139–143. <https://doi.org/10.1016/j.softx.2016.07.003>
- Okoniewska M, Szuminska D (2020) Changes in potential evaporation in the years 1952–2018 in North-Western Poland in terms of the impact of climatic changes on hydrological and hydrochemical conditions. *Water (Switzerland)*. <https://doi.org/10.3390/w12030877>
- Oren R, Sperry JS, Katul GG et al (1999) Survey and synthesis of intra- and interspecific variation in stomatal sensitivity to vapour pressure deficit. *Plant, Cell Environ* 22:1515–1526. <https://doi.org/10.1046/j.1365-3040.1999.00513.x>
- Paschalis A, Fatichi S, Pappas C, Or D (2018) Covariation of vegetation and climate constrains present and future T/ET variability. *Environ Res Lett.* <https://doi.org/10.1088/1748-9326/aae267>
- Paul-Limoges E, Wolf S, Schneider FD et al (2020) Partitioning evapotranspiration with concurrent eddy covariance measurements in a mixed forest. *Agric For Meteorol* 280:107786. <https://doi.org/10.1016/j.agrformet.2019.107786>
- Pieruschka R, Huber G, Berry JA (2010) Control of transpiration by radiation. *Proc Natl Acad Sci U S A* 107:13372–13377. <https://doi.org/10.1073/pnas.0913177107>
- Plaut JA, Yezpe EA, Hill J et al (2012) Hydraulic limits preceding mortality in a piñon-juniper woodland under experimental drought. *Plant, Cell Environ* 35:1601–1617. <https://doi.org/10.1111/j.1365-3040.2012.02512.x>
- Polonik P, Chan WS, Billesbach DP et al (2019) Comparison of gas analyzers for eddy covariance: Effects of analyzer type and spectral corrections on fluxes. *Agric for Meteorol* 272–273:128–142. <https://doi.org/10.1016/j.agrformet.2019.02.010>
- Qubaja R, Amer M, Tatarinov F et al (2020) Partitioning evapotranspiration and its long-term evolution in a dry pine forest using measurement-based estimates of soil evaporation. *Agric For Meteorol* 281:107831. <https://doi.org/10.1016/j.agrformet.2019.107831>
- R Core Team (2020) R: a language and environment for statistical computing. Austria, Vienna
- Rabbel I, Bogen H, Neuwirth B, Dieckrüger B (2018) Using sap flow data to parameterize the Feddes water stress model for Norway spruce. *Water (Switzerland)*. <https://doi.org/10.3390/w10030279>
- Rafi Z, Merlin O, Le Dantec V et al (2019) Partitioning evapotranspiration of a drip-irrigated wheat crop: inter-comparing eddy covariance-, sap flow-, lysimeter- and FAO-based methods. *Agric for Meteorol* 265:310–326. <https://doi.org/10.1016/j.agrformet.2018.11.031>
- Räsänen M, Aurela M, Vakkari V et al (2022) The effect of rainfall amount and timing on annual transpiration in a grazed savanna grassland. *Hydrol Earth Syst Sci* 26:5773–5791. <https://doi.org/10.5194/hess-26-5773-2022>
- Reichstein M, Falge E, Baldocchi D et al (2005) On the separation of net ecosystem exchange into assimilation and ecosystem respiration: review and improved algorithm. *Glob Chang Biol* 11:1424–1439. <https://doi.org/10.1111/j.1365-2486.2005.001002.x>
- Renninger HJ, Schäfer KVR (2012) Comparison of tissue heat balance and thermal dissipation-derived sap flow measurements in ring-porous oaks and a pine. *Front Plant Sci* 3:1–9. <https://doi.org/10.3389/fpls.2012.00103>
- Savi T, Bertuzzi S, Branca S et al (2015) Drought-induced xylem cavitation and hydraulic deterioration: risk factors for urban trees under climate change? *New Phytol* 205:1106–1116. <https://doi.org/10.1111/nph.13112>
- Schlesinger WH, Jasechko S (2014) Transpiration in the global water cycle. *Agric for Meteorol* 189–190:115–117. <https://doi.org/10.1016/j.agrformet.2014.01.011>
- Soubie R, Heinesch B, Granier A et al (2016) Evapotranspiration assessment of a mixed temperate forest by four methods: eddy covariance, soil water budget, analytical and model. *Agric for Meteorol* 228–229:191–204. <https://doi.org/10.1016/j.agrformet.2016.07.001>
- Stoy PC, El-Madany TS, Fisher JB et al (2019) Reviews and syntheses: turning the challenges of partitioning ecosystem evaporation and transpiration into opportunities. *Biogeosciences* 16:3747–3775. <https://doi.org/10.5194/bg-16-3747-2019>
- Sulman BN, Roman DT, Scanlon TM et al (2016) Comparing methods for partitioning a decade of carbon dioxide and water vapor fluxes in a temperate forest. *Agric for Meteorol* 226–227:229–245. <https://doi.org/10.1016/j.agrformet.2016.06.002>
- Szatniewska J, Zavadilova I, Nezval O, Krejza J, Petrik P, Čater M, Stojanović M (2022) Species-specific growth and transpiration response to changing environmental conditions in floodplain forest. *For Ecol Manag* 516:120248. <https://doi.org/10.1016/j.foreco.2022.120248>
- Tang J, Bolstad PV, Ewers BE et al (2006) Sap flux-upscaled canopy transpiration, stomatal conductance, and water use efficiency in

- an old growth forest in the Great Lakes region of the United States. *J Geophys Res Biogeosci*. <https://doi.org/10.1029/2005JG000083>
- Trugman AT, Anderegg LDL, Anderegg WRL et al (2021) Why is tree drought mortality so hard to predict? *Trends Ecol Evol* 36:520–532. <https://doi.org/10.1016/j.tree.2021.02.001>
- Verbeeck H, Steppe K, Nadezhdina N et al (2007) Stored water use and transpiration in Scots pine: a modeling analysis with ANAFORE. *Tree Physiol* 27:1671–1685. <https://doi.org/10.1093/treephys/27.12.1671>
- Vicente-Serrano SM, Beguería S, López-Moreno JI (2010) A multiscale drought index sensitive to global warming: The standardized precipitation evapotranspiration index. *J Clim* 23:1696–1718. <https://doi.org/10.1175/2009JCLI2909.1>
- Wang L, Wei X, Bishop K et al (2018) Vegetation changes and water cycle in a changing environment. *Hydrol Earth Syst Sci* 22:1731–1734. <https://doi.org/10.5194/hess-22-1731-2018>
- Webb EK, Pearman GI, Leuning R (1980) Correction of flux measurements for density effects due to heat and water vapour transfer. *Q J R Meteorol Soc* 106:85–100. <https://doi.org/10.1002/qj.49710644707>
- Wieser G, Gruber A, Oberhuber W (2018) Growing season water balance of an inner alpine scots pine (*Pinus sylvestris* L.) forest. *Iforest* 11:469–475. <https://doi.org/10.3832/ifor2626-011>
- Wilson KB, Hanson PJ, Mulholland PJ et al (2001) A comparison of methods for determining forest evapotranspiration and its components: Sap-flow, soil water budget, eddy covariance and catchment water balance. *Agric for Meteorol* 106:153–168. [https://doi.org/10.1016/S0168-1923\(00\)00199-4](https://doi.org/10.1016/S0168-1923(00)00199-4)
- WRB-IUSS (2007) World reference base for soil resources 2006, first update 2007. *World Soil Resour Reports No 103*:128
- Wutzler T, Lucas-Moffat A, Migliavacca M et al (2018) Basic and extensible post-processing of eddy covariance flux data with REddyProc. *Biogeosci Dis*. <https://doi.org/10.5194/bg-2018-56>
- Yong JWH, Wong SC, Farquhar GD (1997) Stomatal responses to changes in vapour pressure difference between leaf and air. *Plant, Cell Environ* 20:1213–1216. <https://doi.org/10.1046/j.1365-3040.1997.d01-27.x>
- Zhou S, Yu B, Huang Y, Wang G (2014) The effect of vapor pressure deficit on water use efficiency at the subdaily time scale. *Geophys Res Lett* 41:5005–5013. <https://doi.org/10.1002/2014GL060741>
- Zhou S, Yu B, Huang Y, Wang G (2015) Daily underlying water use efficiency for ameriflux sites. *J Geophys Res Biogeosciences* 120:887–902. <https://doi.org/10.1002/2015JG002947>
- Zhou S, Yu B, Zhang Y et al (2016) Partitioning evapotranspiration based on the concept of underlying water use efficiency. *Water Resour Res* 52:1160–1175. <https://doi.org/10.1002/2015WR017766>
- Ziemblińska K, Urbaniak M, Chojnicki BH et al (2016) Net ecosystem productivity and its environmental controls in a mature scots pine stand in north-western Poland. *Agric for Meteorol* 228–229:60–72. <https://doi.org/10.1016/j.agrformet.2016.05.022>
- Zimmermann R, Schulze ED, Wirth C et al (2000) Canopy transpiration in a chronosequence of central Siberian pine forests. *Glob Chang Biol* 6:25–37. <https://doi.org/10.1046/j.1365-2486.2000.00289.x>

Publisher's Note Springer Nature remains neutral with regard to jurisdictional claims in published maps and institutional affiliations.

7. Oświadczenia kandydata oraz współautorów

Oświadczenie autora pracy doktorskiej o jej oryginalności, samodzielności jej przygotowania i o nienaruszeniu praw autorskich

Paulina Dukat

Niniejszym oświadczam, że przedłożoną pracę doktorską pt.: *Ocena wymiany wody i dwutlenku węgla pomiędzy różnowiekowymi lasami sosnowymi a atmosferą w skali drzewa i ekosystemu*. Napisałam samodzielnie, tj.

- nie zleciłam opracowania pracy lub jej części innym osobom,
- nie przepisałam pracy lub jej części z innych opracowań i prac związanych tematycznie z moją pracą,
- korzystałam jedynie z niezbędnej konsultacji,
- wszystkie elementy pracy, które zostały wykorzystane do jej realizacji (cytaty, ryciny, tabele, programy itp.), a nie będące mojego autorstwa, zostały odpowiednio zaznaczone oraz zostało podane źródło ich pochodzenia,
- praca nie była wcześniej podstawą nadania stopnia doktora innej osobie

Mam świadomość, że złożenie nieprawdziwego oświadczenia skutkować będzie niedopuszczeniem do dalszych czynności przewodu doktorskiego lub cofnięciem decyzji o nadaniu mi stopnia doktora oraz wszczęciem postępowania dyscyplinarnego.

Data i podpis autora

Paulina Dukat
17.04.2023

Oświadczenie autora o zgodności elektronicznej wersji pracy z jej formą wydrukowaną

Paulina Dukat

Niniejszym oświadczam, że załączona, wydrukowana wersja mojej pracy doktorskiej pt. *Ocena wymiany wody i dwutlenku węgla pomiędzy różnowiekowymi lasami sosnowymi a atmosferą w skali drzewa i ekosystemu.*, jest zgodna z plikiem w wersji elektronicznej, znajdującym się na załączonym nośniku, przeznaczonym do sprawdzenia w systemie antyplagiatowym.

Data i podpis autora

17.01.2023 Paulina
Dukat

Oświadczenie promotorów pracy doktorskiej

Oświadczamy, że niniejsza rozprawa została przygotowana pod naszym kierunkiem i stwierdzamy, że spełnia ona warunki do przedstawienia jej w postępowaniu o nadanie stopnia naukowego.

Data

18.04.2023

Podpis promotora rozprawy

Michał Urbaniak

Podpis promotora pomocniczego rozprawy

Remigiusz

Poznań 26.03.2023

Mgr Paulina Dukat
Pracownia Meteorologii, Katera Budownictwa i Geoinżynierii,
Wydział Inżynierii Środowiska i Inżynierii Mechanicznej,
Uniwersytet Przyrodniczy w Poznaniu
Piątkowska 94, 60-649 Poznań
Nr tel: : +48 665723673
paulina.dukat05@gmail.com

Oświadczenie o współautorstwie

Niniejszym oświadczam, że w pracy:

Dukat P., Ziemblińska K., Olejnik J., Małek S., Vesala T., Urbaniak M., *Estimation of Biomass Increase and CUE at a Young Temperate Scots Pine Stand Concerning Drought Occurrence by Combining Eddy Covariance and Biometric Methods*, 2021, *Forests*, DOI: 10.3390/f12070867 – **Mój indywidualny udział w jej powstawaniu polegał na – przygotowaniu oryginalnego tekstu pracy, konceptualizacji, opracowaniu metodologii oraz wizualizacji co stanowi 61% całej pracy.**

Podpis

Paulina
Dukat

Poznań 26.03.2023

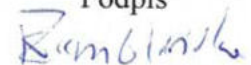
Dr inż. Klaudia Ziemblińska
Pracownia Meteorologii, Katera Budownictwa i Geoinżynierii,
Wydział Inżynierii Środowiska i Inżynierii Mechanicznej,
Uniwersytet Przyrodniczy w Poznaniu
Piątkowska 94, 60-649 Poznań
Nr tel: +48519755460
klaudiazziem@wp.pl

Oświadczenie o współautorstwie

Niniejszym oświadczam, że w pracy:

Dukat P., Ziemblińska K., Olejnik J., Małek S., Vesala T., Urbaniak M., *Estimation of Biomass Increase and CUE at a Young Temperate Scots Pine Stand Concerning Drought Occurrence by Combining Eddy Covariance and Biometric Methods*, 2021, Forests, DOI: 10.3390/f12070867 – **Mój indywidualny udział w jej powstawaniu polegał na – konceptualizacji, edytowaniu oraz redakcji pracy, co stanowi 7.8% całej pracy.**

Podpis



Poznań 26.03.2023

Prof. Dr hab. inż. Janusz Olejnik
Pracownia Meteorologii, Katera Budownictwa i Geoinżynierii,
Wydział Inżynierii Środowiska i Inżynierii Mechanicznej,
Uniwersytet Przyrodniczy w Poznaniu
Piątkowska 94, 60-649 Poznań
Nr tel: +48 512453888
janusz.olejnik@up.poznan.pl

Oświadczenie o współautorstwie

Niniejszym oświadczam, że w pracy:

Dukat P., Ziemblińska K., Olejnik J., Małek S., Vesala T., Urbaniak M., *Estimation of Biomass Increase and CUE at a Young Temperate Scots Pine Stand Concerning Drought Occurrence by Combining Eddy Covariance and Biometric Methods*, 2021, *Forests*, DOI: 10.3390/f12070867 – **Mój indywidualny udział w jej powstawaniu polegał na – analizie formalnej, administracji projektu oraz zapewnieniu zasobów do powstania pracy, co stanowi 7.8 % całej pracy.**



Podpis

Kraków, 14.04.2023

prof. dr hab. inż. Stanisław Małek
Katedra Ekologii i Hodowli Lasu,
Wydział Leśny,
Uniwersytet Rolniczy w Krakowie,
Al. 29-go Listopada 46;
31-425 Kraków,
Nr tel.: +48 691373182
rlmalek@cyf-kr.edu.pl

Oświadczenie o współautorstwie

Niniejszym oświadczam, że w pracy:

Dukat P., Ziemblińska K., Olejnik J., Małek S., Vesala T., Urbaniak M., *Estimation of Biomass Increase and CUE at a Young Temperate Scots Pine Stand Concerning Drought Occurrence by Combining Eddy Covariance and Biometric Methods*, 2021, *Forests*, DOI: 10.3390/f12070867 – 100 punktów na liście MNiSW - **Mój indywidualny udział w jej powstawaniu polegał na administracji projektu oraz zapewnieniu zasobów do powstania pracy co stanowi 7.8% całej pracy.**



Podpis

Poznań 26.03.2023

Prof. Timo Vesala
Institute for Atmospheric and Earth System Research/Physics,
Faculty of Science, University of Helsinki
P.O. Box 64 (Gustaf Hällströmin katu 2)
FI-00014 University of Helsinki
Finland
Nr tel: +358405779008
timo.vesala@helsinki.fi

Oświadczenie o współautorstwie

Niniejszym oświadczam, że w pracy:

Dukat P., Ziemblińska K., Olejnik J., Małek S., Vesala T., Urbaniak M., *Estimation of Biomass Increase and CUE at a Young Temperate Scots Pine Stand Concerning Drought Occurrence by Combining Eddy Covariance and Biometric Methods*, 2021, Forests, DOI: 10.3390/f12070867 – **Mój indywidualny udział w jej powstawaniu polegał na – analizie formalnej, komentowaniu oraz edytowaniu pracy, co stanowi 7.8 % całej pracy.**

Podpis



Poznań 26.03.2023

Dr inż. hab. Marek Urbaniak

Pracownia Meteorologii, Katera Budownictwa i Geoinżynierii,

Wydział Inżynierii Środowiska i Inżynierii Mechanicznej,

Uniwersytet Przyrodniczy w Poznaniu

Piątkowska 94, 60-649 Poznań

Nr tel: +48505273436

marek.urbania@up.poznan.pl

Oświadczenie o współautorstwie

Niniejszym oświadczam, że w pracy:

Dukat P., Ziemblińska K., Olejnik J., Małek S., Vesala T., Urbaniak M., *Estimation of Biomass Increase and CUE at a Young Temperate Scots Pine Stand Concerning Drought Occurrence by Combining Eddy Covariance and Biometric Methods*, 2021, Forests, DOI: 10.3390/f12070867 – **Mój indywidualny udział w jej powstawaniu polegał na analizie formalnej, przechowywaniu i analizowaniu danych, recenzowaniu, weryfikacji i nadzorze nad powstawaniem pracy, co stanowi 7.8 % całej pracy.**



Podpis

Poznań 26.03.2023

Mgr Paulina Dukat
Pracownia Meteorologii, Kateru Budownictwa i Geoinżynierii,
Wydział Inżynierii Środowiska i Inżynierii Mechanicznej,
Uniwersytet Przyrodniczy w Poznaniu
Piątkowska 94, 60-649 Poznań
Nr tel: +48 665723673
paulina.dukat05@gmail.com

Oświadczenie o współautorstwie

Niniejszym oświadczam, że w pracy:

Dukat P., Bednorz E., Ziemblińska K., Urbaniak M., *Trends in drought occurrence and severity at mid-latitude European stations (1951–2015) estimated using standardized precipitation (SPI) and precipitation and evapotranspiration (SPEI) indices*, 2022, Meteorology and Atmospheric Physics, DOI: 10.1007/s00703-022-00858-w –**Mój indywidualny udział w jej powstawaniu polegał na – przygotowaniu oryginalnego tekstu parcy, konceptualizacji, opracowaniu metodologii, oraz wizualizacji, co stanowi 61% całej pracy.**

Podpis

Paulina
Dukat

Poznań 26.03.2023

Prof. dr hab. Ewa Bednorz
Uniwersytet im. Adama Mickiewicza w Poznaniu
Wydział Nauk Geograficznych i Geologicznych
Zakład Meteorologii i Klimatologii
Bogumiła Krygowskiego 10, 61-680 Poznań, Polska
Nr tel: 694048319
Email: ewabedno@amu.edu.pl

Oświadczenie o współautorstwie

Niniejszym oświadczam, że w pracy:

Dukat P., Bednorz E., Ziemblińska K., Urbaniak M., *Trends in drought occurrence and severity at mid-latitude European stations (1951–2015) estimated using standardized precipitation (SPI) and precipitation and evapotranspiration (SPEI) indices*, 2022, Meteorology and Atmospheric Physics, DOI: 10.1007/s00703-022-00858-w – 70 punktów na liście MNiSW - **Mój indywidualny udział w jej powstawaniu polegał na – pomocy w konceptualizacji, edytowaniu oraz redakcji pracy co stanowi - 13% całej pracy.**

Ewa Bednorz

Poznań 26.03.2023

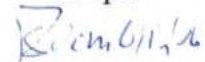
Dr inż. Klaudia Ziemblińska
Pracownia Meteorologii, Katera Budownictwa i Geoinżynierii,
Wydział Inżynierii Środowiska i Inżynierii Mechanicznej,
Uniwersytet Przyrodniczy w Poznaniu
Piątkowska 94, 60-649 Poznań
Nr tel: +48519755460
klaudiaziem@wp.pl

Oświadczenie o współautorstwie

Niniejszym oświadczam, że w pracy:

Dukat P., Bednorz E., Ziemblińska K., Urbaniak M., *Trends in drought occurrence and severity at mid-latitude European stations (1951–2015) estimated using standardized precipitation (SPI) and precipitation and evapotranspiration (SPEI) indices*, 2022, Meteorology and Atmospheric Physics, DOI: 10.1007/s00703-022-00858-w – **Mój indywidualny udział w jej powstawaniu polegał na – komentowaniu oraz edytowaniu pracy, co stanowi 13% całej pracy.**

Podpis



Poznań 26.03.2023

Dr inż. hab. Marek Urbaniak
Pracownia Meteorologii, Katera Budownictwa i Geoinżynierii,
Wydział Inżynierii Środowiska i Inżynierii Mechanicznej,
Uniwersytet Przyrodniczy w Poznaniu
Piątkowska 94, 60-649 Poznań
Nr tel: +48505273436
marek.urbania@up.poznan.pl

Oświadczenie o współautorstwie

Niniejszym oświadczam, że w pracy:

Dukat P., Bednorz E., Ziemblińska K., Urbaniak M., *Trends in drought occurrence and severity at mid-latitude European stations (1951–2015) estimated using standardized precipitation (SPI) and precipitation and evapotranspiration (SPEI) indices*, 2022, Meteorology and Atmospheric Physics, DOI: 10.1007/s00703-022-00858-w – **Mój indywidualny udział w jej powstawaniu polegał na – komentowaniu, edytowaniu oraz nadzorze nad pisaniem pracy, co stanowi 13% całej pracy.**



Podpis

Poznań 26.03.2023

Mgr Paulina Dukat

Pracownia Meteorologii, Katera Budownictwa i Geoinżynierii,

Wydział Inżynierii Środowiska i Inżynierii Mechanicznej,

Uniwersytet Przyrodniczy w Poznaniu

Piątkowska 94, 60-649 Poznań

Nr tel: : +48 665723673

paulina.dukat05@gmail.com

Oświadczenie o współautorstwie

Niniejszym oświadczam, że w pracy:

Dukat P., Ziemblińska K., Räsänen M., Olejnik J., Vesala T., Urbaniak M. *Scots pine responses to drought investigated with eddy covariance and sap flow methods, 2023, European Journal of Forest Research*, DOI: 10.1007/s10342-023-01549-w – 100 punktów na liście MNiSW – **Mój indywidualny udział w jej powstawaniu polegał na – napisaniu oryginalnego tekstu pracy, udziale w opracowaniu metodologii, wizualizacji oraz konceptualizacji pracy co stanowi 61% udziału w całej pracy.**

Podpis

Paulina
Dukat

Poznań 26.03.2023

Dr inż. Klaudia Ziemblińska
Pracownia Meteorologii, Katera Budownictwa i Geoinżynierii,
Wydział Inżynierii Środowiska i Inżynierii Mechanicznej,
Uniwersytet Przyrodniczy w Poznaniu
Piątkowska 94, 60-649 Poznań
Nr tel: +48519755460
klaudiaziem@wp.pl

Oświadczenie o współautorstwie

Niniejszym oświadczam, że w pracy:

Dukat P., Ziemblińska K., Räsänen M., Olejnik J., Vesala T., Urbaniak M. *Scots pine responses to drought investigated with eddy covariance and sap flow methods*, 2023, *European Journal of Forest Research*, DOI: 10.1007/s10342-023-01549-w –**Mój indywidualny udział w jej powstawaniu polegał na – komentowaniu, edycji i nadzorze powstawania pracy co stanowi 7.8% całej pracy.**

Podpis



Poznań 26.03.2023

Dr Matti Räsänen

Institute for Atmospheric and Earth System Research/Physics,

Faculty of Science, University of Helsinki

P.O. Box 64 (Gustaf Hällströmin katu 2)

FI-00014 University of Helsinki

Finland

Nr tel: +358400600047

matti.rasanen@helsinki.fi

Oświadczenie o współautorstwie

Niniejszym oświadczam, że w pracy:

Dukat P., Ziemblińska K., Räsänen M., Olejnik J., Vesala T., Urbaniak M. *Scots pine responses to drought investigated with eddy covariance and sap flow methods*, 2023, *European Journal of Forest Research*, DOI: 10.1007/s10342-023-01549-w – 100 punktów na liście MNiSW – **Mój indywidualny udział w jej powstawaniu polegał na – udziale w opracowaniu metodologii, komentowaniu, edytowaniu oraz weryfikacji poprawności pracy co stanowi 7.8% całej pracy.**



Podpis

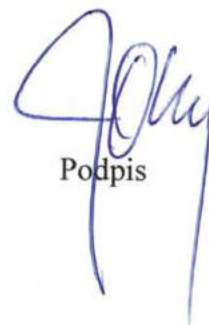
Poznań 26.03.2023

Prof. Dr hab. inż. Janusz Olejnik
Pracownia Meteorologii, Katera Budownictwa i Geoinżynierii,
Wydział Inżynierii Środowiska i Inżynierii Mechanicznej,
Uniwersytet Przyrodniczy w Poznaniu
Piątkowska 94, 60-649 Poznań
Nr tel: +48 512453888
janusz.olejnik@up.poznan.pl

Oświadczenie o współautorstwie

Niniejszym oświadczam, że w pracy:

Dukat P., Ziemblińska K., Räsänen M., Olejnik J., Vesala T., Urbaniak M. *Scots pine responses to drought investigated with eddy covariance and sap flow methods, 2023, European Journal of Forest Research*, DOI: 10.1007/s10342-023-01549-w – 100 punktów na liście MNiSW – **Mój indywidualny udział w jej powstawaniu polegał na – administracji projektu, pozyskiwaniu funduszy oraz pomocy w przygotowanie i weryfikacji pracy co stanowi 7.8% całej pracy.**



Podpis

Poznań 26.03.2023

Prof. Timo Vesala
Institute for Atmospheric and Earth System Research/Physics,
Faculty of Science, University of Helsinki
P.O. Box 64 (Gustaf Hällströmin katu 2)
FI-00014 University of Helsinki
Finland
Nr tel: +358405779008
timo.vesala@helsinki.fi

Oświadczenie o współautorstwie

Niniejszym oświadczam, że w pracy:

Dukat P., Ziemblińska K., Räsänen M., Olejnik J., Vesala T., Urbaniak M. *Scots pine responses to drought investigated with eddy covariance and sap flow methods*, 2023, *European Journal of Forest Research*, DOI: 10.1007/s10342-023-01549-w – 100 punktów na liście MNiSW – **Mój indywidualny udział w jej powstawaniu polegał na – edytowaniu, redakcji oraz nadzorowaniu poprawności pracy, co stanowi 7.8% całej pracy.**

Podpis



Poznań 26.03.2023

Dr inż. hab. Marek Urbaniak
Pracownia Meteorologii, Katera Budownictwa i Geoinżynierii,
Wydział Inżynierii Środowiska i Inżynierii Mechanicznej,
Uniwersytet Przyrodniczy w Poznaniu
Piątkowska 94, 60-649 Poznań
Nr tel: +48505273436
marek.urbaniak@up.poznan.pl

Oświadczenie o współautorstwie

Niniejszym oświadczam, że w pracy:

Dukat P., Ziemblińska K., Räsänen M., Olejnik J., Vesala T., Urbaniak M. *Scots pine responses to drought investigated with eddy covariance and sap flow methods*, 2023, *European Journal of Forest Research*, DOI: 10.1007/s10342-023-01549-w – 100 punktów na liście MNiSW – **Mój indywidualny udział w jej powstawaniu polegał na przechowywaniu danych komentowaniu, edycji i nadzorze powstawania pracy co stanowi 7.8% całej pracy.**



Podpis